Francisco Javier Torrijo
Julio Garzón
Miguel Ángel Eguibar
Francesca Trizio

Stability Analysis of Soil and Rock Slopes

edUPV
Universitat Politècnica de València

Collection Académica

To cite this publication please use the following reference: Torrijo, J. F.; Garzón, J.; Eguibar; M. A.; Trizio, F. (2022) *Stability Analysis of Soil and Rock Slopes.* Valencia: edUPV

sale: www.lalibreria.upv.es / Ref.: 0214_05_01_01
ISBN: 978-84-1396-037-1
DL: V-1752-2022
edUPV is committed to eco-printing and uses paper from suppliers that meet environmental sustainability standards https://editorialupv.webs.upv.es/compromiso-medioambiental/

Printed: Byprint Percom, S. L.

If the reader detects a mistake in the book or wishes to contact the authors, he can send an email to edicion@editorial.upv.es

Printed in Spain

Index

Chapter 1
Slope Instabilities

1.1. Introduction

Slope instabilities are one of the geological hazards that more economic and life losses cause each year. This phenomenon can have a natural origin (geological morphology) or an anthropogenic one (slopes made as a complement of other infrastructures, such as the results of excavations and embankments) and can occur both in soils and rocks.

In geology and engineering, slope instabilities are often referred as *landslides*. That term may have different definitions with slight differences, but usually a landslide is understood as any downslope movement of soil or rock under the effects of gravity and the landform that results from such movement (Highland & Bobrowski, 2008). However, it is interesting to note that the term slope instability is more general than landslide.

The analysis of the stability of slopes is a key aspect in the design of any infrastructure such as roads, railways, canals, pipelines and dams as well as in mining operations. For common infrastructures, slopes reach heights up to 40 or 50 m, although slope of more than 200 m can be built on some occasions. These slopes should normally be projected as vertical as possible for economic reasons and must be stable in the long term. On the other hand, mining slopes are designed based on the mineral deposit to be exploited and may need to be stable exclusively for a short or medium term.

The potential instability of slopes is not only related to infrastructures or mining operations, but it is also of high importance in other areas of Civil Engineering like land use planning, urbanism and environmental issues. Although many landslides take place in sparsely populated mountain areas where material damage and deaths are lower than the one produced by other hazards like floods or earthquakes, some slope instabilities around the world resulted in infamous disasters (e.g. Fig. 1.1) with a great amount of life losses, for instance:

- The Vargas landslide (Venezuela) in December 1999, caused between 1500 and 3000 deaths.
- The Monte Elgon landslide (Uganda) in March 2010, caused ca.350 deaths.
- The Niteroi favela landslide (Río de Janeiro, Brazil) in April 2010, caused around 200 missing persons in the Niteroi favela.
- The Leh landslide (Ladakh, India) in August 2010, caused ca.190 deaths and 400 missing persons.
- The Medellin landslide (Colombia) in December 2010, caused ca. 45 deaths.
- The Río de Janeiro landslide (Brazil) in January 2011, caused ca. 800 deaths and a great number of missing persons.
- The Uttarakhand landslide (India) in June 2013 together with an important flooding and both phenomena caused around 6000 deaths.
- The Aab Bareek landslide (Afganistán) in May 2014, caused ca.350 deaths.
- The Salgar landslide (Colombia) in May 2015, caused ca.90 deaths.
- The Santa Catarina Pinula landslide (Guatemala) in November 2015, caused around 280 deaths and 70 missing persons.
- A landslide in the south of Bangladesh in June 2017, caused ca. 150 deaths.
- The Freetown landslide (Sierra Leone) in August 2017, caused around 400 deaths and destroyed more than 100 houses.
- The Petropolis landslide (Río de Janeiro, Brazil) in August 2017, caused ca. 150 deaths.

Slope instabilities are often linked to flooding and sometimes with earthquakes, like the ones occurred in China in 1920 (100000 deaths) and Peru in 1970 (22000 deaths), or even to volcano eruptions, like the Armedo landslide (Colombia) generated by the “Nevado de Ruiz” volcano in December 1999, which caused ca. 23000 deaths after affecting some lahar deposits. However, separating victims generated by floods or earthquakes and by landslides is difficult, since authorities usually do not distinguish between them.

The consequences of these great disasters together with the fact that small landslides, even though can cause just a dozen victims, are very numerous, almost continuous throughout any year and always result in significant economic losses, shows the importance of analyzing slope stability and forecasting and preventing such kind of natural and man-made potential hazards.

Source: Smith, Lawson, US ACE. United States Geological Survey Open File Report 01-0144

Fig. 1.1. Example of the consequences of a slope instability. Aerial view of debris-flow deposition resulting in widespread destruction on the Caraballeda fan of the Quebrada San Julián. Avulsion of the main channel (left side of photo) resulted in deposits up to 6-m in thickness and totaling about 1.8 million cubic meters of bouldery debris. Secondary new flood channels are visible through center of fan to the lower right of photo.

1.2. Slope Instabilities Types

1.2.1. Varnes' Classification

Fig. 1.2 shows the classification of slope instabilities according to Varnes (1978). This is a common classification also used by different national institutions like the British Geological Survey. Varnes' classification defines 5 basic types of instabilities: falls, topples, slides, lateral spreads and flows.

A sixth type is also included as complex movements and it covers the combination of two or more of the basic types (e.g. a slide and a flow).

The next sections describe the features of those six types.

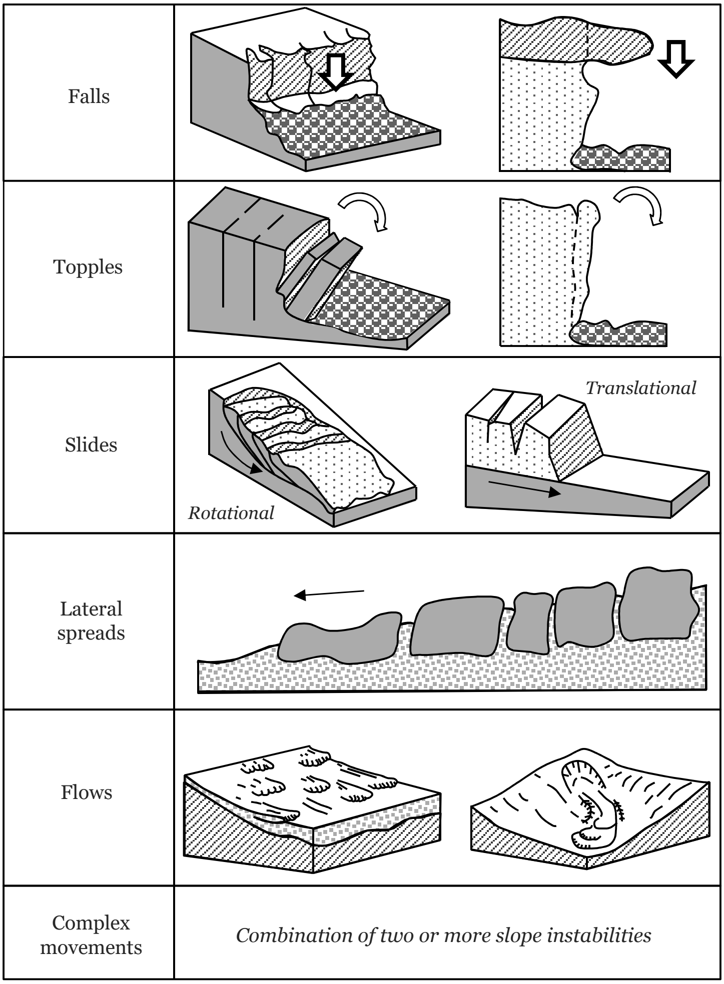

Source: Based on Varnes (1978), modified from British Geological Survey and Corominas & García Yagüe (1997)

Fig. 1.2. Landslides classification.

1.2.2. Falls

Falls are defined as the fall of masses of soil or rock detached with little or no shear displacement which descend mostly through air by free fall, bouncing or rolling.

When a fall occurs in rock masses, it is called *rockfall*. Rockfalls are vertical fast movements and typical of rock masses with steep slopes. They can be identified by the accumulation of blocks of rocks of variable size at the slope toe, as seen in Fig. 1.3.

Source: Self-elaboration

Fig. 1.3. Rockfalls in a slope close to Cenicero village, La Rioja (Spain).

1.2.3. Topples

Topples occur when a set of blocks rotate outward about a pivot axis located below the center of gravity of the unstable mass. Fig. 1.4 shows an example of a rock slope prone to experiment a toppling failure.

Once the material on the slope separates, it impacts on the slope itself, fragmenting into smaller pieces or portions that can bounce and roll.

Topples speed can vary widely, from extremely fast movements to ones that need thousands of years to occur.

1.2.4. Slides

Slides are rigid displacements of a mass of soil or rock that moves downwards along a defined surface that can be identified and discretized.

The mass of soil or rock in a slide moves as a whole, i.e. it behaves as a unique unit, and sliding occurs along a given surface where the shear strength of the ground material is exceeded.

Slides speed is variable, ranging from several m/s to a few mm/year and they usually involve large material volumes.

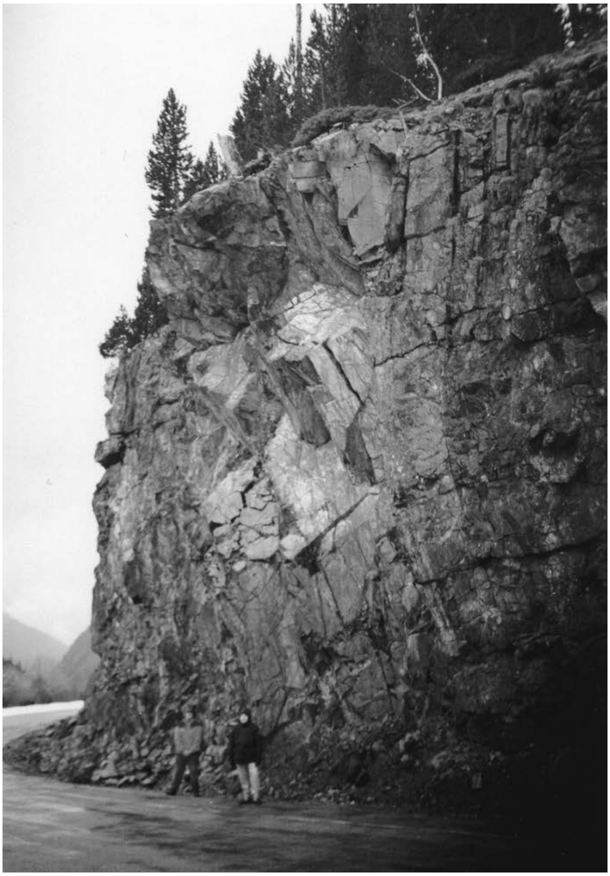

Source: Self-elaboration

Fig. 1.4. Strata close to present a toppling failure mechanism, Benasque Valley, Huesca (Spain).

Depending on the path followed by the sliding mass, two groups can be distinguished:

- *Rotational slides* (also call slumps): in this slides the failure surface is curved with concavity upwards. An unstable mass rotates around an imaginary axis located above the center of gravity, parallel to the slope. The rotation often involves sinking of the slope head and heave of the toe (Fig. 1.5).
- *Translational slides*: in this slides the failure surface is flat and the movement is mainly linear (Fig. 1.6). Two typologies of translational slides exist: planar failures, where the slide takes places along a single planar surface; and wedge failures, when it occurs along the intersection line of two planar surfaces.

Source: Self-elaboration

Fig. 1.5. Rotation slide in a slope close to Formigal, Huesca (Spain).

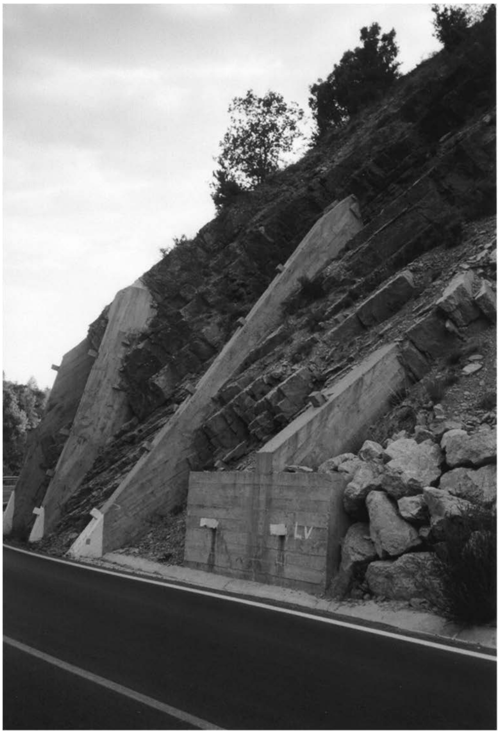

Source: Picture courtesy of J.M. Bescós

Fig. 1.6. Stabilized slope to avoid translational slides due to planar failures, Cuenca (Spain).

1.2.5. Lateral Spreads

Lateral spreads are slope instabilities which involve the lateral extension of the ground due to the movement of coherent rock or soil masses over a soft and deformable material (e.g. a plastic flow or a liquefaction of the subjacent material). As a consequence, a fragmentation of the stiffer upper layers takes place. Fig. 1.7 shows a scheme.

Lateral spreads are not frequent instabilities, although they are usually quite extensive. On many occasions, they are the consequence of the subsidence of a great mass due to the relaxation of a slope after having been excavated by glacial phenomena.

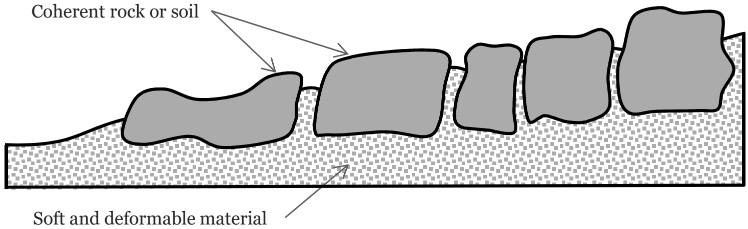

Source: Modified from Corominas & García Yagüe (1997)

Fig. 1.7. Lateral spread by the flow and extrusion of the underlying material.

1.2.6. Flows

Flows are movements of saturated or dry materials which advance by flowing like viscous fluids, i.e. the ground particles do move neither in parallel paths nor at the same speed.

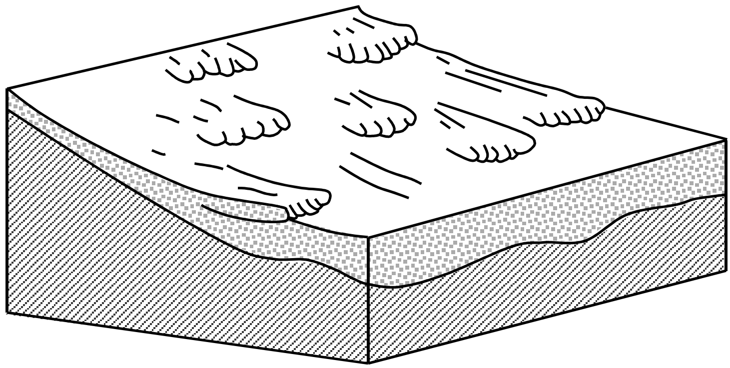

Source: Modified from Corominas & García Yagüe (1997)

Fig. 1.8. Solifluction scheme.

In flows, the unstable mass does not keep the geometry in its movement, giving rise to lobed forms and usually being the sliding surface not well defined.

Flows can range from slow to rapid movements, and the fluidizing effect of water has great influence on them.

These instabilities are quite common in nature and their analysis is normally conducted based on fluid mechanics by assuming the ground to behave as a liquid.

Different types of flow movements are distinguished:

- *Solifluction*: shallow complex phenomenon where the soil flows by deforming, appearing shear surfaces Fig. 1.8 shows a scheme. Ice and soil plasticity are conditioning factors of this instability.
- *Creeps*: extremely slow and continuous shallow movements of soil and rock particles which can be produced by variations of water content and ice-thaw cycles. Fig. 1.9 shows an example of a slope affected by creep.

Source: Self-elaboration

Fig. 1.9. View of a slope affected by creep, Benasque Valley, Huesca (Spain).

- *Mud flow*: elongated and lobed movements at their toe produced in materials with at least 50% of fines and with enough water content for fluidization. Fig. 1.10 shows a scheme. Sudden increases in pore pressure play a critical role in these instabilities, since this significantly reduces the shear strength of the ground material. The loss of shear strength once the material starts its movement due to reorientation of the particles is also an important aspect. For these reasons mud flows reach great distances.

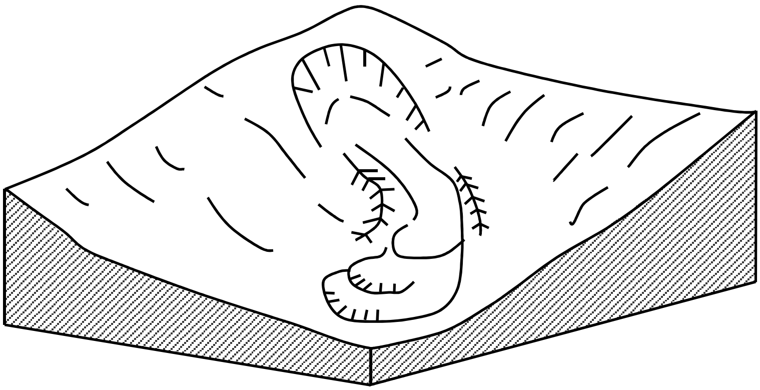

Source: Modified from Corominas & García Yagüe (1997)

Fig. 1.10. Mud flow scheme.

- *Debris flow*: flows in materials with a high percentage of coarse-grained particles. When debris flows are fast and progressive, they are called "rockslides" or "rock avalanches". Fig. 1.11 shows an example of a debris flow.

Varnes classification separates mud flows from debris flows according to the quantity of coarse-grained particles. However, it should be noted that this classification does not directly include *hyperconcentrated flows*. This special case of flows consists of a two-phase flowing mixture of water and sediments with more fluid characteristics than a debris flow, but with a solid and sediment load high enough to make it be considered as a non-Newtonian fluid (behavior of a debris flow). So, a hyperconcentrated flow may be seen as an intermediate case between a mud flow and a debris flow.

1.2.7. Complex Movements

Complex movements are those that result from the combination of two or more types of the five basic movements described in sections above. For instance, a slide and a flow or a slide and a lateral spread.

A complex movement normally involves the triggering of a type of instability followed by two or more of the other movement types. These instabilities generally reach a large size, sometimes affecting an entire slope.

An example of a complex movement is shown in Fig. 1.12.

Source: Picture courtesy of J.M. Bescós

Fig. 1.11. Debris flow in the Pyrenees, Lerida (Spain).

1.3. Triggering Factors

Factors that trigger slope instabilities are basically related to the variations that occur in the intrinsic properties of the ground. Some of those factors include:

- Lithology
- Strength properties of the ground material.
- Geological structure.
- Hydrogeological conditions.
- Morphology of the area.

Such factor may be natural ones, i.e. a direct consequence of natural processes, or anthropogenic factor, i.e. induced by human activity.

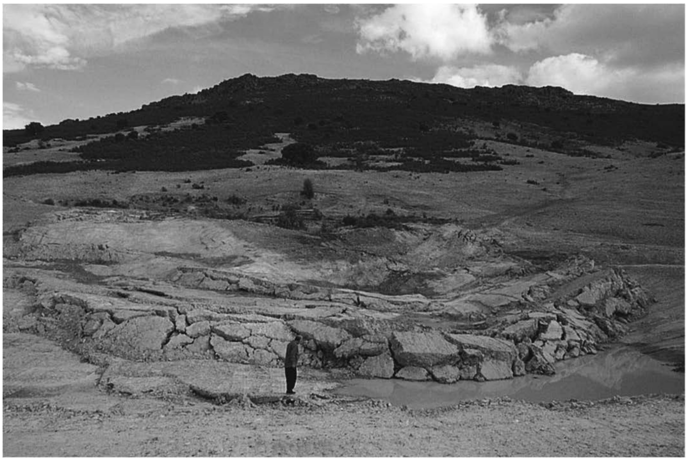

Source: Picture courtesy of Laboratorios Proyex, S.A.

Fig. 1.12. View of a sliding flow (complex movement) produced due to the absence of compaction of materials, Arroba de los Montes, Ciudad Real (Spain).

Natural factors include phenomena such as:

- Weathering and erosion.
- Slope orientation to the geological structure.
- Natural stresses in rock masses.
- Steeper slopes in an area.
- Weather.
- Water (e.g. erosion due to rainfalls, seepage or increase in the water table).
- Seismicity.
- Vegetation.

Anthropogenic (man-made) factors include activities like:

- Excavations for mining or civil works (e.g. roads or railways).
- Blasting.
- Overloads on slopes.
- Changes in the water table.
- Changes in the saturation level in reservoirs (including fast emptying of reservoirs).
- Irrigation.
- Channels.

1.4. Instabilities Identification

It is interesting to mention that the actual state of a slope and the materials that appear on it are the main indicative factors of a potential instability and they also "inform" about the type of movement associated. Thus, the process of identifying potentially unstable areas is carried out by the interpretation of the geomorphology of a region.

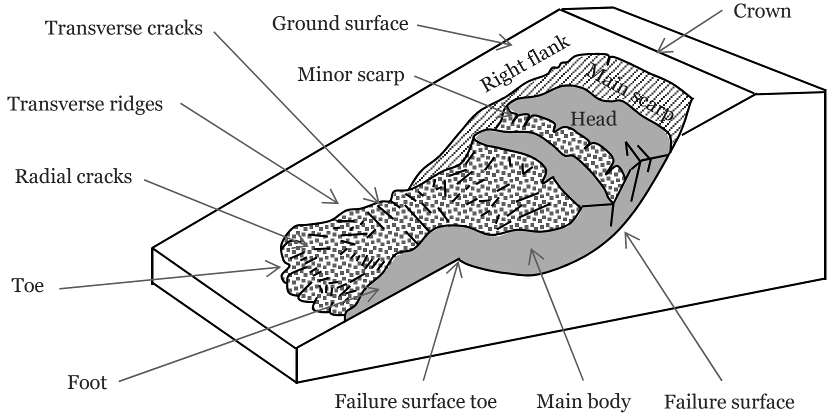

Source: Modified from Highland & Bobrowski (2008)

Fig. 1.13. Rotational slide in soils.

Thus, for the case of rotational slides in soils (slumps) like the one shown in Fig.1.13, typical mechanism of a soil slope instability, a series of observations can be conducted to detect the potential sliding (Corominas, 1989):

- Erosion: scars and scarps are often observed prior to a landslide, as well as sinks in the terrain with displacement of material.
- Deposit at the slope toe: deposits corresponding to a potential landslide usually present heave.
- Structure: sliding mass internal organization is chaotic with scattered blocks; material classification is very small, and mixture of lithology may appear.
- Morphology: cracks that affect the substrate, changes in color and texture as well as a disorganized drainage network are signals of unstable areas.
- Vegetation: the movements and inclinations in the vegetation (e.g. trees) may indicate ground movements where they are located.

1.5. Geological-Geotechnical Investigation of Slopes

The investigations and explorations for addressing slope instabilities must be conducted on two work scales and two steps: a first step at large scale (*general survey*) and a second step at small scale (*detailed surveys*).

General surveys are previous geological-geotechnical investigations carried out at large scale and which involve the use of:

- Topographic maps (including old maps that may have variations in topography or even allusive names), geographic maps, geotechnical maps and geomorphological maps.
- The use of successive aerial photos to appreciate different aspects such as variations of movements, changes in morphology, slopes and drainage network.
- Remote sensing, like the use of DinSAR satellites or LIDAR images.

This first phase should result in zoning the region, establishing areas where the development of potential instabilities is high. This is achieved by combining various data such as slope angles, slope heights, lithology, natural stability, hydrological and hydrogeological parameters, surface formations and degree of weathering.

Detailed surveys are carried out at small scale and usually include two stages:

- In situ interpretation and measurement of the landslide geometry: the morphological evidence of landslides such as cracks, scarps, undulations and the appearance of landslide deposits are studied.

  The slope is measured (slope angle, height and length), the type of movement identified and the position of the head, the toe and the depth of the sliding surface established. In addition, some indicators may be proposed for measuring the movement activity.
- In situ investigations: a series of geological-geotechnical explorations and investigations are carried out for establishing the landslide geometry and the mass involved in the instability.

  These investigations should also obtain the geotechnical parameters of the materials involved, especially in the failure surface (in the case of slides).

  Techniques used in this stage include geomechanical stations, boreholes, trial pits, penetration tests, geophysical prospecting and the use of instrumentation like inclinometers (they allow locating the failure surface position and setting the movement speed).

Chapter 2
Slope Stability in Soils

2.1. Introduction

The study of the stability of a soil slope deals with analyzing the equilibrium of such slope just before the failure of part of the ground take place. Basically, two kinds of forces can be identified in any soil slope failure:

- Driving forces, or forces that produce the movement of the soil mass and eventually cause the soil failure and the instability of the slope. The main unstable load in any soil instability is the self-weight of the soil as well as other gravitational loads.
- Resisting forces, or forces that oppose to the movement of the soil mass and "try" to prevent failure from occurring. The main ground resisting force is the shear strength developed at the failure surface.

Besides, water, as in any geotechnical calculation, conditions the behavior of soil slopes and can contribute to the instability mechanism.

Some slope stability analysis methods can be considered nowadays as classical ones, as they were designed when computers did not exist or its use was not frequent. They are still in use, especially for analyzing simple cases or for doing quick estimations in preliminary design phases. Similarly, the use of charts results in a quick and effective procedure endorsed by years of practice. Nevertheless, today the most common approach for addressing a soil slope stability analysis is the method of slices.

2.2. General Aspects

2.2.1. Soils Features

Soils are not cemented aggregates of mineral particles that are the result of different physical and chemical (sometimes biological too) alteration processes over rocks. A soil is assumed to be formed by three phases: the solid phase (mineral particles); the liquid phase (water located in the pores or voids between the mineral particles); and the gaseous phase (free air found in the pores not filled by water).

Mechanically, depending on their nature, two types of soils are distinguished:

- *Granular soils*: high permeable soils in which there is no attraction between their particles (cohesion is very small or even inexistent). Stresses are resisted in granular soils due to friction between particles. Granular soils include gravels and sands; many types of silts are also granular soils, but due to the small size of their particles, silts usually behave like cohesive soils.
- *Cohesive soils*: low or very low permeability soils characterized by a noticeable interaction between their particles (cohesion). Stresses are resisted in cohesive soils due to a combination of the friction and cohesion between particles. Cohesive soils include clays and some types of silts.

The basic properties of a soil give information about its state. These properties include gradation (distribution of soil particles by size), water content (ratio between the weight of the water found in the soil and the weight of the solid phase), Atterberg limits (water content values for which the soil change its consistency), degree of saturation (ratio between the volume of voids filled by water and the total volume of voids) and density (ratio between the mass and the volume).

Particularly, three kinds of densities are defined in a soil:

- Dry density (γ_d): density of the soil when the degree of saturation is 0% (all voids are filled with air).
- Bulk density or simply "density" (γ): density of the soil for a given degree of saturation.
- Saturated density (γ_{sat}): density of the soil when the degree of saturation is 100% (all voids are filled with water).

It should be noted that here the term density is equivalent to unit weight. Even though both terms are not exactly the same, since an identical value for Earth acceleration gravity is considered elsewhere, both terms may be assumed interchangeable.

Soils show a specific mechanical behavior which is different from other materials. In a saturated soil, the total stresses applied are transmitted both to the mineral particles and the water located in the pores, thus resulting in the relationship:

$$\sigma = \sigma' + u \rightarrow \sigma' = \sigma - u$$ **Equation 2.1**

Where σ is the total stress; u is the *pore pressure* (pressure of the water located in the pores); and σ' is the *effective stress*. Effective stresses act exclusively on the solid phase of the soil, and although not really measurable, they are considered to correspond to the intergranular pressure when the area of contact between particles tends to zero.

When a load is applied to a saturated soil, this is immediately transmitted to the water existing in the soil. That results in an increase in the pore pressures, which is called *overpressure*. If drainage is allowed, some of the water contained in the soil will tend to flow out to alleviate the pore overpressures and eventually all overpressures will dissipate. At that point, volume of soil will have decreased and overpressures stresses will have passed to the solid phase in form of an increase in the effective stresses.

The previous phenomenon is the basis of the well-known Terzaghi's principle which basically says that all appreciable and measurable changes in a soil caused by changes in stresses are exclusively produced by a change in effective stresses. Consequently two geotechnical drainage conditions may exist:

- *Drained conditions*: when the pore overpressures are dissipated as drainage is allowed; this is the usual condition of granular materials (high permeability) as well as cohesive materials in "long term" (regardless a low permeability, after a long time drainage will occur). Soils in this case work in effective stresses.
- *Undrained conditions*: when the pore overpressures are not dissipated as drainage is "not allowed"; this is the usual condition of cohesive materials in "short-term", i.e. after a load is applied, an excavation is performed or a similar change in the stress conditions of the soil occurs. Soils in this case work in total stresses.

Therefore, pore pressures are needed to be evaluated to define the mechanical behavior of a soil. Commonly, pore pressures are due to groundwater and their values can be estimated hydrostatically; in other cases, a water flow exists, requiring establishing and computing a flow net to set the value of pore pressures at each point of the soil.

2.2.2. Shear Strength

Soils are unable of resisting tension stresses, so soil strength is normally considered against shear stresses, with the Mohr-Coulomb criterion defining the failure of a soil:

$$\tau_{\max} = c + \sigma \cdot \tan \phi \qquad \textbf{Equation 2.2}$$

Where τ_{max} is the maximum tangential (shear) stress that can be reached; σ is the normal stress to the failure plane considered; and c and ϕ are the shear strength parameters of the soil, cohesion and friction angle, respectively.

The Mohr-Coulomb criterion of Eq. 2.2 is expressed in generic stresses. When working under drained conditions, the criterion must be expressed in effective stresses, thus replacing σ by σ' and c and ϕ by c' and ϕ', i.e. considering the effective values of the shear strength parameters of the soil (cohesion and friction angle). It is interesting to note that total and effective tangential stresses are equal ($\tau = \tau'$) as pore pressures are water pressures that always act normal to a surface, without a tangential component.

For soils working under undrained conditions, the Mohr-Coulomb criterion is expressed in total stresses and the shear strength parameters (cohesion and the friction angle) are considered in undrained values, c_u and ϕ_u. Commonly, a null value for the undrained friction angle is considered ($\phi_u = 0$), so all the soil shear strength is reduced to its undrained cohesion c_u, which is also call *undrained shear strength*. The value of c_u is equal to a half of the uniaxial compression strength (UCS).

Values of the shear strength parameters (in effective and undrained values) can be obtained by means of laboratory tests. The most common ones are: (i) the direct shear tests, for granular soils and cohesive soils under drained conditions (performed according to standards such as ASTM D30806); and (ii) the uniaxial compression strength tests for obtaining the undrained shear strength (performed according to standards such as ASTM D21666).

Under drained conditions, soils may experiment peak strength. This is observed when carrying out a direct shear test on a granular soil, which may show two main behaviors:

- For dense granular soils, peak strength is observed, i.e. a clear maximum tangential stress value is developed and once obtained the strength of the soil progressively reduces until reaching an asymptotic residual value. The peak appears along with an increase in the volume of the soil due to shear loading (*dilation*). The denser the soil, the sharper the peak and more dilation.
- For loose granular soils, no peak strength is observed, reaching directly the shear strength an asymptotic residual value. Instead of dilation, *contraction* is observed, i.e. a decrease in the volume of the soil due to shear loading.

In the case of cohesive soils, the two previous behaviors are also observed depending on their consolidation state: normally consolidated soils behave similar to loose granular soils, while overconsolidated soils resemble dense granular soils. Nevertheless, this behavior is only considered for cohesive soils under drained conditions.

2.2.3. Types of Instabilities

Based on the shear strength values, instabilities in soils can be classified as (Skempton & Hutchinson, 1969):

- *New landslides*, which occur in a soil where previously no instability took place. The soil strength parameters to be considered in this case are those corresponding to the peak values of cohesion and friction angle.
- *Reactivated or old landslides*, which occur in a soil where previously an instability took place, so the soil structure may be highly oriented due to the old landslide effect, following the direction of the movement. The soil strength parameters to be considered in this case are those corresponding to the residual values of cohesion and friction angle.

Instabilities in soils can also be classified based on the pore pressure values (Skempton & Hutchinson 1969):

- *Landslides under undrained conditions*: instabilities in which the dissipation of pore overpressures does not occur, as drainage is not allowed. The shear strength parameters to consider correspond to total stresses (c_u and $\phi_u = 0$).
- *Landslides under intermediate drainage conditions*: instabilities in which a partial dissipation of pore overpressures occurs.
- *Landslides under drained conditions*: instabilities in which the total dissipation of pore overpressures occurs. The shear strength parameters to consider correspond to the effective stresses (c' and ϕ').

2.2.4. Water Influence

The presence of water on any slope always causes negative effects on its stability. Some aspects that affect the stability of a soil slope due to the presence of water include (González de Vallejo & Ferrer, 2011):

- Pore pressure reduces shear strength (friction angle and cohesion), being especially significant in cohesive materials.
- Water in a soil increases the weight of the slope, thus increasing the driving forces (weight) that tend the sliding to occur.

- Water produces weathering and alteration processes that cause material degradation, thus increasing the instability of slopes. This includes seepage washing down the soil fine particles, changing soil gradation in the long term.
- Rainfall and surface runoff erode slopes, especially contributing to phenomena of surface instability.
- Water induces compositional changes in the mineralogy of materials.
- In expansive materials, water can cause volume increases that contribute to the instability of the slopes.
- In granular materials, a flow net opposed to the gravity direction may result in canceling the effective stresses ($\sigma' = 0$), leading to a quicksand phenomenon.

Therefore, the analysis and location of water on slopes must be carefully considered as it totally conditions the slope stability under study.

2.2.5. Instabilities in Soil Slopes

Instabilities in soil slopes are normally the result of rotational slides materialized in curve failure surfaces. The hypothesis of a circular sliding surface is quite accurate and experimentally many slopes in homogeneous soils are observed to develop instabilities following a circle-shaped failure.

Circular failures are therefore the most common instabilities in soil slopes. They are classified in three typologies, as show in Fig. 2.1, depending on the point where the failure surface daylights (i.e. appears) in the ground:

- Toe failure, when the failure surface exactly daylights at the slope toe.
- Face failure, when the failure surface daylights at the slope face.
- Base failure, when the failure surface daylights beyond the slope toe and consequently it affects the ground below the slope.

Under some circumstances, soil slopes can also develop instabilities due to translational slides. When the ground is composed by strata of different strength, a failure following a plane or a polygonal surface may occur, giving rise to a *planar failure*.

It is interesting to note that simple calculation methods usually assume that the failure mechanism of soil vertical slopes is governed by a planar failure. This is due to an easier analytical approach calculation. However, the general assumption considering a circular failure of the soil slope is still completely valid and even close to the real phenomenon.

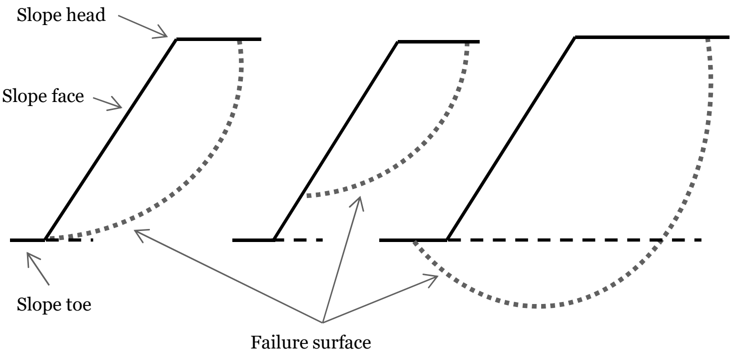

Source: Self-elaboration

Fig. 2.1. Circular failure surfaces in a soil slope: toe failure (left), face failure (center) and base failure (right).

2.2.6. Calculation Methods

The stability analysis of soil slopes can be carried out using stress-strain methods and limit equilibrium methods. In both cases, a two-dimension model is normally assumed, and the problem is solved as plane strain, considering a unit thickness of slope.

Stress-strain methods consider both ground deformations and forces for analyzing soil slopes. They are comprehensive calculation methods capable of dealing with complex geometries, material anisotropy, non-linear behavior, in situ stresses, creep deformation or dynamic loading. However, they have a high complexity and need the use of advance modeling. Strain-stress methods also require gathering knowledge about the constitutive behavior that governs all the materials involved, both geotechnical and structural ones (like anchors). Definition of some geotechnical parameters in soils is sometimes not easy and data needed is commonly poor, difficult to obtain, not measured or not available, which limit the use of these methods.

The most common way of applying stress-strain calculation methods is by finite element modeling (FEM). This technique discretizes a continuous problem into a series of elements defined by their constitutive behavior in which all the kinematic and mechanical conditions are applied. Any forces, water tables, water flows, anchorages or structures can be implemented, and the output provides a complete definition of the stresses and strains in all materials (both geotechnical and structural ones). Other techniques for using stress-strain methods include finite difference modeling (FDM) and discrete element modeling (DEM).

Conversely, *limit equilibrium methods* rely exclusively on the static balance of forces. They solve the problem establishing the equilibrium state of the unstable mass and do not take into account the ground strains and deformations. They assumed the soil shear strength is developed totally and simultaneously along the sliding (failure) surface.

Limit equilibrium methods are aimed at obtaining the *safety factor* of the slope, which is defined as the ratio between the resisting forces opposed to the sliding of the failure surface and the driving forces causing the sliding of the unstable mass: a safety factor less than 1.0 means that the soil mass is unstable; a safety factor equal to 1.0 means a strict balance between the resisting forces and the driving forces; a safety factor greater than 1.0 indicates that the slope is stable. Generally, the different regulations and codes require safety factor values around 1.3 – 1.5 to consider a slope stable.

Some limit equilibrium methods provide a rigorous solution of the safety factor, applying all the static equilibrium equations and without admitting any simplification. This is in general only possible for simple geometries and certain cases. On the other hand, many limit equilibrium methods assume some simplifications; this is the case of the method of slices, the most common method used in the study of soil slopes.

The following sections deal with different limit equilibrium methods used to analyze the stability of a soil slope and obtain its safety factor. The use of FEM for calculating soil slopes is found in ***Chapter 5***.

2.3. Analytical Classical Solutions

2.3.1. Infinite Slope

The infinite slope model assumes the slope length is much greater than the thickness of the unstable mass, being the plane parallel to the ground surface. This model is suitable when the failure surface is defined by the contact between the soil and the underlying bedrock located in a plane almost parallel to the slope (González de Vallejo & Ferrer, 2011).

In an infinite slope, the expression for the safety factor F (defined as the ratio between the resisting forces and the driving forces) can be obtained considering that the potential sliding plane will be located at a depth z.

Fig. 2.2 shows the balance of forces on a slice of soil of thickness t. An earth thrust E will act on each vertical plane of the slice, but as the slope is assumed infinite, the value of such earth thrust at both sides of the slice will be the same with opposed direction, thus canceling each other. The weight of the slice W is therefore the main acting force and needs a reaction force at the slice base to balance it. That reaction force is decomposed into a normal force to the slice N and a tangential force parallel to the slice S_m which corresponds to the shear force mobilized in the sliding plane (failure surface).

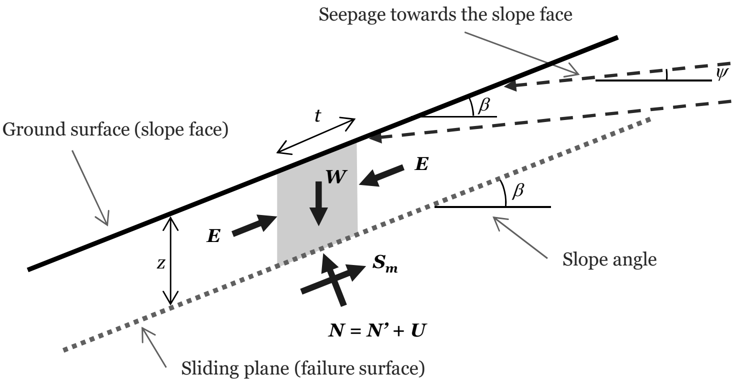

Source: Self-elaboration

Fig. 2.2. Balance of forces on an infinite soil slope (Acting forces: *E*: earth thrust; *W*: weight of the soil slice; *N*: normal force at the base of the slice; *N'*: effective normal force at the base of the slice; *U*: water force due to the pore pressures at the base of the slice; S_m: tangential force developed by the ground along the slice).

The Mohr-Coulomb failure criterion is considered:

$$\tau_{\max} = c' + \sigma' \cdot \tan \phi' \qquad \textbf{Equation 2.3}$$

Where τ_{max} is the maximum tangential stress in the failure plane; σ' is the effective normal stress in the failure plane; c' is the effective cohesion; and ϕ' is the effective friction angle. Introducing the safety factor *F* in this expression, this can be written as:

$$\tau_{available} = \frac{c'}{F} + \frac{\sigma' \cdot \tan \phi'}{F} \qquad \textbf{Equation 2.4}$$

Where $\tau_{available}$ is the maximum tangential stress that can be developed in the failure plane affected by a safety factor *F* (equal for the cohesion and the friction angle).

If shear strength parameters (c' and ϕ') are assumed constant along the sliding surface, the maximum tangential force S_m that can be developed at the base of the slide considering a safety factor *F* will be:

$$S_m = \frac{c' \cdot t}{F} + \frac{N' \cdot \tan \phi'}{F} \qquad \textbf{Equation 2.5}$$

Where *N′* is the effective normal force at the base of the slice, therefore:

$$N' = N - U = N - u \cdot t$$ **Equation 2.6**

Where *U* is the resultant force due to pore pressures and *u* the pore pressure acting at the failure surface.

The static balance of perpendicular forces to the failure surface requires:

$$N' = W \cdot \cos\beta - U = \gamma \cdot z \cdot t \cdot \cos^2\beta - u \cdot t$$ **Equation 2.7**

Where γ is the soil density (bulk density or saturated density, depending on the case) and *β* is the angle of the slope.

The static balance of parallel forces to the failure surface requires:

$$W \cdot \sin\beta = S_m \rightarrow \gamma \cdot z \cdot t \cdot \sin\beta \cdot \cos\beta = \frac{c' \cdot t}{F} + \frac{N' \cdot \tan\phi'}{F}$$ **Equation 2.8**

Carrying out some mathematical arrangements, the expression for the safety factor is:

$$F = \frac{c'}{\gamma \cdot z \cdot \sin\beta \cdot \cos\beta} + \left(1 - \frac{r_u}{\cos^2\beta}\right)\frac{\tan\phi'}{\tan\beta}$$ **Equation 2.9**

Where r_u is a non-dimensional coefficient which depends on the pore pressure at the failure plane and is given by:

$$r_u = \frac{u}{\gamma \cdot z}$$ **Equation 2.10**

For instance, given a straight seepage towards the slope that makes an angle *ψ* with the horizontal, the value of coefficient r_u is (Alonso Pérez de Ágreda, 2009):

$$r_{u,straigth\ seepage\ angle\ \psi} = \frac{\cos\beta \cdot \cos\psi}{\cos(\psi - \beta)}$$ **Equation 2.11**

If the seepage is parallel to the slope, $\psi = \beta$, therefore coefficient r_u would result:

$$r_{u,parallel\ seepage} = \cos^2\beta$$ **Equation 2.12**

For a granular soil, where commonly cohesion is neglected and all soil strength is assumed to be developed due to friction between its particles, safety factor yields:

$$F = \left(1 - \frac{r_u}{\cos^2 \beta}\right) \frac{\tan \phi'}{\tan \beta}$$ **Equation 2.13**

In that case, if pore pressures are null, i.e. the soil is dry, coefficient r_u will be null, so:

$$F = \frac{\tan \phi'}{\tan \beta}$$ **Equation 2.14**

This result indicates that the maximum angle ($F = 1$) withstand by a non-cohesive soil where no pore pressures exist is exactly its effective friction angle. Particularly, this is the conceptual definition of the effective friction angle ϕ' of a soil.

2.3.2. Vertical Soil Slope

A vertical slope in a soil can only be stable if some cohesion exists. In the case of a purely cohesive saturated soil with reduced permeability, the safety factor *F* of a vertical slope of height *H* can be obtained considering undrained conditions and establishing the balance of forces shown in Fig. 2.3 (for the sake of the simplicity, the possibility of a tension crack is not taken into account).

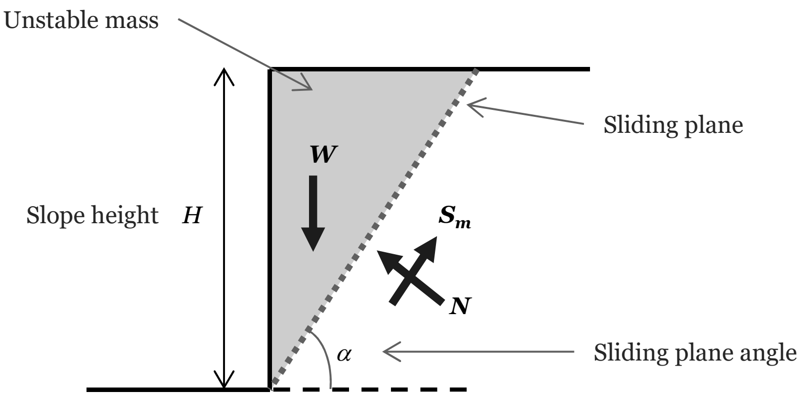

Source: Self-elaboration

Fig. 2.3. Balance of forces on a vertical slope in an undrained cohesive soil (Acting forces: *W*: weight of the unstable mass; *N*: normal force at the sliding plane; S_m: tangential force developed by the ground along the sliding plane).

In a vertical slope, the soil failure takes place at a certain plane (sliding plane) defined by an angle α and sliding occurs when the shear strength given by the Mohr-Columb criterion is exceeded. It should be noted that the Mohr-Columb criterion must be written with the parameters corresponding to a saturated soil under undrained conditions ($c = c_u$ and $\phi = \phi_u = 0$), so:

$$\tau_{\max} = c_u + \sigma \cdot \tan\phi_u = c_u \rightarrow \tau_{available} = \frac{c_u}{F}$$ **Equation 2.15**

If undrained shear strength (c_u) is assumed constant along the sliding plane, the maximum tangential force S_m that can be developed will be:

$$S_m = \frac{c_u \cdot l}{F}$$ **Equation 2.16**

Where l is the length of the sliding plane, geometrically equal to:

$$l = \frac{H}{\sin\alpha}$$ **Equation 2.17**

The static balance of tangential forces at the sliding plane requires:

$$W \cdot \sin\alpha = S_m = \frac{c_u \cdot l}{F} = \frac{c_u}{F} \cdot \frac{H}{\sin\alpha}$$ **Equation 2.18**

Where W is the weight of the potentially unstable soil wedge, which can be expressed in terms of its geometry as:

$$W = \frac{1}{2} \cdot \gamma_{sat} \cdot \frac{H^2}{\tan\alpha}$$ **Equation 2.19**

Where γ_{sat} is the saturated density of the soil.

Carrying out some mathematical arrangements the safety factor F can be computed:

$$F = \frac{4 \cdot c_u}{\gamma_{sat} \cdot H} \cdot \frac{1}{\sin 2\alpha}$$ **Equation 2.20**

The safety factor depends on the sliding plane angle α, so it appears that several values of α should be computed for analyzing the vertical slope, selecting the minimum safety factor obtained.

However, this case can be analytically solved by finding the minimum value of function *F(α)* mathematically:

$$\min[F(\alpha)] \leftrightarrow \frac{dF}{d\alpha} = 0 \rightarrow \cos 2\alpha = 0 \leftrightarrow \alpha = 45^{o}$$ **Equation 2.21**

Therefore, the minimum safety factor is given for a sliding plane angle of 45º and the expression that defines such safety factor will be:

$$F = \frac{4 \cdot c_u}{\gamma_{sat} \cdot H}$$ **Equation 3.22**

For the case of a soil under drained conditions, the safety factor of a vertical slope may also be obtained by establishing a balance of forces and assuming the Mohr-Coulomb criterion, now written in effective stresses with the effective parameters *c'* and *ϕ'*; doing some arrangements the expression yields (Alonso Pérez de Ágreda, 2009):

$$F = \frac{2 \cdot c'}{\gamma \cdot H} \cdot \frac{1}{\sin\alpha \cdot \cos\alpha} + \frac{\tan\phi'}{\tan\alpha}$$ **Equation 2.23**

The minimum value of function *F(α)* leads to the expression:

$$\tan\alpha = \sqrt{1 + \frac{\gamma \cdot H}{2 \cdot c'} \cdot \tan\phi'}$$ **Equation 2.24**

Therefore, the safety factor of a vertical slope for a soil under drained conditions is:

$$F = 2 \cdot \sqrt{\frac{2 \cdot c'}{\gamma \cdot H} \cdot \left(\frac{2 \cdot c'}{\gamma \cdot H} + \tan\phi'\right)}$$ **Equation 2.25**

The analysis of this expression indicates that, as expected, non-cohesive soils ($c' = 0$) such as sands or gravels without fines, can never withstand vertical slopes ($F = 0$).

It is important to mention that the safety factors obtained in this section for vertical slopes (for cohesive soils under undrained conditions and granular/cohesive soils under drained conditions) normally lead to conservative results. Such values can be useful in a preliminary design phase and for analyzing simple cases and small slopes.

2.3.3. Circular Failures

The computation of the safety factor considering a circular failure in a soil which has only cohesion, as is the case of a cohesive material under undrained conditions ($c = c_u$ and $\phi = \phi_u = 0$) may be addresses by a establishing the balance of forces given in Fig. 2.4. This procedure is also called "Petterson's circle method".

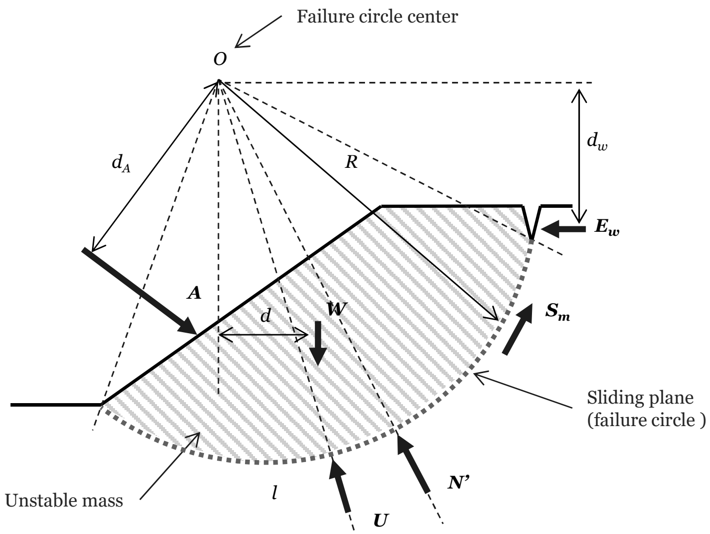

Source: Self-elaboration

Fig. 2.4. Balance of forces on a circular failure (Acting forces: *E_w*: water thrust in the tension crack; *W*: weight of the unstable mass; *N'*: effective normal force at the sliding plane; *U*: water force due to pore pressures at the sliding plane; *S_m*: tangential force developed by the ground along the sliding plane; *A*: exterior forces).

Following a mathematical procedure similar to the one used for an indefinite slope, but with the additional consideration of the existence of a tension crack and exterior forces, the safety factor *F* for a circular failure in a soil with only cohesion is given by:

$$F = \frac{c_u \cdot l}{W \cdot d - A \cdot d_A + E_w \cdot d_w} \cdot R$$ **Equation 2.26**

Where c_u is the undrained shear strength (or undrained cohesion); l is the arch length of the failure circle in the soil; R is the radius of the failure circle; W is the saturated weight of the unstable mass; d is the lever arm of W with respect to the center of the failure circle; A is the resultant of all exterior forces acting over the unstable mass and tending to its instability; d_A is the lever arm of all the exterior forces A with respect to the center of the failure circle; E_w is the resultant of the water thrust in the tension crack and d_w its corresponding is the lever arm. The depth of the tension crack can be calculated as:

$$z_{tension\ crack} = \frac{2 \cdot c_u}{\gamma_{sat}}$$ **Equation 2.27**

Where γ_{sat} is the saturated density of the soil.

The Petterson's circle method provides an easy and quick estimation of the safety factor of a general slope in a cohesive material under undrained conditions. However, since the method is applied to a given failure circle of radius R, the method requires performing several iterations considering different positions of the center of the circle and its radius until finding the worst failure circle, i.e. the minimum safety factor value.

It is interesting to note that the safety factor expression for the Petterson's circle method can be easily extended to terrains with several horizontal soil layers simply by adding the contribution of each layer to the strength, i.e.:

$$F = \frac{\sum c_{u,j} \cdot l_j}{W \cdot d - A \cdot d_A + E_w \cdot d_w} \cdot R$$ **Equation 2.28**

Where $c_{u,j}$ and l_j correspond to such values for the stratum j intersected by the proposed failure circle.

Unfortunately, the generalization of the Petterson's circle method to a general case of a material with non-zero values of friction and cohesion involves proposing a balance of forces which leads to an indeterminate system of equations with more unknowns than equations. Such general slope stability problem may be solved using the "friction circle method" (Alonso Pérez de Ágreda, 2009; Taylor 1948). This method considers that all effective normal stresses acting at the failure circle can be concentrated in given point P (unknown) and the result of adding the normal force and the tangential force component related to friction is tangent to a "friction circle" with the same center as the failure circle and passing through the point P.

The friction circle method requires proposing an initial value of safety factor as well as conducting an iterative process to be solved. Similar to the Petterson's circle method, the friction circle method requires studying a series of failure circles of different centers and radius to find the correct safety factor value. All in all, the friction circle method is quite complex and laborious. Instead, Taylor (1948) and the Hoek & Bray (1981) charts are used, both of which are built based on that method.

2.4. Use of Charts

2.4.1. Taylor Charts

Using the friction circle method, Taylor analyzed a series of soil slope stability problems for dimensionless cases and homogeneous soils and obtained two charts (Taylor 1937, 1948). This tabulated solution provides the safety factor of a soil slope when the only driving force is the self-weight of the soil and the ground is completely dry or totally saturated (i.e. completely under the water table).

The use of Taylor charts requires a homogeneous soil (constant values of c and ϕ), no significant external forces that can destabilize or stabilize the slope (e.g. they cannot be used with anchors) and the absence of seepage. Furthermore, they do not consider the existence of tension cracks. However, they are easy to apply and useful to make estimations or to solve simple cases.

Chart no. 1 (Fig. 2.5) is the general chart and represents the slope angle ψ in abscises and the *stability number* N_e in ordinates, being N_e defined as:

$$N_e = \frac{c}{F_c \cdot \gamma \cdot H} = \frac{c^*}{\gamma \cdot H}$$ **Equation 2.29**

Where c is the soil cohesion (undrained cohesion or effective cohesion, according to the case under study); F_c is the safety factor for the cohesion; γ is the soil density, which must be considered saturated (γ_{sat}) when the slope is under the water table and equal to the bulk density otherwise; H is the slope height; and c^* is the reduced cohesion due to the application of the corresponding safety factor (i.e. c / F_c).

This chart provides the values for N_e depending on the slope angle ψ and the reduced friction angle ϕ^* defined as:

$$\tan \phi^* = \frac{\tan \phi}{F_\phi}$$ **Equation 2.30**

Where ϕ is the soil friction angle and F_ϕ is the safety factor for the friction angle, which may be different to the safety factor for the cohesion (F_c), but commonly both values are considered to be the same ($F_c = F_\phi$).

When the soil friction angle ϕ is null (case of a saturated cohesive soil working under undrained conditions where $\phi = \phi_u = 0$) and the slope angle ψ is less than 54º, the stability analysis must be conducted considering one of the following cases:

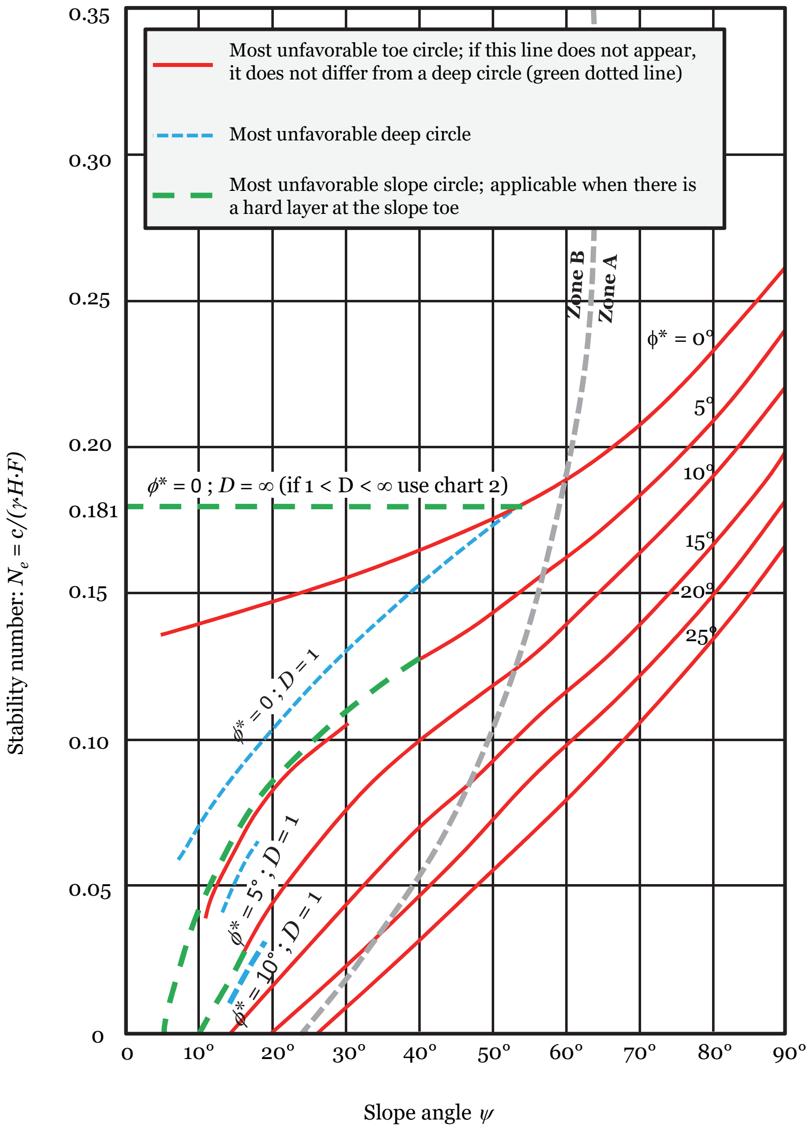

Source: Modified from González de Vallejo & Ferrer (2011)

Fig. 2.5. Taylor's chart no. 1; in zone A the critical circle is above the slope toe (resulting in face or toe failures); in zone B the critical circle results in base failures.

- If there is neither a hard layer (a much more rigid and resistant stratum than the one under study) below the slope nor any type of horizontal limitation that forces the critical circle to emerge at a specific point, N_e is always 0.181.

- If there is a hard layer below the slope and such layer is just located at the same level as the excavation, i.e. the toe of the slope corresponds to the hard layer, then the curve indicated as "*D* = 1" in chart no. 1 is followed. The existence of a hard layer restricts the development of the failure circle and therefore substantially influences the stability of the slope.
- If there is a hard layer below the slope at a different depth from that of the previous point ($D \neq 1$), chart no. 2 is used (Fig. 2.6). Once the depth of the hard layer is known, this depth is called D·H, where *H* is the height of the slope. In chart no. 2 the stability number N_e is replaced by the *stability coefficient* N_s, which is the inverse of N_e:

$$N_s = \frac{F_c \cdot \gamma \cdot H}{c} = \frac{\gamma \cdot H}{c^*}$$

Equation 2.31

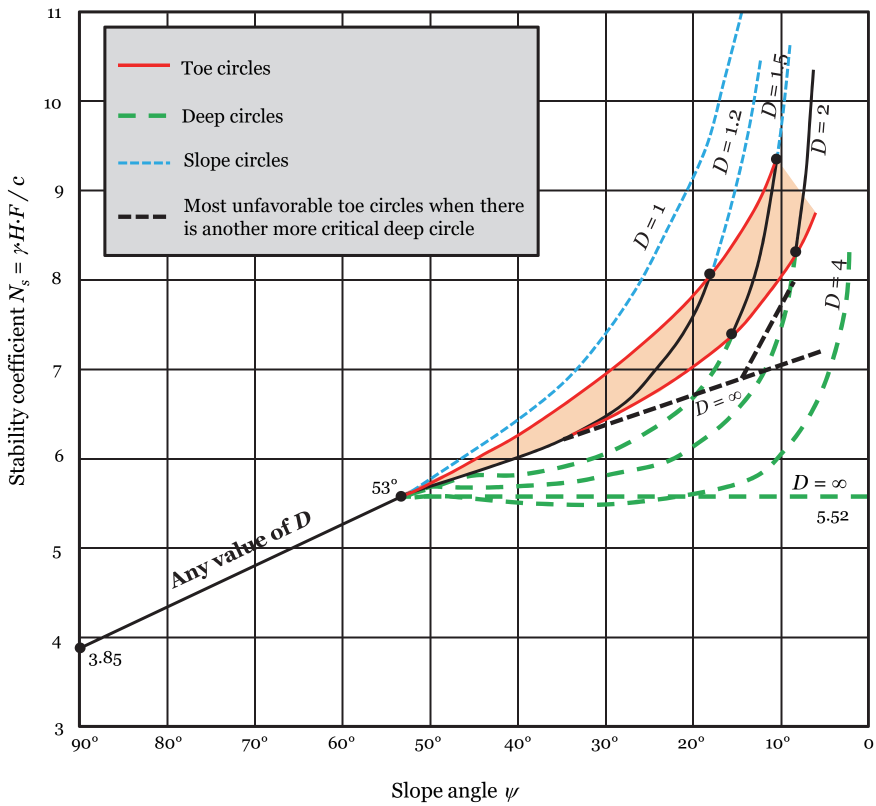

Source: Modified from González de Vallejo & Ferrer (2011)

Fig. 2.6. Taylor's chart no. 2 ($\phi = 0$).

2.4.2. Hoek & Bray Charts

Hoek & Bray charts (1981) provide the safety factor of a slope in a homogeneous soil (constant values of c and ϕ) where the only driving force is the self-weight of the ground (they are not valid when existing external forces that can destabilize or stabilize the slope) considering 5 hydrological conditions (Fig. 2.7) as well as the existence of tension cracks. Hoek & Bray charts are much more comprehensive (Alonso Pérez de Ágreda, 2005) than Taylor charts and are also used to make estimations prior to conduct more advanced calculations or to solve simple cases. However, according to their own authors, the assumptions considered to build the charts are valid for friction angles greater than 5º; therefore, Hoek & Bray charts should not be used for undrained conditions (null friction angle); in that case, Taylor charts should be used.

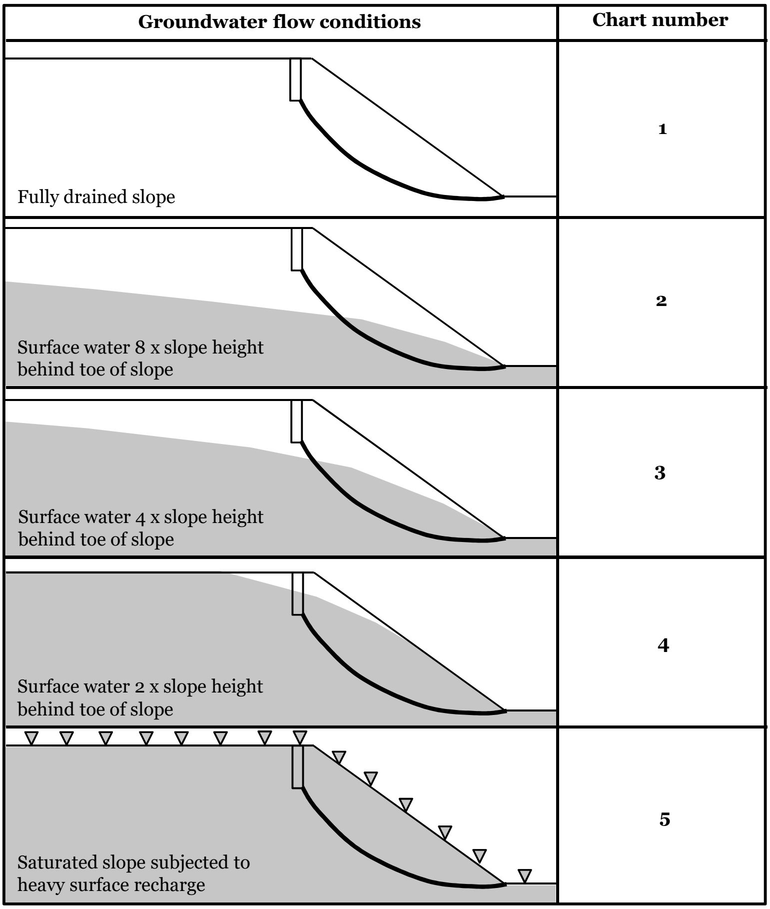

Source: Modified from Hoek & Bray (1981)

Fig. 2.7. Hydrological conditions considered by Hoek & Bray and corresponding chart.

The five Hoek & Bray charts are given in Figs. 2.8 – 2.12; each chart corresponds to a given hydrological condition (Fig. 2.7) from a totally dried soil to a totally saturated soil; in case of doubt, the condition on the safe side should be chosen. Fig. 2.13 shows the general scheme for the use of a Hoek & Bray chart.

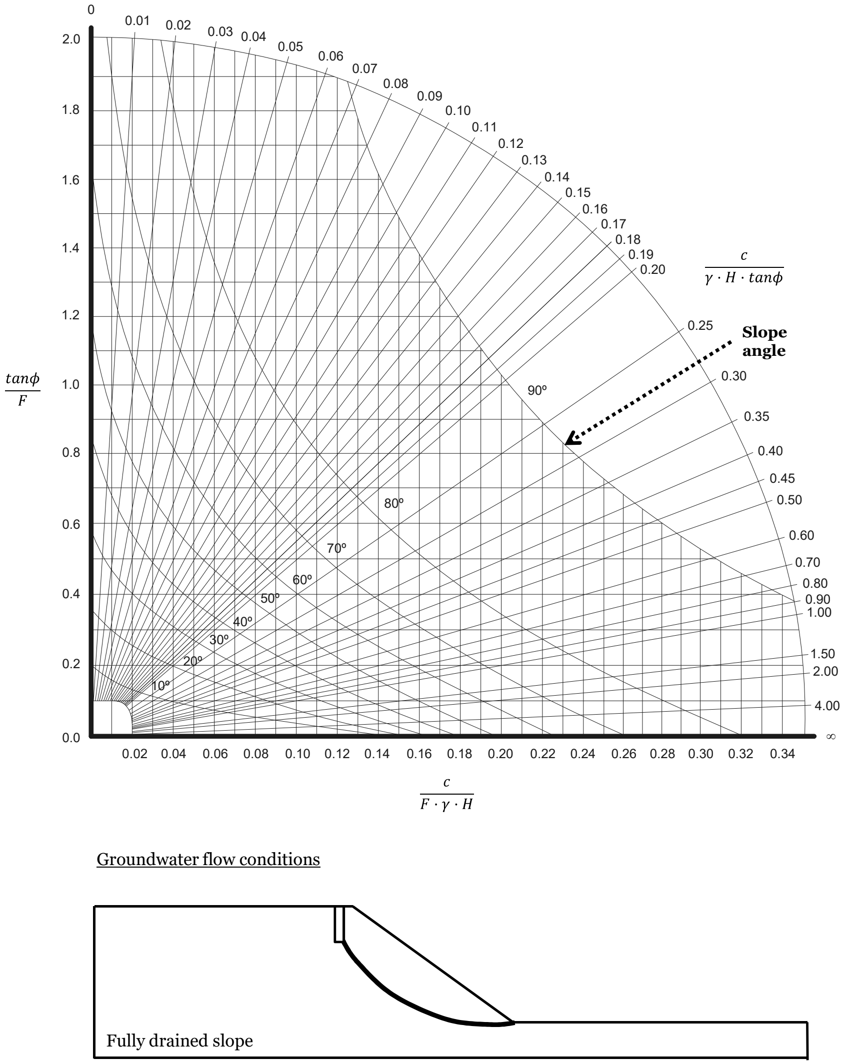

Source: Modified from Hoek & Bray (1981)

Fig. 2.8. Hoek & Bray chart no. 1. Groundwater flow conditions for applying this chart are shown below it.

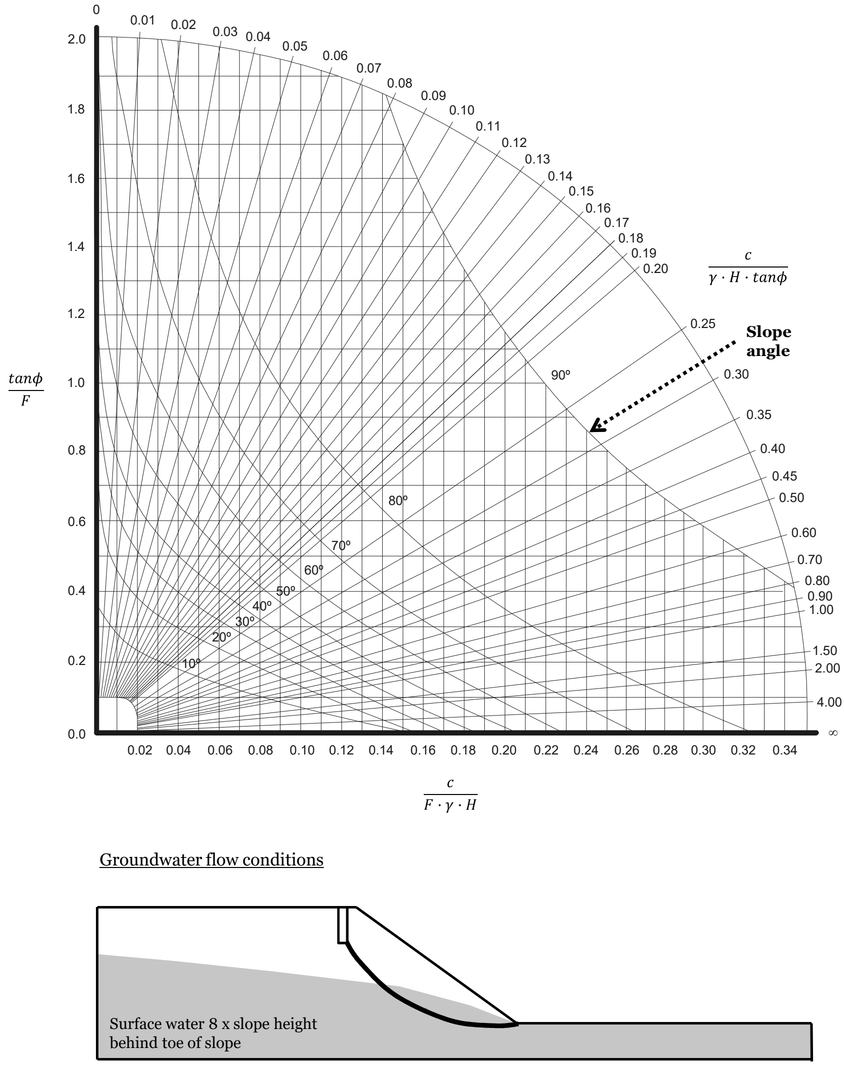

Source: Modified from Hoek & Bray (1981)

Fig. 2.9. Hoek & Bray chart no. 2. Groundwater flow conditions for applying this chart are shown below it

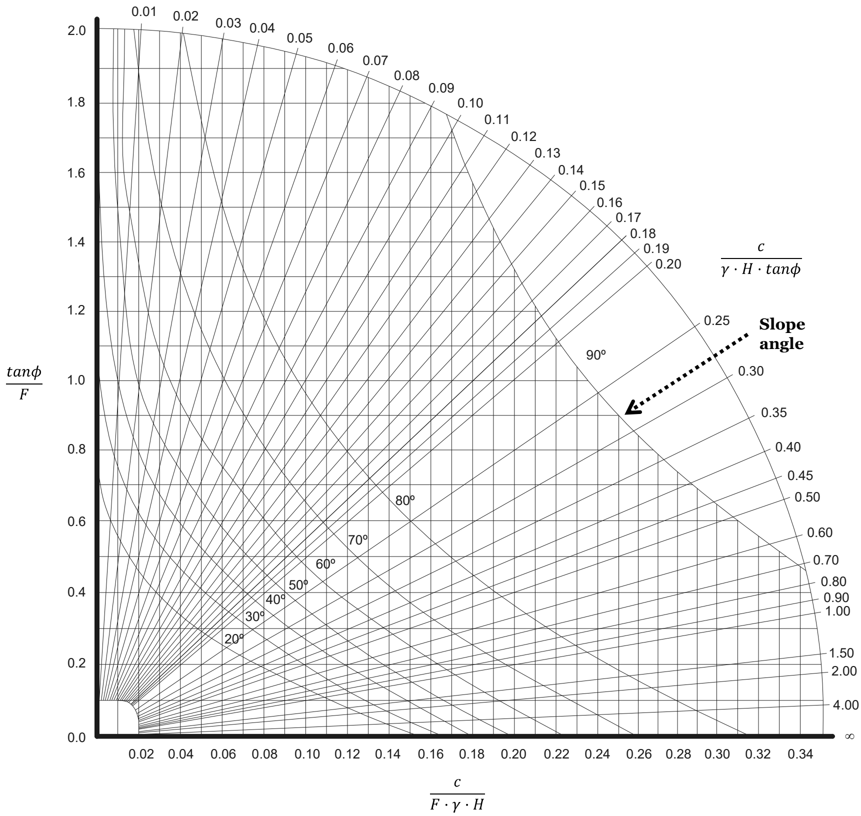

Groundwater flow conditions

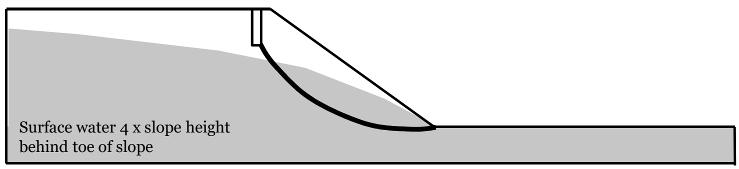

Source: Modified from Hoek & Bray (1981)

Fig. 2.10. Hoek & Bray chart no. 3. Groundwater flow conditions for applying this chart are shown below it

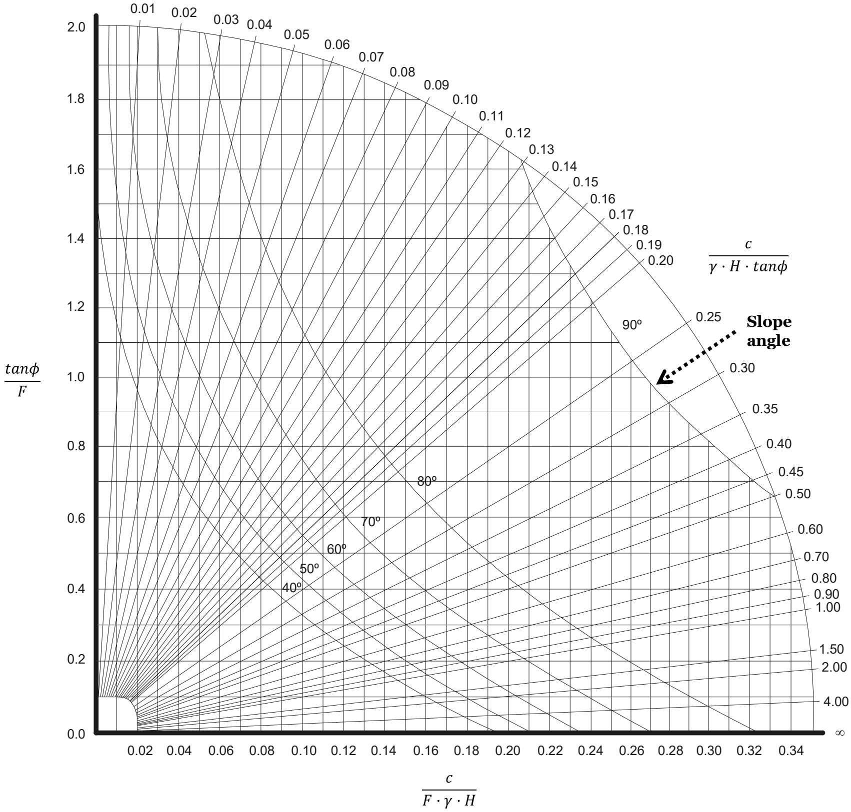

Groundwater flow conditions

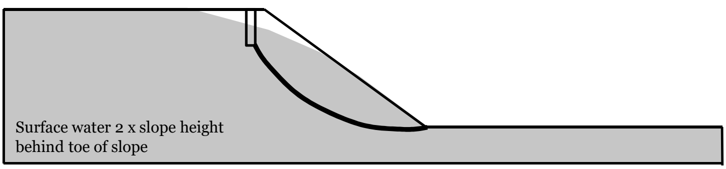

Source: Modified from Hoek & Bray (1981)

Fig. 2.11. Hoek & Bray chart no. 4. Groundwater flow conditions for applying this chart are shown below it

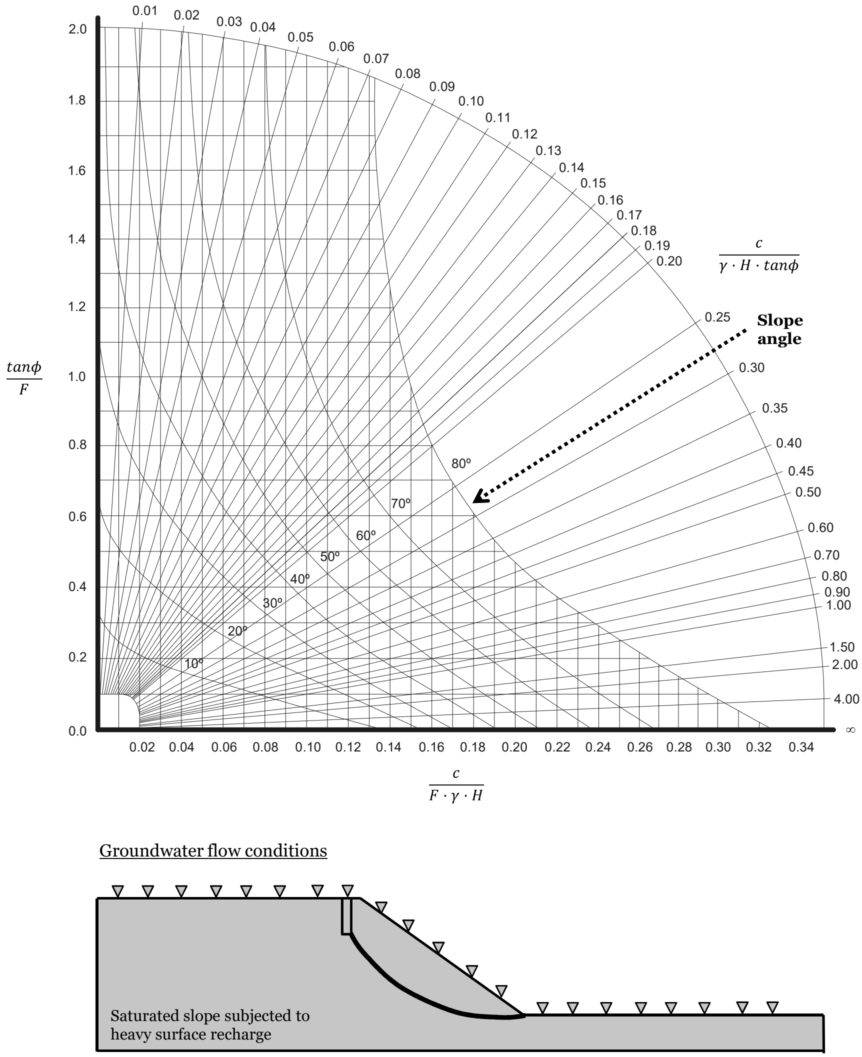

Source: Modified from Hoek & Bray (1981)

Fig. 2.12. Hoek & Bray chart no. 5. Groundwater flow conditions for applying this chart are shown below it

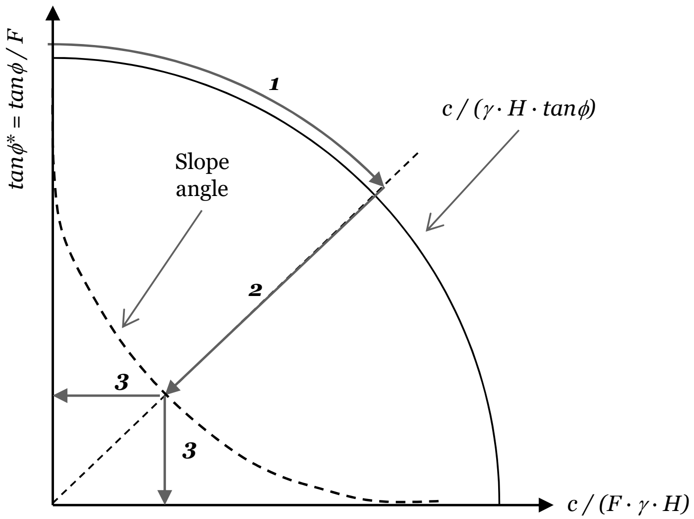

Source: Adapted from Hoek & Bray (1981)

Fig. 2.13. Use of a Hoek & Bray chart.

2.5. The Method of Slices

2.5.1. Generalities

The method of slices is a limit equilibrium method in which the potentially unstable soil mass is divided, for calculation purposes, into a series of vertical slices. The slices are considered rigid solids and a balance of forces is established at each slice. This method is the most common one used today to analyze the stability of soil slopes.

The method of slices makes three main assumptions:

- The soil failure is governed by the Mohr-Coulomb criterion.
- The static balance must be fulfilled at each slice.
- There are no forces or stresses inside each slice.

The existence of anchors or similar stabilization measures, as well as water thrusts, tension cracks and any exterior force like the seismic action, can also be considered just by directly introducing all these aspects as forces in the static balance. Besides, the method can be applied to heterogeneous grounds by appropriately choosing the number and location of the different slices.

As any limit equilibrium method, the objective of the method of slices is obtaining the safety factor of the soil slope defined as the ratio of the resisting forces to the driving forces. However, when the static balance of forces (horizontal forces, vertical forces and moments) is established at each slice, a statically indeterminate problem occurs.

Therefore, the method needs assuming some additional hypotheses, which leads to having different solution procedures (Ortuño, 1992; Alonso Pérez de Ágreda, 2005; González de Vallejo & Ferrer, 2011).

2.5.2. Fellenius' Method

Fellenius' method (1927) considers the static balance of moments and perpendicular forces to the base of each slice, neglecting the balance of horizontal forces. Following the scheme showed in Fig. 2.14, the static balance of moments applied to all slices leads to:

$$\sum W \cdot d = \sum S_m \cdot R$$ **Equation 2.32**

Where *W* is the weight of the soil slice; *d* is the lever arm of *W* with respect to the center of gravity of the soil slice; S_m is the maximum tangential force that can be developed at the failure surface (base of the slice); and *R* is the failure circle radius.

An inspection of the geometry of the problem results in the relationship:

$$d = R \cdot \sin\alpha$$ **Equation 2.33**

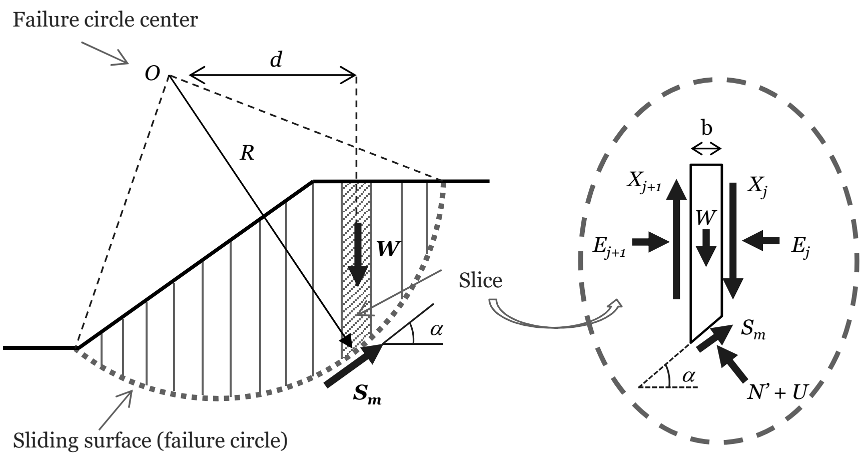

Source: Self-elaboration

Fig. 2.14. Fellenius' method general scheme.

Where *α* is the angle of the slice base. Therefore:

$$\sum W \cdot d = \sum S_m \cdot R \rightarrow \sum S_m = \frac{R}{\sum W \cdot d} = \frac{R}{\sum W \cdot R \cdot \sin\alpha} = \frac{1}{\sum W \cdot \sin\alpha} \qquad \textbf{Equation 2.34}$$

Assuming the Mohr-Coulomb failure criterion, the maximum tangential force S_m developed at the failure surface for a safety factor *F* is equal to (see Eqs. 3.3 and 3.4):

$$S_m = \frac{c' \cdot b}{F} + \frac{N' \cdot \tan\phi'}{F} \qquad \textbf{Equation 2.35}$$

Where *c′* is the effective soil cohesion; *b* is the slice thickness; *N′* is the effective normal force to the failure surface; and *ϕ′* is the effective soil friction angle.

Considering that tangential force at each slice, Eq. 2.32 may be written as:

$$\sum\left(\frac{c' \cdot b}{F} + \frac{N' \cdot \tan\phi'}{F}\right) = \frac{1}{\sum W \cdot \sin\alpha} \qquad \textbf{Equation 2.36}$$

The static balance of perpendicular forces to the base of the slice (i.e. in the direction corresponding to force *N′*) may be established as:

$$N' + U = \left(W + X_j - X_{j+1}\right) \cdot \cos\alpha - \left(E_j - E_{j+1}\right) \cdot \sin\alpha \qquad \textbf{Equation 2.37}$$

Where *U* is the water force due to pore pressures at the failure surface at the slice; E_j and E_{j+1} are the earth thrusts at each side of the slice; and X_j and X_{j+1} are the tangential forces at the each of the edges of the slice (note that both *E* and *X* forces are the reactions of the adjacent slices on the slice under study).

If both earth thrusts and tangential forces at each sides of a slice are equal, the previous expression leads to:

$$N' + U = W \cdot \cos\alpha \rightarrow N' = W \cdot \cos\alpha - U \qquad \textbf{Equation 2.38}$$

From that point, considering Eqs. 3.36 and 3.38 and making some mathematical arrangements, the Fellenius' method safety factor expression is obtained:

$$F = \frac{1}{\sum W \cdot \sin\alpha} \sum\left(c' \cdot b + \left(W \cdot \cos\alpha - U\right) \cdot \tan\phi'\right) \qquad \textbf{Equation 2.39}$$

Fellenius' method does not verify the balance of forces in the sliding direction and tends to overestimate the value of the safety factor, not being common its use as a final calculation method. However, it can be used to estimate the value of the safety factor and it is normally applied for setting a starting point for other iterative methods.

2.5.3. Bishop's Method

Bishop's method (1955, 1967) follows a similar development as the Fellenius' method, establishing the static balance of moments, but instead of using the static balance of perpendicular forces to the base of the slice, the Bishop's method establishes the static balance of vertical forces. Thus, the complementary equation to the static balance of moments (Eq. 2.32) is:

$$N' + U \cdot \cos\alpha + S_m \cdot \sin\alpha = W + \left(X_j - X_{j+1}\right) \qquad \textbf{Equation 2.40}$$

Considering the Mohr-Coulomb failure criterion in similar way as was made for the Fellenius' method, the value of *N'* can be obtained as:

$$N' = \frac{W + \left(X_j - X_{j+1}\right) - \left(U \cdot \cos\alpha + \dfrac{c' \cdot b}{F} \cdot \sin\alpha\right)}{\cos\alpha + \dfrac{\tan\phi'}{F} \cdot \sin\alpha} \qquad \textbf{Equation 2.41}$$

And from this point, the static equilibrium of moments can be solved. After some mathematical arrangements, the Bishop's method safety factor expression is obtained:

$$F = \frac{1}{\sum W \cdot \sin\alpha} \sum \left[\frac{c' \cdot b + \left(W - U \cdot \cos\alpha + \left(X_j - X_{j+1}\right)\right) \cdot \tan\phi'}{\cos\alpha \cdot \left(1 + \dfrac{\tan\phi'}{F} \cdot \tan\alpha\right)} \right] \qquad \textbf{Equation 2.42}$$

The previous expression corresponds to the *rigorous Bishop's method* and needs setting the value of forces X_j and X_{j+1}. Bishop himself showed that the safety factor is not sensitive to the value of such forces and recommended to consider the hypothesis $X_j = X_{j+1}$. As a result, the safety factor for the *simplified Bishop's method* is obtained:

$$F = \frac{1}{\sum W \cdot \sin\alpha} \sum \left[\frac{c' \cdot b + \left(W - U \cdot \cos\alpha\right) \cdot \tan\phi'}{\cos\alpha \cdot \left(1 + \dfrac{\tan\phi'}{F} \cdot \tan\alpha\right)} \right] \qquad \textbf{Equation 2.43}$$

In the Bishop's method (both rigorous and simplified) the safety factor *F* is implicit in the expression, so an iterative process is required and a first value is needed to start the calculation. That starting value is usually the one obtained by the Fellenius' method.

The simplified Bishop's method provides results of low errors and can be adapted to unconventional geometries and heterogeneous soils. However, it does not verify the balance of forces in the sliding and horizontal direction. Anyway, this method is the most common one used for analyzing the stability of soil slopes.

2.5.4. Janbu's Method

Janbu's method (1954) has a similar mathematical development as the Bishop's method, but it establishes both static balance of forces in the horizontal direction and the vertical direction, thus neglecting the moment balance.

The Janbu's method safety factor expression is given by:

$$F = \frac{1}{\sum\left(W + \left(X_j - X_{j+1}\right)\right)\cdot \tan\alpha} \sum \left[\frac{c'\cdot b + \left(W - U + \left(X_j - X_{j+1}\right)\right)\cdot \tan\phi'}{1 + \frac{\tan\phi'}{F}\cdot \tan\alpha} \cos^2\alpha \right]$$

Equation 2.44

This expression corresponds to the *rigorous Janbu's method*; if hypothesis $X_j = X_{j+1}$ is considered, the *simplified Janbu's method* is obtained:

$$F = \frac{1}{\sum W \cdot \tan\alpha} \sum \left[\frac{c'\cdot b + \left(W - U\right)\cdot \tan\phi'}{1 + \frac{\tan\phi'}{F}\cdot \tan\alpha} \cos^2\alpha \right]$$

Equation 2.45

The safety factor is also implicit in the Janbu's method, so both an iterative process is required to compute it and a starting value of *F* is needed (normally obtained using the Fellenius' method). Janbu's method does not verify the static balance of moments but unlike Bishop's or Fellenius' methods, Janbu's method is especially suitable for studying failures where the depth/length ratio is low (planar failures).

2.5.5. Exact Methods

Exact methods are a group of methods in which all equilibrium equations are satisfied, thus leading to using different hypotheses to solve the statically indeterminate problem. These methods are more accurate than the other methods but they are also more complex and more expensive in computational terms.

Even though they are not as common as Bishop's and Janbu's methods, exact methods should be used when one of the forces acting on the slope under study is the seismic action.

Two exact methods that are usually used are:

- Morgenstern – Price' method (1965): this method can be applied to any failure surface (not only a circular failure) and establishes the stability problem using the three equilibrium conditions in slices of differential thickness. The method assumes that the inclination of the forces between slices is $\lambda \cdot f(x)$, where λ is a scale factor and $f(x)$ a given function (Alonso Pérez de Ágreda, 2005).
- Spencer's method (1967): this method can be applied to circular failures, fulfills both the balance of horizontal forces and moments and assumes that the inclination of the forces between slices is equal to a given constant value, which is also an unknown to find by solving the equilibrium (Alonso Pérez de Ágreda, 2005).

2.5.6. Grid of Centers

The method of slices following any of the procedures seen is applied for an assumed failure circle defined by a given center and radius. However, many other failure circles may exist and the critical circle producing the instability of the slope is unknown.

Therefore, different possible failure circles must be considered, the method of the slices applied and the corresponding safety factor obtained. This is normally done in a standardize way by defining a grid of centers, computing the safety factor for the corresponding failure circle at each center.

Ideally, the minimum value of safety factor obtained will correspond to the critical failure surface and this will be the safety factor of the slope. Clearly, the higher the resolution of the grid (i.e. more possible centers), the greater the accuracy of the safety factor of the slope obtained, but the calculation cost also increases.

The normal approach normally followed consists of selecting a medium resolution grid and once computed the different safety factors for each proposed center, tracing the isovalues (lines with the same value of the safety factor) at the grid. The safety factor of the slope will be located in the "valley" corresponding to the lowest safety factor.

It is important to mention that when conducting this process, the resulting safety factor of the slope (i.e. the minimum value of the safety factors) must always be located in the central area of the grid of centers defined. Otherwise the calculation may not be correct, as possible failure circles with lower safety factors may have been ignored.

Chapter 3
Slope Stability in Rocks

3.1. Introduction

The stability of a slope in a rock mass is fundamentally a geometrical problem related to the orientation of the slope under study and the structural configuration of the discontinuities of the rock mass. Besides rockfalls and depending on the previous aspects, rock slopes can develop three main types of instabilities: planar failures, wedge failures and toppling failures.

The study of the instability in rock slopes is a process that usually involves two stages:

- Firstly, a kinematic analysis is carried out to verify if a series of kinematic and mechanical conditions are fulfilled in the rock slope for triggering one or more instabilities; this analysis is normally conducted with the help of the stereographic projection.
- Secondly, if the kinematic analysis identifies that one or more instabilities can appear in a rock slope, a stability analysis is conducted to verify the stability of the slope and quantify its safety (and/or decide the use of corrective measures).

The potential instability problem in a rock slope must never be underestimated. Although apparently rocks are “strong” materials that can resist “anything”, historical events have shown this argument to be false. The most notorious accident occurred at Vaiont dam (Italy), where on October 1963 a huge landslide poured 270 million cubic meters at 110 km/h into the reservoir, resulting in a wave that over topped the dam by 250 m and swept onto the valley below, with the loss of about 2500 lives.

3.2. General Aspects

3.2.1. The Rock Mass: Intact Rock and Discontinuities

Rocks are natural hard and compact materials composed of mineral particles with strong cohesive bonds. Unlike soils, rocks have a very variable composition and characteristics. They are heterogeneous and anisotropic materials and are affected by geological and environmental processes that give rise to fracturing and weathering.

Geologically, rocks are classified in three main groups: sedimentary rocks (e.g. sandstone and limestone), igneous rocks (e.g. granite and basalt) and metamorphic rocks (e.g. slate and gneiss). In Structural Geology and Rock Mechanics what is usually addressed as “rock” is called *intact rock*, and refers to the raw material, i.e. fragments or blocks which can be tested in laboratory. In their natural state, rocks almost never appear as big masses of intact rock, but they are affected by a series of *discontinuities* which cause their individualization in blocks. The result of composing both the intact rock and their discontinuities conforms the *rock mass*.

The mechanical behavior of a rock mass is governed by their discontinuities and the number of sets. The greater the number of sets and the smaller the size of the rock blocks, the greater the probability of them to rotate, move and break. Fig. 3.1 shows examples of discontinuities in the rock mass. Discontinuities may be classified according to their origin and characteristics as (the typical symbol associated with each type is shown in brackets):

- *Stratification or bedding planes* (S_0): depositional surfaces generally associated with a lithological change, typical of sedimentary rocks.
- *Schistosity or foliation planes* (S_1, S_2 ...): deformational surfaces, perpendicular to the main stress direction, generally associated with metamorphic rocks.
- *Joints* (J_1, J_2 ...): surfaces of tectonic origin that correspond to fragile failure surfaces, along which no displacement is visible.
- *Faults* (F_1, F_2 ...): surfaces of tectonic origin where relative displacement between the two lips occurs.

Discontinuities are described based on their orientation, spacing, persistence, roughness, aperture, filling and seepage (ISMR 1981, 2007, 2014), while their mechanical behavior is normally defined by cohesion and friction angle. For addressing a rock slope stability analysis, the most important features are orientation and shear strength:

- Orientation: corresponds to the spatial arrangement of the discontinuity; in Geotechnical Engineering planes are spatially positioned by their dip vector, i.e. by means of *dip direction* and *dip* (Fig. 3.2):
    - Dip vector: the vector that has the direction of the line of maximum slope of the plane and towards the descending direction.

Source: Taken from Torrijo *et al.* (2020)

Fig. 3.1. Stratification or bedding planes and presence of a fault (crossing approximately diagonal from top right to bottom left).

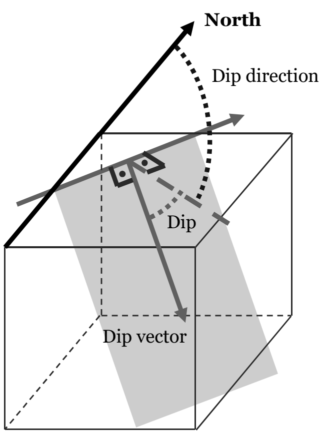

Source: Self-elaboration

Fig. 3.2. Dip vector, dip direction and dip of a plane.

- Dip direction: angle formed by the horizontal projection of the dip vector with the north, measured from the north and clockwise.
- Dip: angle formed by the dip vector with its horizontal projection.

The generic notation α / β is normally used for define a dip vector, where α is the dip direction given by three digits, from 000 to 360 and measured from the north clockwise and with the dip vector pointing downwards; and β is the dip, given by two digits, from 00 to 90. The degree symbol (º) is normally omitted.

- Shear strength: normally cohesion is neglected so all the shear strength of a discontinuity is reduced to the friction angle, ϕ. This parameter may be obtained conducting a direct shear test (by a cutting box or Hoek cell), but for slope stability analyses is usually obtained on field by performing in situ "tilt tests" on materials extracted directly from the discontinuities.

Intersection of two or more discontinuity planes produces a line called *intersection line*. Orientation of lines is given by their vector, defined by two components: *trend* and *plunge*. The former is the angle to the north of the projection of the line vector in the horizontal plane (equivalent to the dip direction of a plane) while the latter is the angle formed by the line with the horizontal plane (equivalent to the dip of a plane). Notation β / α is used to define the orientation of a line, where α is the trend of the line (from 000 to 360) and β is its plunge (from 00 to 90). In essence, lines are defined the same as planes, but with their plunge ("dip") before the trend ("dip direction") to indicate that the element is a line.

3.2.2. Stereographic Projection

The stereographic projection is a technique used to solve geometric problems in Structural Geology and Geotechnical Engineering (Goodman 1976; Hoek & Brown 1980; Hoek & Bray 1981). While an orthographic projection (e.g. topographic maps) preserves spatial relationships, a stereographic projection only preserves relative positions and angular relationships. That makes stereographic projection a very powerful tool for the analysis of rock slopes where the stability is governed by the orientation and relative position of the discontinuities and the slope under study.

The stereographic projection is a type of azimuthal projection obtained by intersecting lines and planes with the surface of a sphere (with all lines and planes passing through the center of it) and then projecting such intersection onto the equatorial plane. A line intersects the surface of the sphere at two diametrically opposite points, producing a point in stereographic projection, while a plane intersect the surface of the sphere generating a circle, which result in a curve line in stereographic projection.

The stereographic projection reduces a 3D geometry to a 2D one, so that planes are represented as circular lines, called *plane traces*, and lines as points. The result of plotting lines and planes in of stereographic projection is called *stereogram*. When using this type of projection, both the location of the elements and the distance between them is out of interest. Their relative position is the key.

In Structural Geology and Geotechnical Engineering the hemisphere of the sphere used to intersect lines and planes is the lower hemisphere as seen in Fig. 3.3. The intersection of the equatorial plane (projection plane) with the sphere is called the *primitive circle* and has the same radius as the original projection sphere, so any point on the surface of the lower hemisphere must always be plotted within the primitive circle.

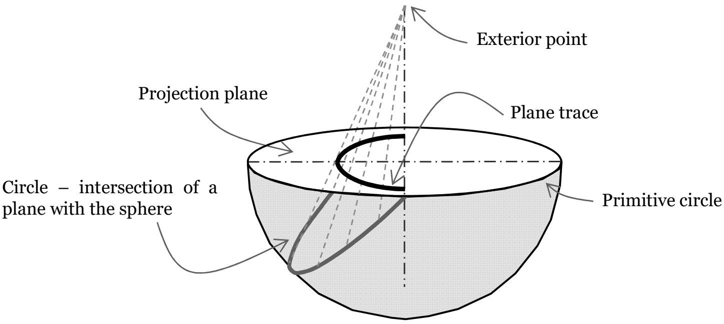

Source: Self-elaboration

Fig. 3.3. Stereographic projection.

3.2.3. Planes Poles and Discontinuities Sets

Information about the discontinuities of a rock mass is gathered by performing *geomechanical stations* (Torrijo et al. 2020). At each geomechanical station the orientation of the different discontinuities observed is recorded and plotted in stereographic projection, resulting in a stereogram (Fig. 3.4). Such amount of graphical information may be reduced by replacing plane traces by their *poles*.

In stereographic projection, the pole corresponds to the normal vector to a plane. As any plane is uniquely defined by its dip vector, a normal line can be drawn to that plane, also being unique: the normal to a plane (the pole in stereographic projection) completely define the plane. Thus, planes can be reduced to lines, i.e. plane traces can be transformed into points.

In rock masses, discontinuities usually appear as sets that share the same type, similar orientation and analogous mechanical characteristics, with the exception of faults which commonly appear alone. Therefore it is possible to group the discontinuities in sets. This is normally done by grouping the poles according to their “density” in the stereogram.

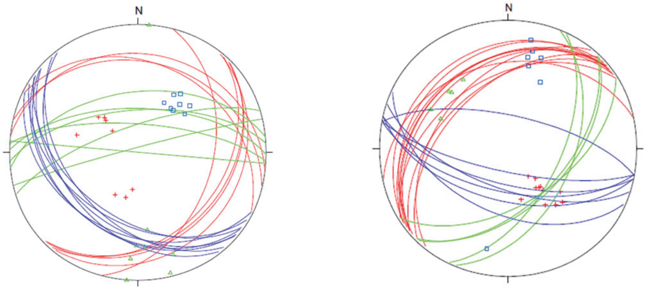

Source: Self-elaboration

Fig. 3.4. Example of two stereograms representing two geomechanical stations (note that the poles of the different planes are also plotted).

A simple statistical rule considers significant any pole concentration higher than 6%, so it defines a set of discontinuities. Isolated poles are usually related to faults. However, if there are isolated poles or zones of poles with a density less than 6% and those are associated to joints, schistosity or stratification, data may be considered anomalous, since these types of discontinuities never appear alone. This may be put down to errors like mistakes in the transcription to the geomechancial station (therefore those points should be removed) or may indicate the need to extend the investigation of the rock mass (some sets of discontinuities may not have been clearly detected).

Once the poles of the rock mass are grouped in sets, a characteristic pole is defined for each set (usually taken as a point located in the center of densities and it does not need to be a “true” pole) and the equivalent plane to that pole may be plotted, representing the corresponding discontinuity set.

3.2.4. Instabilities in a Rock Slope

The most common rock slope instabilities are rockfalls, topples, translational slides and rotational slides.

Rockfalls (fall of masses of rock detached from the rock mass which descend mostly through air by free fall) present an intrinsic arbitrariness that makes its calculation relatively complex and makes it difficult to predict in which area of the slope the rockfall will take place and consequences will arise (e.g. collisions, bouncings and rollings). The work of Ritchie (1963) provides a series of charts to design toe ditches (*Ritchie ditches*) capable of containing the rocks detached from a rock mass given the angle and height of the slope. However, for more in depth analyses, statistical simulation programs are used. Rockfalls analyses are beyond the scope of this work.

Rotational slides in rock masses only occur in highly fractured rock masses or when the intact rock has of very low strength (e.g. marls and flysch materials). The analysis and calculation of these instabilities is carried out considering the rocky material a soil-type material and applying the common methods used for analyzing soil slopes seen in ***Chapter 2***. The values of the shear parameters c and ϕ needed to use such methods may be obtained following the indications given in ***Chapter 5*** for highly fractured rock masses. Thus, rotational slides in rock masses may be solved using classical methods like the Petterson's circle, the method of slices (Bishop method, Janbu method, Morgerstern-Price method or Spence method) as well as Taylor (1937, 1948) and Hoek & Bray (1981) charts. The latter, showed in Figs. 2.8 – 2.12, are particularly suitable to use in preliminary phases, as Hoek & Bray charts where developed for highly rock masses, although later their use was extended to soils.

Topples and translational slides (due to either *planar failures* or *wedge failures*) are the most common instabilities of rock slopes. Addressing the stability of a rock slope against planar failures, wedge failures and toppling failures requires a process which is divided into two parts:

- Kinematic analysis: the orientations of the discontinuities must fulfill a series of geometric and mechanical requirement in relation to the slope under study. Otherwise, the instability cannot occur. The kinematic analysis (Piteau & Peckover, 1978) establishes those discontinuities potentially problematic for the slope considered and is usually carried out using stereographic projection.
- Stability analysis: if the kinematic analysis establishes the existence of some potential instability in a slope, a slope stability analysis is carried out to define the level of safety of the slope considered, the need of introducing corrective measures or the performance of such measures. This analysis is conducted by:
    - Limit equilibrium methods: they are exclusively based on the static balance of forces, defining the equilibrium state of the unstable mass, and do not take into account the ground deformations. The objective of limit equilibrium methods is comparing the forces that oppose to the instability to the forces causing it, thus obtaining a safety factor.
    - Stress-strain methods: these methods consider ground deformations in addition to the balance of forces. They are the most complete calculation methods but require the use of advanced numerical procedures such as finite elements modeling (see ***Chapter 5***).

The following sections deal with the kinematic and stability analysis by limit equilibrium methods of planar failures, wedge failures and toppling failures. As rock masses may have various sets of discontinuities, their interaction with slopes under study may result in the potential activation of one or more instabilities. Thus, in the analysis of a slope, each type of failure must always be studied separately and independently, evaluating the kinematic conditions for each one of them and conducting the corresponding stability analysis if any potential instability is detected.

3.3. Planar Failures

3.3.1. Definition

Planar failures occur when part of a rock mass slides on a single discontinuity plane that daylights (i.e. appears) on the slope (Fig. 3.5). In a planar failure, both the sliding mass and the rest of the rock mass are continuously in contact, so the movement of the unstable mass is governed by the angle and the roughness of the discontinuity plane that triggers the unstable mechanism.

Planar failures are typical of rock masses formed by stratified sedimentary rock formations, where that type of failure is associated with the bedding planes. It is also common of metamorphic rock formations like slate and shale, where schistosity creates natural weakness planes of small roughness which are prone to cause a planar failure.

The amount of unstable material involved in a planar failure may largely vary from a few cubic meters to great landslides covering entire mountains.

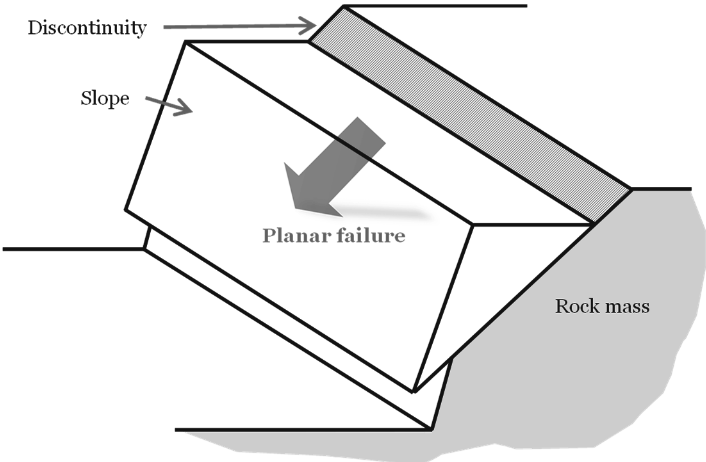

Source: Modified from Hoek & Bray (1981)

Fig. 3.5. Planar failure general scheme.

3.3.2. Kinematic Conditions

Geometrically, the occurrence of a planar failure depends on the orientation of the discontinuity to the one of the slope, as well as on the dip of the discontinuities to the one of the slope. Mechanically, sliding can only take place if the friction force in the sliding plane is exceeded.

The structural conditions required for planar failures to take place are three (Hoek & Bray, 1981; Norrish & Wyllie, 1996a):

- The dip direction of the discontinuity (assimilated to a plane) must be approximately parallel to the dip direction of the slope. Commonly, the term "approximately parallel" considers that the difference between the discontinuity dip direction and the slope dip direction is found within a range of ± 20º.
- The dip of the discontinuity (β_{disc}) must be less than the dip of the slope (β_{slope}) so that the discontinuity must daylight on the surface of the slope.
- The dip of the discontinuity (β_{disc}) must be greater than the friction angle (ϕ) of the sliding plane (the friction angle of the discontinuity is normally taken).

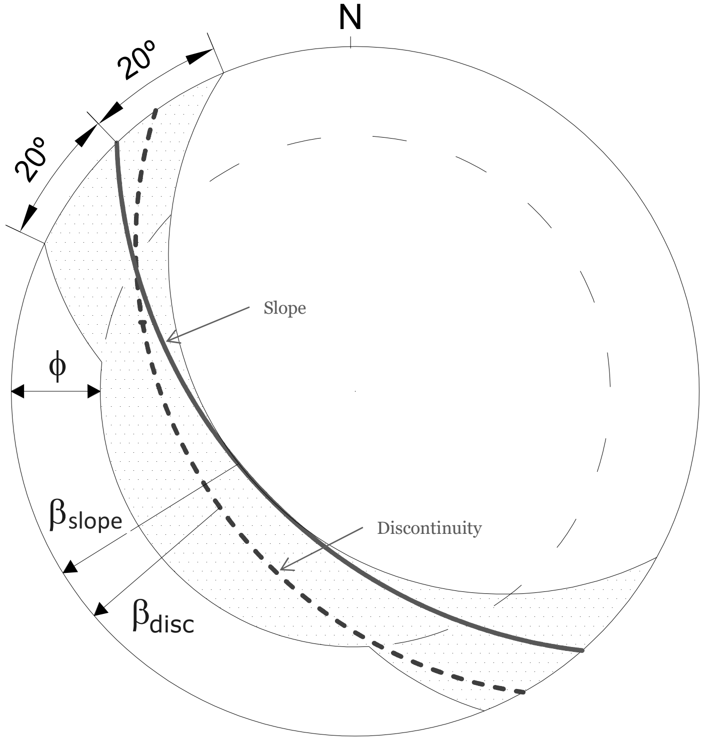

Any discontinuity that falls within the shaded area has a potential risk of planar failure, i.e. fulfills all the structural conditions:

- Dip direction of the discontinuity = dip direction of the slope ± 20º
- Dip of discontinuity (β_{disc}) < dip of the slope (β_{slope})
- Dip of discontinuity (β_{disc}) > sliding plane (discontinuity) friction angle (ϕ)

Source: Adapted from Hoek & Bray (1981)

Fig. 3.6. Kinematic analysis of the stability of a rock slope due to a planar failure.

This kinematic analysis must be carried out independently for each discontinuity (or set of discontinuities) and each slope under study. Additionally, a planar failure needs the existence of “release surfaces” to occur, i.e. lateral joints or tensile cracks which enable that part of the rock mass can slide and separate from the rest of it.

The three previous structural conditions can be evaluated graphically using stereographic projection as shown in Fig. 3.6. The existence of release surfaces can also be observed in the representation of the rock mass structure in a stereogram.

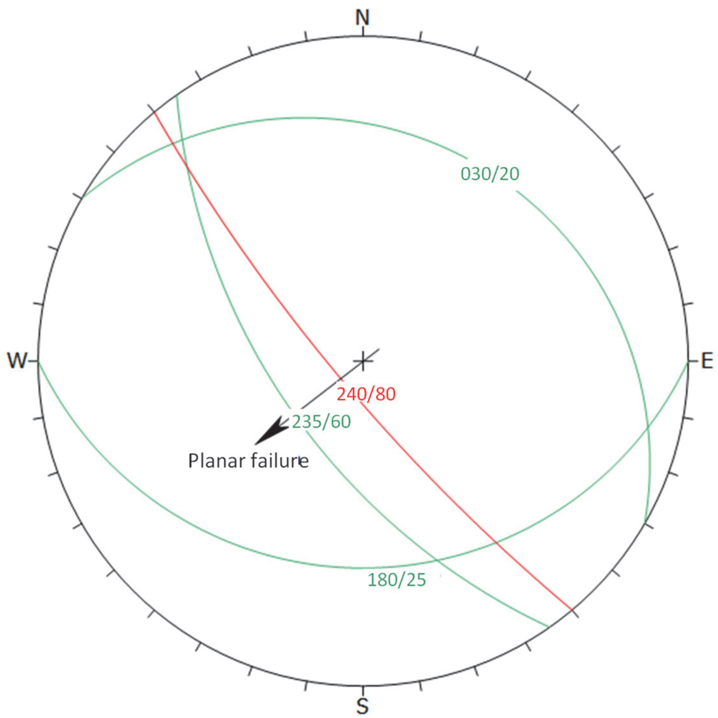

- Rock mass defined by three joint sets (in green) with orientations (dip direction / dip): 180/25, 235/60, 030/20
- A slope with orientation 240/80 (in red) is planned to be built
- The friction angle of the discontinuities is considered to be 20º
- Joint set defined by orientation 235/60 represents a potential risk of planar failure (fulfills all the structural conditions)

Source: Self-elaboration

Fig. 3.7. Analysis of the possibility of planar failures.

Fig. 3.7 shows an example of a potential planar failure in a rock mass where a slope is planned to be built. The case is presented making use of the stereographic projection. The rock mass is defined by three joint sets (in green) with orientations (dip direction/dip): 180/25, 235/60 and 030/20. Joints friction angle is assumed equal to 20º. The slope (in red) is defined by the orientation 240/80.

As can be observed, the joint sets 180/25 and 030/20 cannot cause a planar failure since the dip direction of the slope and those of the joint sets are not parallel: the difference between the dip directions of the joint sets and the slope face is greater than 20º in both cases (240 – 180 = 60º for the first set and 240 – 30 = 210º for the second set). However, the joint set defined by orientation 235/60 represents a potential risk of planar failure as the three required kinematic conditions are fulfilled:

- The joint set dip direction (235º) is within the range ± 20º to the slope dip direction (240º).
- The joint set dip (60º) is lower than the slope dip (80º).
- The joint set dip (60º) is greater than the sliding plane friction angle (20º).

Besides, the stereographic projection shows that this joint set is intersected by other discontinuities (in fact it is intersected by the others two joint sets). These intersections define the release surfaces required for the occurrence of the planar failure.

3.3.3. Safety Factor Calculation

The safety factor of a rock slope due to a planar failure can be obtained following limit equilibrium methods (Hoek & Bray, 1981; Giani, 1992; Norrish & Wyllie, 1996a) by establishing the forces acting perpendicular and parallel to the potential failure surface and solving the system. Forces include the self-weight of the unstable mass, the effects of the pore pressures, the shear strength at the failure surface and the influence of external forces (e.g reinforcing elements or seismic accelerations). Shear strength is computed following the Mohr-Coulomb criterion, considering that this strength is completely developed along the sliding surface.

Although calculations can be carried out in two or three dimensions, the most common approach is to assimilate the problem to a plane strain case and solve it in two dimensions, considering a unit thickness of the slope. Besides, all point forces are commonly assumed to pass through the center of gravity of the sliding mass so that moments are ignored and no toppling can occur.

For addressing the stability analysis of planar failures, the existence of a tension crack in the slope should be taken into account. Two cases are defined: (i) tension crack located in the slope face and (ii) tension crack located in the upper slope surface. The approximate location of the tension crack on the ground can be predicted in most real cases by conducting field studies of small-scale movements. This makes it possible to apply the appropriate case of the previous two, and also fix the horizontal distance from the crest of the slope to the location of the tension crack.

Pore pressures are commonly considered by a simplified model consisting of assuming a certain depth of water (z_w) in the tension crack and defining a phreatic surface that decreases linearly towards the slope and exits at the toe of the slope.

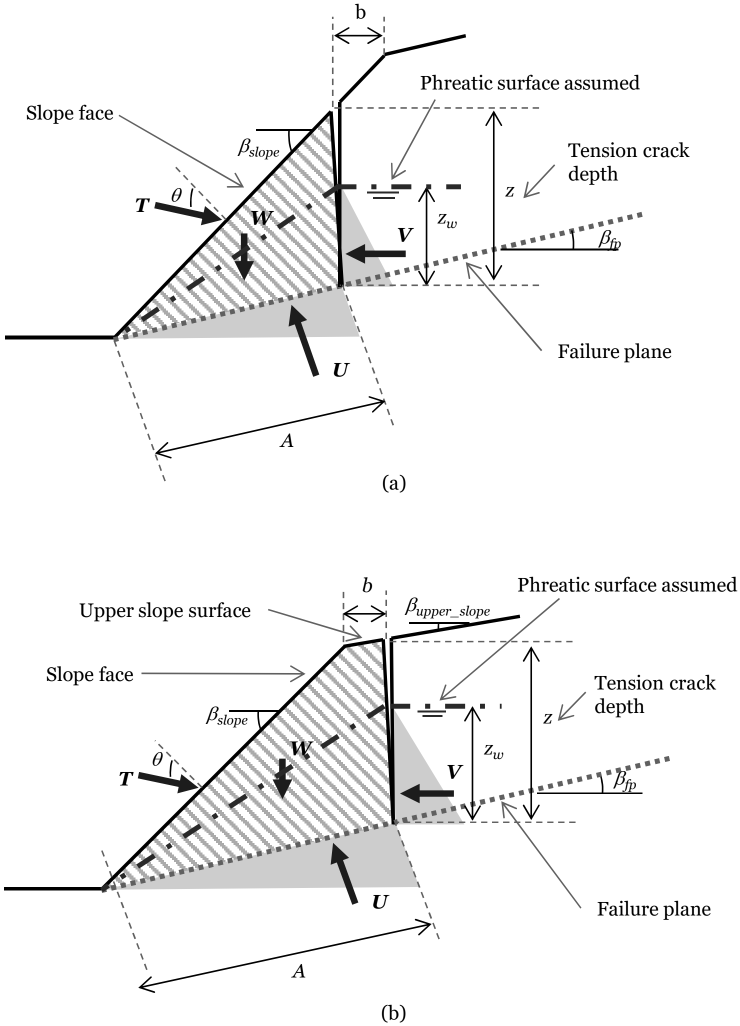

Source: Modified from Hoek & Bray (1981)

Fig. 3.8. Planar failure calculation scheme: (a) tension crack located in the slope face; (b) tension crack located in the upper slope surface.

Taking into account the previous hypothesis and considering the schemes of forces showed in Fig. 3.8, the safety factor of a rock slope due to a planar failure *F*, defined as the ratio between the resisting forces and the driving forces, may be written as:

$$F = \frac{c \cdot A + W \cdot \left[\left(\cos\beta_{fp} - a \cdot \cos\beta_{fp}\right) - U - V \cdot \sin\beta_{fp} + T \cdot \cos\theta\right] \cdot \tan\phi}{W \cdot \left(\sin\beta_{fp} - a \cdot \sin\beta_{fp}\right) + V \cdot \cos\beta_{fp} - T \cdot \sin\theta} \quad \textbf{Equation 3.1}$$

Where c and ϕ are the cohesion and the friction angle of the failure plane (discontinuity that produces the sliding); A is the failure plane length; W is the weight of the unstable mass; U and V are the pore pressure forces, the former being the uplift water force (normal direction to the sliding plane) and the latter the driving water force (tangential direction to the sliding plane); β_{fp} is the failure plane dip; a is the possible horizontal acceleration due to blasting or an earthquake acting at the slope; and T is the possible exterior force opposed to the sliding (e.g. the force introduced by a bolt or an anchor) which is tilted an angle θ with respect to the orthogonal direction to the slope face. Note that an exterior force which is a driving force must be introduced as negative.

The values of W and A depend on the location of the tension crack. For a tension crack located in the slope face:

$$W = \frac{1}{2} \cdot \gamma \cdot H^2 \cdot \left[\left(1 - \frac{z}{H}\right)^2 \cdot \cot\beta_{fp} \cdot \left(\cot\beta_{fp} \cdot \cot\beta_{slope} - 1\right)\right] \quad \textbf{Equation 3.2}$$

$$A = \left(H \cdot \cot\beta_{slope} - b\right) \cdot \sec\beta_{fp} \quad \textbf{Equation 3.3}$$

Where γ is the unit weight of the intact rock; H is the height of the slope face; b is the horizontal distance from the crest of the slope to the location of the tension crack; β_{slope} is the slope dip; and z is the depth of the tension crack, computed as:

$$z = \left(H \cdot \cot\beta_{slope} - b\right) \cdot \left(\tan\beta_{slope} - \tan\beta_{fp}\right) \quad \textbf{Equation 3.4}$$

For a tension crack located in the upper slope surface:

$$W = \frac{1}{2} \cdot \gamma \cdot \left[H^2 \cdot \cot\beta_{slope} \cdot X + b \cdot H \cdot X + b \cdot z\right];\ X = 1 - \tan\beta_{fp} \cdot \cot\beta_{slope} \quad \textbf{Equation 3.5}$$

$$A = \left(H \cdot \cot\beta_{slope} + b\right) \cdot \sec\beta_{fp} \quad \textbf{Equation 3.6}$$

And the depth of the tension crack (z) may be computed in this case as:

$$z = H + b \cdot \tan \beta_{upper\_slope} - \left(b + H \cdot \cot \beta_{slope}\right) \cdot \tan \beta_{fp}$$ **Equation 3.7**

Both for the case of a tension crack located in the slope face or in the upper slope surface, the values for water forces U and V are equal to:

$$U = \frac{1}{2} \cdot \gamma_w \cdot z_w \cdot A$$ **Equation 3.8**

$$V = \frac{1}{2} \cdot \gamma_w \cdot z_w^2$$ **Equation 3.9**

Where γ_w is the water unit weight and z_w the phreatic surface depth in the tension crack.

It is interesting to note that the equation obtained for the safety factor (Eq. 3.1) applied to a dried rock mass ($U = V = 0$) without any reinforcing element ($T = 0$), no seismic action ($a = 0$) and neglecting the discontinuity cohesion ($c = 0$) is reduced to:

$$F = \tan \phi / \tan \beta_{fp}$$ **Equation 3.10**

In this case, $F = 1$ when the discontinuity dip (inclination of the failure plane) equals the friction angle.

3.4. Wedge Failures

3.4.1. Definition

Wedge failures occur when part of the rock mass slides along two intersecting discontinuities which dip out of the slope at an oblique angle to the slope face, forming a wedge-shaped block (Fig. 3.9). In a wedge failure, the resulting intersection line always daylights on the slope. The sliding of the wedge-shaped block can occur along the two discontinuities planes simultaneously or along the steeper one. In both cases, a contact edge continuously exists between the sliding mass and the rock mass.

Wedge failures are typical of rock masses with several sets of discontinuities, the size of the wedge (Gonzalez de Vallejo & Ferrer, 2011) being defined by the spacing, orientation and persistence of the sets. Shales, thin-bedded siltstones, claystones, limestones, and slaty lithologies tend to be more prone to wedge failure development than other rock types (Hoek & Bray, 1981). The amount of unstable material involved in a wedge failure may range from a few cubic meters to very large slides with an important potential for destruction.

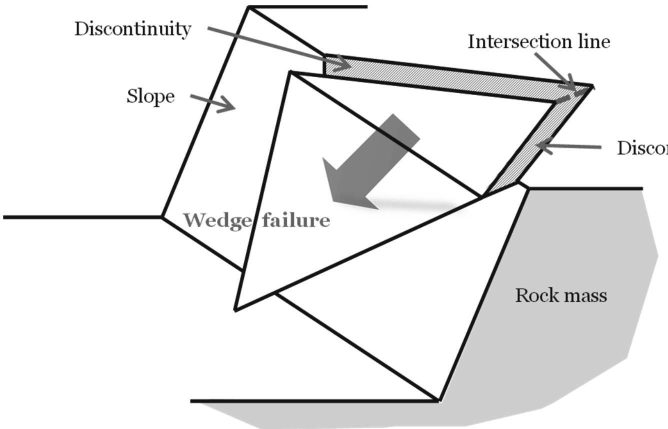

Source: Modified from Hoek & Bray (1981)

Fig. 3.9. Wedge failure general scheme.

3.4.2. Kinematic Conditions

Geometrically, the occurrence of a wedge failure depends on the orientation of the plunge of the intersection lines to the dip of the slope. Mechanically, sliding can only take place if the friction force in the sliding planes defining the wedge is exceeded.

The structural conditions required for wedge failures to take place are three (Hoek & Bray, 1981; Norrish & Wyllie, 1996a):

- The intersection line must daylight on the surface of the slope, so its trend must be "similar" to the slope dip direction, i.e. they should not be opposite one to another.
- The plunge of the intersection line ($\beta_{intersection}$) must be lower than the dip of the slope (β_{slope}).
- The plunge of the intersection line ($\beta_{intersection}$) must be greater than the friction angle (ϕ) of the sliding planes. The friction angle of the two discontinuities that form the unstable wedge must be considered; if these values are significantly different, an average value is taken for the friction angle.

This kinematic analysis must be carried out independently for each intersection line detected (which may result from the interaction of different sets of discontinuities) and for each slope under study, as in a rock mass some of the existing discontinuities may result in a potential wedge failure risk for a given slope.

The three previous structural conditions can be evaluated graphically using stereographic projection as shown in Fig. 3.10. In that case, the last condition can be easily considered: the condition is fulfilled if the point that represents the intersection line falls outside the friction cone. That friction cone is defined as a concentric circle to the primitive circle with a radius equal to the radius of the primitive circle minus the friction angle (ϕ) of the sliding planes. So, all intersection lines which are "inside" that circle are outside the friction cone and therefore fulfill the last condition.

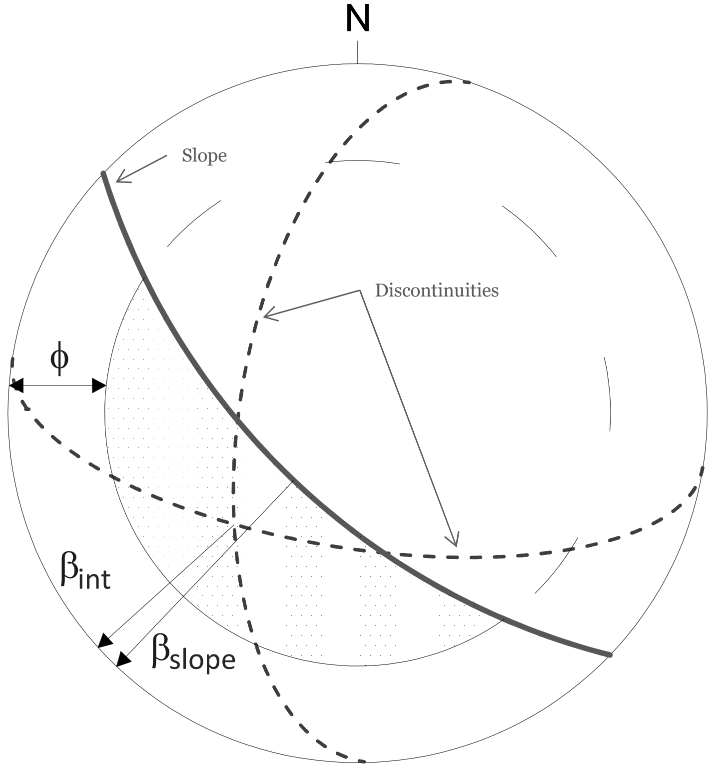

Any intersection that falls within the shaded area has a potential risk of wedge failure, i.e. fulfills all the structural conditions:

- Trend of the intersection line is at the same side as the slope
- Plunge of intersection line (β_{int}) < dip of the slope (β_{slope})
- Plunge of intersection line (β_{int}) > sliding planes (discontinuities) friction angle (ϕ)

Source: Adapted from Hoek & Bray (1981)

Fig. 3.10. Kinematic analysis of the stability of a rock slope due to a wedge failure.

Fig. 3.11 shows an example of a potential wedge failure in a rock mass where a slope is planned to be built. The case is presented making use of the stereographic projection. The rock mass is defined by three joint sets (in green) with orientations (dip direction/dip): 180/25, 235/60 and 030/20. Joints friction angle is assumed equal to 20º. The slope (in red) is defined by the orientation 240/80.

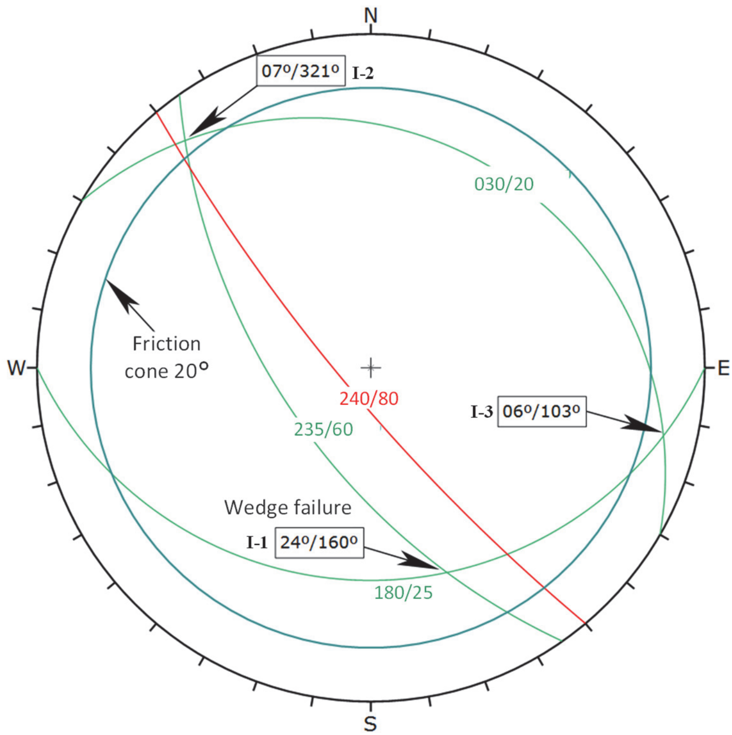

- Rock mass defined by three joint sets (in green) with orientations (dip direction / dip): 180/25, 235/60, 030/20
- A slope with orientation 240/80 (in red) is planned to be built
- The friction angle of the discontinuities is considered to be 20º
- Intersection I-1 (defined by 24/160) represents a potential risk of wedge failure

Source: Self-elaboration

Fig. 3.11. Analysis of the possibility of wedge failures.

As can be observed, the joint sets of the rock mass result in three intersections: 24/160, 07/321 and 06/103, named I-1, I-2 and I-3 hereafter. The trend of intersections I-2 and I-3 is opposed to the slope dip direction so they cannot result in wedge failures. These intersections will never daylight on the slope (they are "behind" the slope). However, the intersection I-1 (defined by 24/160) represents a potential risk of wedge failure as the three required kinematic conditions are fulfilled:

- The intersection line is "at the same side" as the slope (daylights on the slope).
- The intersection line plunge (24º) is lower than the slope dip (80º).
- The intersection line plunge (24º) is greater than the friction angle of the sliding planes (20º); graphically the point is "inside" the friction cone.

3.4.3. Safety Factor Calculation

The safety factor of a rock slope due to a wedge failure can be obtained following limit equilibrium methods (Hoek & Bray, 1981; Giani, 1992; Norrish & Wyllie, 1996a) by establishing the forces acting perpendicular to the discontinuities forming the wedge and parallel to the intersection line and solving the system. Forces include the self-weight of the unstable wedge mass, external forces like foundations, seismic accelerations and reinforcing elements, the effects of the pore pressures and the shear strength developed along the failure surfaces.

The assessment of wedge failures is usually carried out by a rigid-block analysis in which failure is assumed to occur due to a linear sliding along the intersection line formed by the discontinuities generating the wedge, or sliding along one of those discontinuities. The possibility of a toppling or rotational sliding is not considered.

The analysis requires the geometry of the wedge to be completely defined. This means knowing and defining the location and orientation of the five boundary surfaces shown in Fig. 3.12. These include the two intersecting discontinuities, the slope face, the upper slope surface and the plane representing a possible tension crack if present. The size of the unstable wedge is defined by the vertical distance from the crest of the slope to the intersection line. If a tension crack exists, the location of the crack to the crest of the slope must be taken into account to evaluate the size.

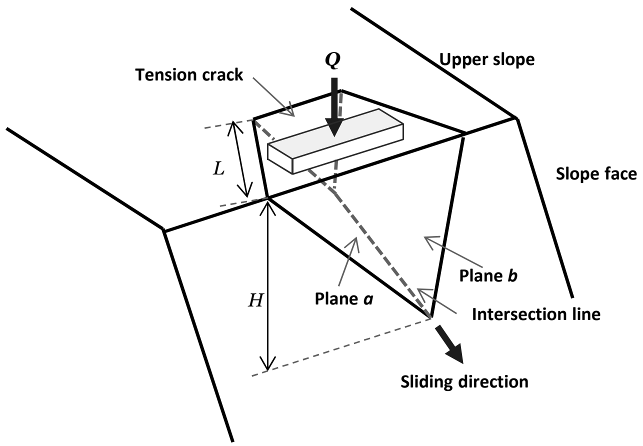

Source: Modified form Hoek & Bray (1981)

Fig. 3.12. Wedge failure calculation scheme.

The analytical study of the stability of an unstable rock wedge is quite complex and was developed by Hoek & Bray (1981), who presented the equations for its general analysis and a methodology to conduct the calculation systematically. Due to the complexity and length of these calculations, analyses of wedge failure for obtaining the safety factor is not usually done by hand but is carried out with the assistance of computer tools and software.

Some assumptions can be made to significantly simplify the equations and solve the problem. This provides a starting point and is sometimes used as an indication of the sensitivity of the wedge stability to different combinations of strength and loads, such as the sensitivity of the ground to be fully saturated or fully drained (dry).

When there is no tension crack and the rock mass is fully saturated (Fig. 3.13) the safety factor of a rock slope due to a wedge failure *F*, defined as the ratio between the resisting forces and the driving forces, may be written as:

$$F = \frac{3}{\gamma \cdot H} \cdot (c_a \cdot X + c_b \cdot Y) + \left(A - \frac{\gamma_w}{2 \cdot \gamma} \cdot X \right) \cdot \tan \phi_a + \left(B - \frac{\gamma_w}{2 \cdot \gamma} \cdot Y \right) \cdot \tan \phi_b \qquad \textbf{Equation 3.11}$$

If there is no tension crack and the rock mass is fully drained, the safety factor is:

$$F = \frac{3}{\gamma \cdot H} \cdot (c_a \cdot X + c_b \cdot Y) + A \cdot \tan \phi_a + B \cdot \tan \phi_b \qquad \textbf{Equation 3.12}$$

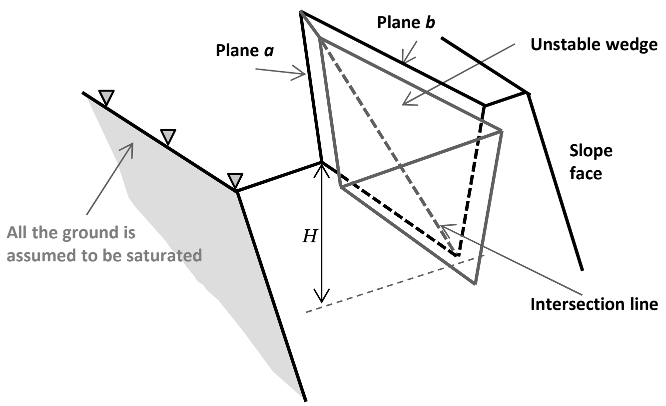

Source: Modified form Hoek & Bray (1981)

Fig. 3.13. Wedge failure calculation scheme for cases without tension crack.

In the previous expressions, the wedge is assumed to be formed by two discontinuities named *a* and *b*. The different terms included in those expressions include: c_a and c_b are the cohesion of the discontinuities *a* and *b*; ϕ_a and ϕ_b are the friction angle of the discontinuities *a* and *b*; γ is the unit weight of the intact rock; γ_w is the water unit weight; *H* is the height of the wedge; and *X*, *Y*, *A* and *B* are four coefficients which depend on angular relationships and which are defined as:

$$X = \frac{\sin\theta_{2,4}}{\sin\theta_{4,5}\cdot\sin\theta_{n_a,2}}$$ **Equation 3.13**

$$Y = \frac{\sin\theta_{1,3}}{\sin\theta_{3,5}\cdot\sin\theta_{n_b,1}}$$ **Equation 3.14**

$$A = \frac{\cos\beta_a - \cos\beta_b\cdot\cos\theta_{n_a,n_b}}{\sin\beta_{intersection}\cdot\sin^2\theta_{n_a,n_b}}$$ **Equation 3.15**

$$B = \frac{\cos\beta_b - \cos\beta_a\cdot\cos\theta_{n_a,n_b}}{\sin\beta_{intersection}\cdot\sin^2\theta_{n_a,n_b}}$$ **Equation 3.16**

Where β_a and β_b are the dips of the discontinuities *a* and *b*; $\beta_{intersection}$ is the plunge of the intersection line; and the values $\theta_{i,j}$ correspond to a series of angles defined by the following intersections:

- *1*: intersection of the discontinuity *a* that forms the wedge with the slope face.
- *2*: intersection of the discontinuity *b* that forms the wedge with the slope face.
- *3*: intersection of the discontinuity *a* that forms the wedge with the upper slope surface.
- *4*: intersection of the discontinuity *b* that forms the wedge with the upper slope surface.
- *5*: intersection of the discontinuities *a* and *b* that form the wedge (intersection line).
- n_a: pole of the discontinuity *a* that forms the wedge.
- n_b: pole of the discontinuity *b* that forms the wedge.

For instance, $\theta_{2,4}$ refers to the angle formed by the intersection of the discontinuity *b* with the slope face (intersection *2*) and the intersection of the discontinuity *b* with the upper slope surface (intersection *4*). Similarly, $\theta_{nb,1}$ refers to the angle formed by the pole of the discontinuity *b* (intersection n_b) and the intersection of the discontinuity *a* with the slope face (intersection *1*).

3.5. Toppling Failures

3.5.1. Definition

Toppling failures occur when the existing discontinuities in a rock mass give rise to a series of blocks or column elements with a very pronounced dip, opposed to the slope dip, which tends to produce a rotation towards the outside of the slope (Fig. 3.14). In a toppling failure, the rock column rotates about a fixed point located at or near the base of the slope and at the same time slippage occurs between the layers.

Toppling failures are typical of rock masses that are subdivided by fractures into a series of approximately vertical blocks or columns. Some rock types susceptible to this failure mode include columnar basalts, sedimentary formations with well-defined bedding planes and metamorphic rocks with foliation planes (schistosity).

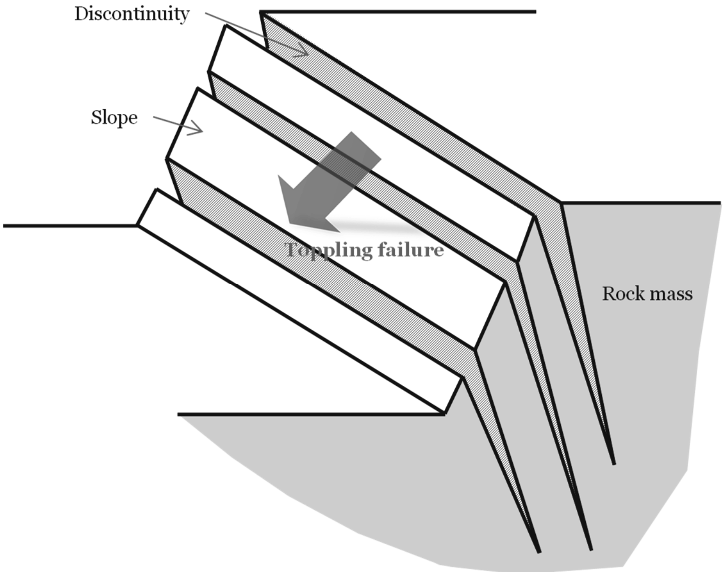

Source: Modified from Hoek & Bray (1981)

Fig. 3.14. Toppling failure general scheme.

3.5.2. Kinematic Conditions

Toppling failures can only occur if the discontinuity planes of the rock mass are substantially parallel to the slope and daylight abruptly and with great inclination in it. Besides, the center of gravity of the rock blocks or columns in which the discontinuities subdivide the rock mass must fall outside the dimension of its base. Toppling failures are characterized by showing significant horizontal movements in their upper part, but very small ones at their toe. To make compatible this differential movement between the toe and the upper part of the slope, the movement of the entire block must occur. This means that exceeding the maximum frictional force between blocks is necessary to trigger the failure mechanism. Therefore, a toppling failure does not occur until failure by shear of the rock blocks happens at the base of the slope.

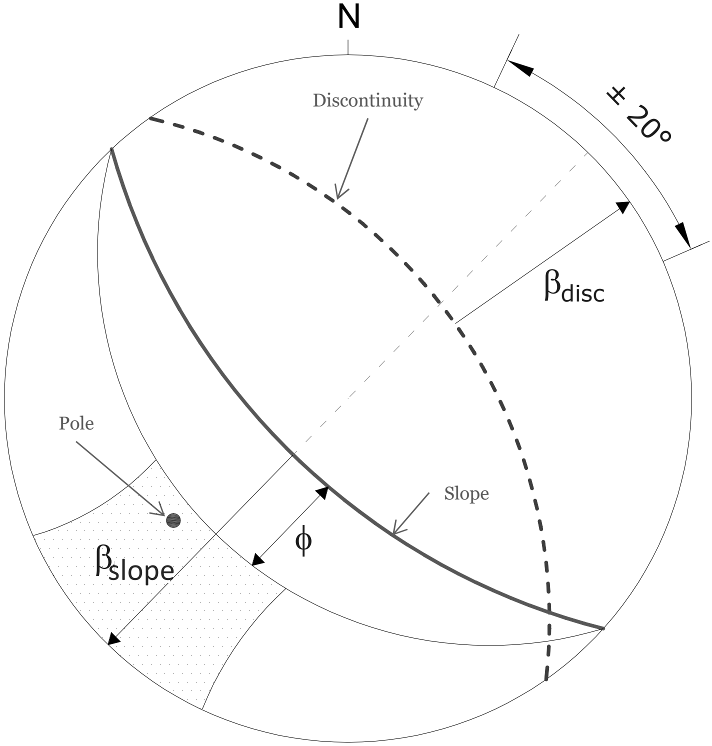

Any pole that falls within the shaded area has a potential risk of failure due to toppling, i.e. fulfills all the structural conditions:

- Dip direction of the discontinuity = dip direction of the slope + 180° ± 20°
- Plunge of the pole < dip of the slope (β_{slope}) – friction angle (ϕ)

Source: Adapted from Hoek & Bray (1981)

Fig. 3.15. Kinematic analysis of the stability of a rock slope due to a toppling failure.

The structural conditions required for toppling failures to take place are two (Hoek & Bray, 1981; Norrish & Wyllie, 1996a):

- The dip direction of the discontinuity (assimilated to a plane) must be approximately opposed to the dip direction of the slope. Commonly, the term "approximately opposed" considers that the difference between the discontinuity dip direction and the slope dip direction is found within a range of 160º and 200º, i.e. 180º ± 20°.

- The plunge of the normal to the discontinuity planes (pole) must be lower than the dip resulting from subtracting the dip slope from the friction angle of the discontinuity planes (the discontinuities friction angle is commonly assumed)

This kinematic analysis must be carried out independently for each discontinuity (or sets of discontinuities) and each slope under study.

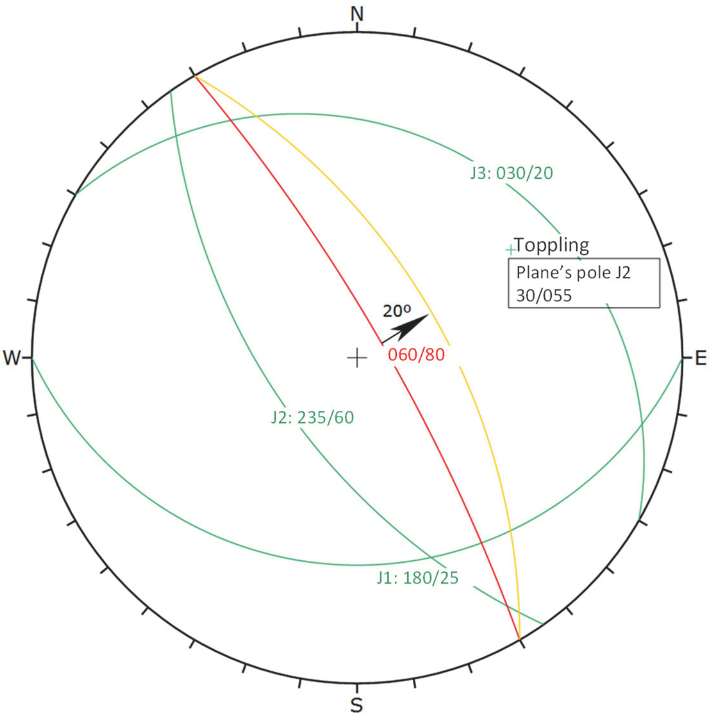

- Rock mass defined by three joint sets (in green) with orientations (dip direction / dip): 180/25, 235/60, 030/20
- A slope with orientation 060/80 (in red) is planned to be built
- The friction angle of the discontinuities is considered to be 20º
- Joint set defined by orientation 235/60 (pole defined by 30/055) represents a potential risk of toppling failure (fulfills all the structural conditions)

Source: Self-elaboration

Fig. 3.16. Analysis of the possibility of toppling failure.

The two previous structural conditions can be evaluated graphically using stereographic projection as shown in Fig. 3.15. The second condition refers to the plunge of the normal to the discontinuity planes, which in a stereogram is equivalent to the plunge corresponding to the poles of such discontinuity planes.

Fig. 3.16 shows an example of a potential toppling failure in a rock mass where a slope is planned to be built. The case is presented making use of the stereographic projection. The rock mass is defined by three joint sets (in green) with orientations (dip direction/dip): 180/25, 235/60 and 030/20. Joints friction angle is assumed equal to 20º. The slope (in red) is defined by the orientation 060/80.

As can be observed, the joint sets defined by 180/25 and 030/20 cannot cause a toppling failure: the difference between the dip directions of the joint sets and the slope face is not within the range 180º ± 20° in both cases (180 – 60 = 120º for the first set and 60 – 30 = 30º for the second set). However, the joint set defined by orientation 235/60 (whose pole corresponds to a line defined by 30/055) represents a potential risk of toppling failure as the two required kinematic conditions are fulfilled:

- The joint dip direction (235º) is within the range 180º ± 20° with respect to the slope dip direction (060º, so 235 – 60 = 175º).
- The pole plunge of the joint (30º) is lower than the result of subtracting the friction angle of the discontinuities (20º) to the slope dip (80º).

3.5.3. Safety Factor Calculation

The analysis of the toppling failure is based on studying the equilibrium conditions of each block that forms the slope (Hoek & Bray, 1981; Norrish & Wyllie, 1996a). Existing techniques and methods try to verify that the center of gravity of a specific rock block is within the base area of that block, otherwise a toppling failure can occur. Cases can be quite complex and cannot generally be represented by simple models. Therefore they cannot be analyzed by limit equilibrium methods.

Toppling failures were investigated by several authors who proposed different ways of solving the problem and obtaining a safety factor for the slope. One of the first successful methods for the analysis of toppling failures was developed by Goodman & Bray in 1976. That method can be applied to study simple cases assuming schematic blocks and assumes that each block (considered from its crest to its toe) may belong to one of the three stability conditions given Fig. 3.17: stable, plane sliding or toppling. The stability condition of the blocks depends on the geometry of the block and the shear strength parameters at the edges of the block, as well as the presence of any external acting force (such as reinforcing elements and an earthquake).

Basically, the method of Goodman & Bray considers that the sliding of a block is only possible if the block friction is lower than the inclination of the base plane of the unstable block. Similarly, the toppling of a block is possible if the ratio between the width of the block and its length is lower than the friction force at the block.

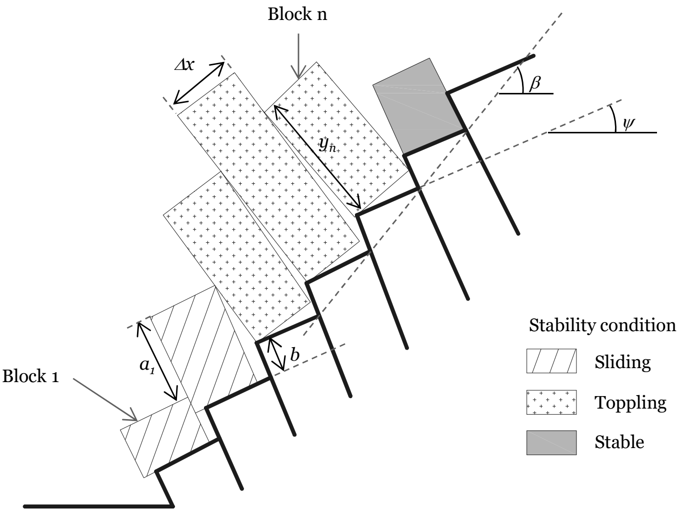

Source: Modified form Hoek & Bray (1981)

Fig. 3.17. Toppling failure, stability conditions.

Those blocks prone to slide or topple will exert a force on the adjacent blocks in the downward direction of the slope. Thus, given a block *n*, one of the forces opposing to slide or topple is the force $P_{(n-1)}$ transmitted by the block immediately located below it. By establishing equilibrium of moments for the block *n* according to Fig. 3.18a, the value of force P_{n-1} can be written as:

$$P_{n-1} = \frac{P_n \cdot (y_n - \Delta x \cdot \tan\phi) + \frac{W_n}{2} \cdot (y_n \cdot \sin\beta - \Delta x \cdot \cos\beta)}{y_n - a_1}$$ **Equation 3.17**

Where P_n is the normal force exerted on the block *n* by the upper adjacent block; y_n, Δx and W_n are the height, width and weight of the block *n*, respectively; ϕ is the friction angle in the vertical of the block *n*; β is the inclination of the base plane of the unstable blocks; and a_1 is the height difference of the first unstable block to the second one.

By establishing a balance of forces in the tangential and perpendicular directions to the plane defined by the base of the unstable blocks according to Fig. 3.18b, the force exerted by a block *n* on the adjacent lower one which opposes to sliding (P_{n-1}) may be written as:

$$P_{n-1} = P_n - \frac{W_n \cdot (\tan\phi \cdot \cos\beta - \sin\beta)}{1 - \tan^2\phi}$$ **Equation 3.18**

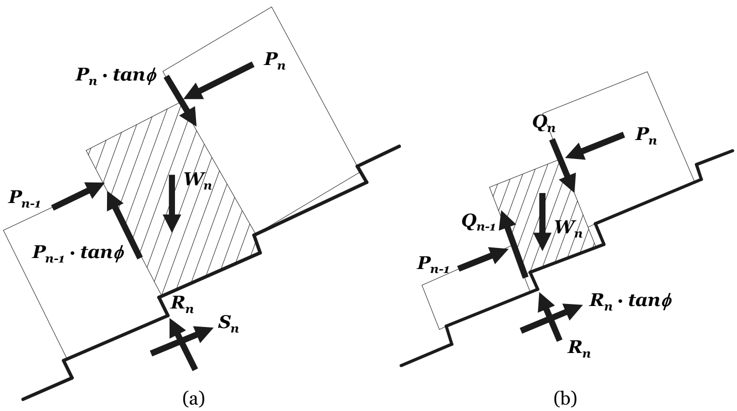

Source: Modified form Hoek & Bray (1981)

Fig. 3.18. Toppling failure stability analysis: (a) forces opposing toppling; (b) forces opposing a planar sliding.

The method proposed by Goodman & Bray requires applying the following process to compute the stability of a slope subjected to a potential toppling failure:

- The blocks to be analyzed are defined and starting from the top of the slope, the first block that meets the toppling condition is found ($\Delta x/y_n < tan\phi$); it is then assumed $P_n = 0$ for that block.
- The force P_{n-1} due to toppling and sliding is calculated for the previous block as the one defined in the previous point. The highest of the obtained values for toppling and sliding is taken as the P_n value for the immediately lower block.
- For the next (lower) block, the P_{n-1} forces for toppling and sliding are calculated. The highest of the obtained values for toppling and sliding is taken as the P_n value of the immediately lower block. If the largest value corresponds to sliding, that block is considered in a sliding condition, otherwise is considered in toppling condition.
- The procedure continues for all the blocks of the slope. When a block is reached in which the toppling condition is not meet (i.e. if $\Delta x/y_n > tan\phi$), the analysis considers only the sliding condition from that point.
- Once the toe of the slope is reached and the last P_{n-1} value is computed, three situations can occur:
  - $P_{n-1} = 0$, which means that the slope is in limit equilibrium for the friction angle ϕ considered.

- $P_{n-1} > 0$, which means that the slope is not stable for the friction angle ϕ considered.
- $P_{n-1} < 0$, which means that the calculation is not valid, so it must be done again for the friction angle ϕ greater than the one considered.

The method of Goodman & Bray does not allow defining the stability of the slope studied in terms of a traditional safety factor. However, the ratio between the friction value required to limit the equilibrium (i.e. ϕ value to attain $P_{n-1} = 0$) and the one available along the base of the blocks is usually considered as the safety factor.

Despite its limitation, the method Goodman & Bray is the most common method used to analyze toppling failures and is implemented in specialized software of rock mechanics. It is also a very flexible method. For instance, by doing some simple modifications, the method also provides the force needed to be introduced by a reinforcing element to stabilize the slope against toppling and sliding conditions.

Other methods used to analyze toppling failures include the nomograms proposed by Choquet and Tanon (1985) based on the solution developed by Hittinger (1978). This is a graphical method that provides the "maximum block limit width" from which the toppling failure can take place (slenderer blocks activate the failure mechanism).

3.6. Analysis of Rock Slopes using the SMR (Slope Mass Rating)

The previous methods are based on stereographic projection for conducting the kinematic analysis and the use of limit equilibrium method for computing the safety factor and define the need a performance of stabilization measures. As alternative to these methods, the analysis of the stability of rock slopes against planar failures, wedge failures and toppling failures may also be carried out using the SMR (Slope Mass Rating). This is a geomechanical index (Romana, 1985, 1995) specifically designed for being used in slope stability problems.

The SMR is a correction of the well-known Rock Mass Rating (RMR) index (Bieniawski, 1979) widely used for classifying and assessing the quality of rock masses in excavation projects and tunnels. The RMR consider five parameters of the rock mass:

- The uniaxial compression strength (UCS) of the rock mass, estimated by uniaxial compression tests or point load tests.
- The degree of fracture of the rock mass, estimated using the RQD.
- The spacing of the discontinuities.
- The conditions of the discontinuities, qualitatively and quantitatively estimated by observing the persistence, aperture, roughness and infilling of the discontinuities and the degree of weathering and alteration of the discontinuities walls.

- The hydrogeological conditions of the rock mass that affect the stability of the slopes, estimated based on a qualitative observation of the surface of the rock mass.

$$SMR = RMR_{basic} + F_1 \cdot F_2 \cdot F_3 + F_4$$

F_1, F_2 and F_3 are three factor that depend on the structural geology of the rock mass and its relationship with the slope

	Failure type	Mathematical condition	Very favorable	Favorable	Medium	Unfavorable	Very unfavorable
F_1	Planar	$\lvert\alpha_j - \alpha_s\rvert$					
	Wedge	$\lvert\alpha_i - \alpha_s\rvert$	> 30º	30º - 20º	20º - 10º	10º - 5º	< 5º
	Toppling	$\lvert\alpha_j - \alpha_s - 180°\rvert$					
		Score F_1	0,15	0,40	0,70	0,85	1,00
F_2	Planar	$\lvert\beta_j\rvert$	< 20º	20º - 30º	30º - 35º	35º - 45º	> 45º
	Wedge	$\lvert\beta_i\rvert$					
		Score F_2	0,15	0,40	0,70	0,85	1,00
	Toppling	-	-	-	-	-	-
		Score F_2	1,00	1,00	1,00	1,00	1,00
F_3	Planar	$\beta_j - \beta_s$	> 10º	10º - 0º	0º	0º - (-10º)	< -10º
	Wedge	$\beta_i - \beta_s$					
	Toppling	$\beta_j + \beta_s$	< 110º	110º - 120º	> 120º	-	-
		Score F_3	0	-6	-25	-50	-60

* Notation: α_j: dip direction of the discontinuity considered; α_i: dip direction of the intersection line considered; α_s: slope dip direction; β_j dip of the discontinuity considered; β_i: dip of the intersection line considered; β_s: slope dip

F_4 is an adjustment factor defined by the excavation method:

- Natural ground: F_4 = +15
- Presplitting: F_4 = +10
- Smooth basting: F_4 = +8
- Basting /mechanical excavation: F_4 = 0
- Deficient blasting: F_4 = -8

PROBABLE FAILURES ACORDING TO THE SMR VALUE

Planar failure		MAJOR	MINOR	NONE
Wedge failure	MANY	SOME	VERY FEW	NONE
Toppling failure		MAJOR	MINOR	NONE
Circular failure	MAJOR	POSSIBLE	NONE	

SMR: 0 | 5 | 10 | 15 | 20 | 30 | 40 | 45 | 50 | 55 | 60 | 65 | 70 | 75 | 80 | 90 | 100

Reexcavation	Reexcavation Walls
Drainage	Surface drainage Deep drainage
Concrete	Shotcrete Dental concrete Ribs and/or beams Toe walls
Reinforcement	Bolts Anchors
Protection	Toe ditches Toe or slope fences Nets
No support	Scaling None

RECOMMENDED SUPPORTS

Source: Self-elaboration, based on Romana (1985, 1995)

Fig. 3.19. Flow chart summary for applying the SMR index.

From the RMR, the SMR is obtained by introducing four new parameters that that depend on the structural geology of the rock mass and its relationship with the slope and the slope excavation method (natural ground, presplitting, smooth blasting, blasting, mechanical excavation and deficient blasting). Bieniawski himself (1989) endorsed the use of the correction factors proposed in the SMR for slope instabilities.

The SMR also provides recommendations for the support and correction methods to be used in a rock slope depending on the SMR value obtained (similar to the RMR, which provides recommendations for tunnel support).

All in all, the SMR may be a very useful engineering tool for assessing the stability of rock slopes in a preliminary design phase and to set the expected support elements needed in an unstable slope. However, it does not provide deep information about the mechanical behavior of the slope. In that case, a limit equilibrium method and/or the use of a stress-strain method (e.g. finite element modeling analysis) should be used to complement the analysis and/or refine it.

Fig. 3.19 shows a flow chart summarizing the SMR use.

Chapter 4
Corrective Measures

4.1. Introduction

Corrective measures include all those actions, elements and construction procedures proposed, install and/or implemented in a soil or rock slope to solve one or more instabilities. In other words, corrective measures help in the stability and safety of a slope.

When stability analyses indicate that a slope is unstable, corrective measures must be taken. The consideration of such measures must be then introduced in the slope model and the stability analysis conducted again. If the new state is still unstable, additional, new or alternative measures must be taken into account. This "trial and error" process finishes when the measures considered achieve the slope to be stable.

There are several corrective measures that can be grouped in four main actions:

- Modifying the geometry of the unstable slope.
- Introducing elements that facilitate the slope drainage.
- Installing reinforcing elements (like anchors and bolts) in the ground that opposed to the driving forces
- Installing retaining elements (e.g. walls) that solve the problem by preventing the sliding of the unstable mass (but they do not stabilize the slope).

Besides, the use of superficial protection measures is always highly recommended to avoid erosion of the most superficial layers of the slope and prevent local instabilities.

4.2. Geometrical Corrective Measures

4.2.1. Soil Slopes

The stabilization of an unstable soil slope by correcting its geometry takes into account the definition of the safety factor F as the ratio between the resisting forces opposed to the sliding of the failure surface and the driving forces causing the sliding of the unstable mass:

$$F = \frac{resisting\ \ forces}{driving\ \ forces}$$ **Equation 4.1**

Either increasing the numerator or decreasing the denominator of such ratio will result in a higher safety factor and consequently a more stable slope. Therefore, for achieving the stabilization of a soil slope, there are two main ways: decreasing the driving forces and/or increasing the resisting forces.

One simple way of decreasing the driving forces is reducing the slope inclination angle, as the tangential component of the weight is the main driving force. Similarly, all driving forces involved in the slope tend to reduce when the slope inclination angle is deceased. However, a low slope inclination angle implies more space used, more occupation area needed and more material to be removed, thus resulting in economic issues.

Other ways of decreasing the driving forces include (Ayala et al. 1987):

- Removing the whole unstable mass and/or those unstable materials which are producing the instability, a solution that can completely eliminate the slope instability problem, but with a high economic cost.
- Removing earth material at the slope head (Fig. 4.1a), since the weight which contributes most to the instability of a slope is that one located at the upper part of the unstable mass.
- Building intermediate benches (Fig. 4.1b), transforming the slope into a stepped slope and thus reducing the equivalent slope angle.

It is interesting to note that intermediate benches are commonly implemented during the design phase of a slope. They do not only increase the safety factor of a slope but intermediate benches have a series of advantages also, such as facilitating the slope construction, helping future conservation operations, controlling partial instabilities, reducing the water erosive effect and facilitating the installation of drainage ditches.

Regarding to increasing the resisting forces opposed to the sliding, this can be achieved by (Ayala et al. 1987) increasing the mass at the toe of the slope, which is usually done by installing earth or rock berms (Fig. 4.2) at that area. The weight of such berms results in an increment of normal stresses in the lower part of the failure surface, which increases the resisting forces and helps in the stabilization of the slope.

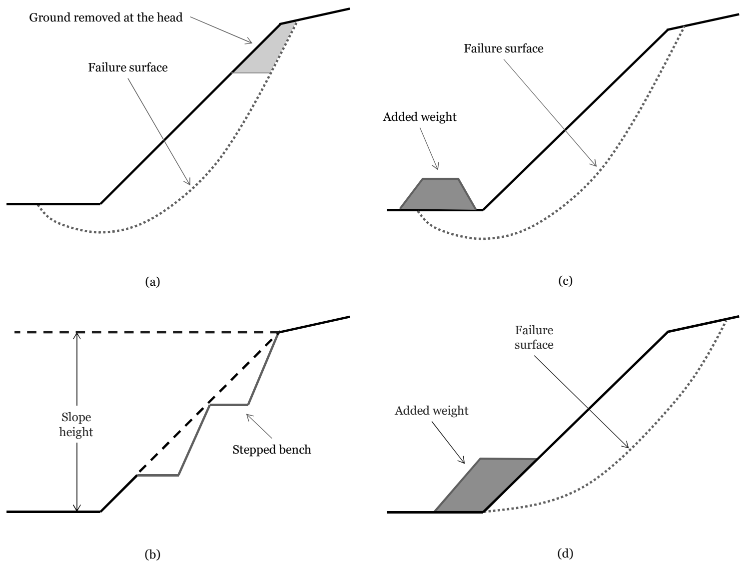

Source: Modified from Ayala et al. (1987)

Fig. 4.1. Geometry correction: (a) removing the ground at the slope head; (b) construction of stepped benches; (c) berm at the slope base; (b) berm at the slope toe.

Sometimes the execution of berms is combined with removing the material at the head of the slope, since the material excavated at that location can be placed at the slope toe. In those cases, two correction measures are implemented at the same time, significantly increasing the safety factor.

In any case, the base of the toe berms should always allow drainage to enable the dissipation of any possible pore pressures generated.

4.2.2. Rock Slopes

The stabilization of a rock slope varying its geometry seeks to avoid the fulfillment of the kinematic conditions that trigger the three main rock failure mechanisms: planar failure, wedge failure and toppling failure (Norrish & Wyllie, 1996a).

The geometric actions to be considered are:

- For planar failures, one of the following procedures may be conducted:
    - Reducing the slope angle, so that the slope dip reaches a value equal to or less than the dip of the discontinuity that causes the planar failure; this prevents the discontinuity from daylighting at the slope face.

    - Changing the orientation of the slope, so that the difference between the dip direction of the slope and the dip direction of the discontinuity that causes the planar failure is greater than 20º.
- For wedge failures, one of the following procedures may be conducted:
    - Reducing the slope angle, so that the slope dip reaches a value equal to or less than the plunge of the intersection line that causes the wedge failure; this prevents the intersection line from daylighting at the slope face.
    - Changing the orientation of the slope, so that the intersection line that causes the wedge failure falls outside the critical region.
- For toppling failures, one of the following procedures may be conducted:
    - Reducing the slope angle, so that the poles of the discontinuity that causes the toppling failure fall outside the critical region.
    - Changing the orientation of the slope, so that the difference between the dip direction of the slope and the dip direction of the discontinuity that causes the toppling failure falls outside the range 160º - 200º.

Making modifications in the geometry of a slope according to the previous points is the best and most efficient way to deal with slope instabilities problems in rock masses: if the kinematic conditions defining any failure (planar, wedge or toppling) are not fulfill, the rock slope is guaranteed to be stable regardless other parameters and factors.

However, changing the geometry of a slope is not always possible given the project, execution and / or economic conditions involved. Especially, changing the orientation of a slope can only be done normally at a design or a preliminary design phase, and not always is plausible.

Besides the indication given above, other geometrical corrective measures on rock slopes include building intermediate benches or implementing similar measures that tend to reduce the high of the slopes and/or reduce the equivalent slope angle.

4.3. Drainage Measures

4.3.1. General Aspects

The presence of water reduces the stability of slopes (both in soil and rock slopes) and can contribute to trigger any potential instability. In general, water appears in a slope due to groundwater or as result of run-off and infiltrations caused by precipitations. Therefore, carrying out drainage measures in a slope is always recommended.

The drainage of a slope has as a main objective removing the water from the slope (or at least reducing it). This produces several positive effects including the dissipation of pore pressures and any overpressures that may exist on sliding surfaces as well as the reduction of the total weight of the unstable mass (the water adds weight, so removing it reduces the weight of the soil). Besides, some drainage measures also result in the protection of the slope against erosion, reducing future potential local instabilities.

As water is often the main cause of slope instabilities (González de Vallejo & Ferrer, 2011), implementation of drainage in a slope is probably the most effective corrective measure that contributes to the general stability of a slope.

There are two main drainage correction measures: surface drainage and deep drainage. Fig. 4.2 shows different drainage measures implemented in a slope.

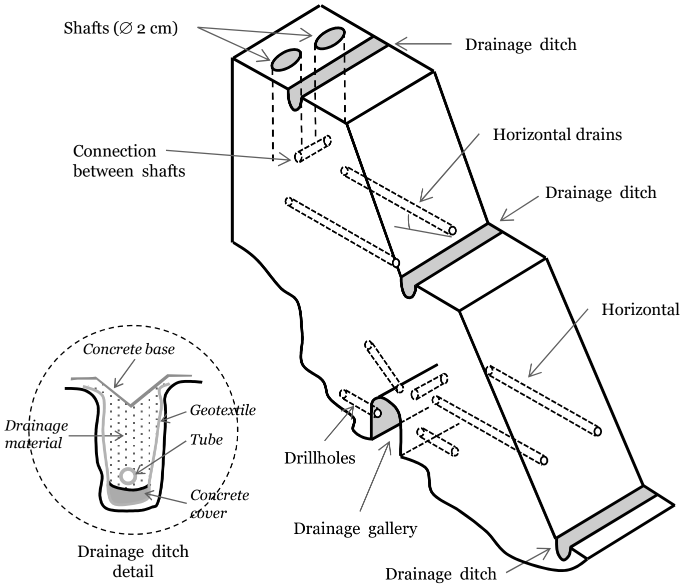

Source: Modified from González de Vallejo & Ferrer (2011)

Fig. 4.2. Drainage and protection measures in slopes.

4.3.2. Surface Drainage

Surface drainage measures are carried out with two objectives:

- Preventing run-off water from infiltrating directly into the ground or get into it by any discontinuity and crack. That can result in an elevation of the water table, the apparition of pore pressures and the ground saturation. In rock masses, water can also reduce the friction angle due to a lubrication effect.
- Preventing run-off water from acting on the slope surface where it may produce an erosive phenomenon that contributes to potential instabilities.

Surface drainage measures normally include building drainage ditches at both the head and the toe of the slope. These two ditches are recommended to be included in any slope design, even though the slope is expected to be stable. Drainage ditches can also be introduced at intermediate benches when the slope includes such elements. Drainage ditches may be designed based on the expected flow to evacuate and taking into account that water must be conducted outside the landslide area.

4.3.3. Deep Drainage

Deep drainage measures basically consist of making holes in the ground to evacuate the water contained in it and/or lowering the water table. Those measures include:

- Horizontal drains: these are horizontal or sub-horizontal holes of small diameter made in the surface of the slope. The system requires the installation of a high density of drills to be effective since drains tend to be blocked in a high percentage as well as the use of geotextiles to avoid their silting with fines.
- Vertical wells: these are large diameter vertical drills in which water is usually evacuated by pumping using submerged pumps. To avoid the maintenance involved in having the pumping equipment running, they are sometimes connected to a drainage gallery, so water is evacuated by gravity.
- Drainage galleries: these are galleries excavated in the ground quite separated from the surface of the slope and parallel to it. It is a very effective but very expensive system and it is usually only used in special cases. They are often combined with radial drain drilling from the gallery itself, encompassing a larger cross section, which greatly improves drainage.
- Drainage trenches: ditches filled with a filtering material, built below the slope surface along it that allow water to be extracted from its surface and control phreatic levels.
- Drainholes: typical of rock slopes, they create outlets for the water. Perforations should be placed at the toe of the slope and crossing fractures with great persistence through which the water circulates, since the intact rock hardly contains water (Norrish & Wyllie, 1996b).

4.4. Reinforcing and Resisting Elements

4.4.1. Anchors

Anchors are elements formed by cables or steel bars located inside drilled holes which work in tension. Anchors stabilize a slope by providing a force which opposes to the movement of the unstable mass as well as by increasing the normal stresses on the failure surface, thus leading to an increment in the sliding resistance.

There are three types of anchors:

- Passive anchors: normally made up of steel bars, these anchors are not tensioned, so they begin to work when the ground begins to move.
- Active: materialized by steel bars or cables, these anchors are post-tensioned until reaching their maximum load, so they provide a stabilizing force on the slope from the moment they are installed.
- Mixed: active-like anchors that are post-tensioned until reaching a lower load than their maximum one.

All anchors have three basic parts: the anchor grout body, the free length body and the anchor head (Fig. 4.3). When a tension is applied to the anchor, this is transmitted to the ground through the head of the anchor, producing a compression force.

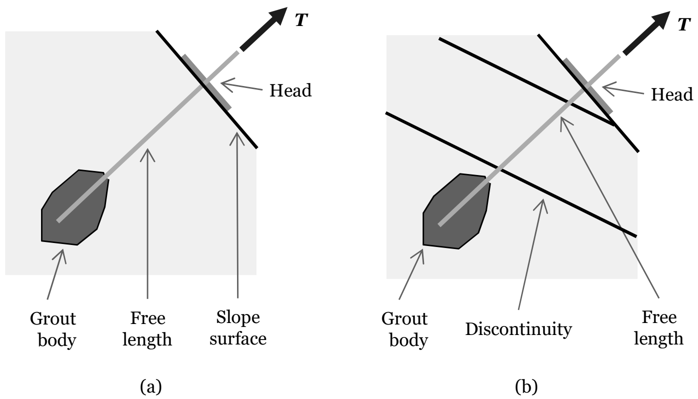

Source: Self-elaboration

Fig. 4.3. Scheme of an anchor in a soil slope (a) and in a rock slope (b); if *T* is null, the anchor is passive; otherwise the anchor is active or mixed.

A proper calculation of each of these parts must be carried out to avoid the anchor failure, which is usually made based on different regulations and recommendations. For instance, the Spanish "Guide for the design and execution of ground anchors in road works" (Ministerio de Fomento, 2001) consider the following checks:

- Admissible tension of the steel tie rod.
- Sliding of the tie rod inside the grout body.
- Safety against the grout body pull-out.

The first two checks are solved directly from the geometric and mechanical data of the anchor and its different parts. The last check needs estimating the value of the adhesion between the cement grout and the geological materials where the grout body is installed, which can be determined from experimental tests or based on empirical results.

Anchors are used in both soil and rocks slopes, although their purpose is different:

- In soil slopes, anchors are used for covering large soil masses with deep failure surfaces. They are normally used together with walls that collect all the anchor heads and distribute the compression forces transmitted to the ground.
- In rock slopes, anchors are used as a stabilization measures against planar, wedges and toppling failures. They are installed so that they cross all potential failure surfaces and they should be anchored in healthy rock. They are especially effective in stabilizing planar failures. The necessary force to be provided by anchors can be estimated using limit equilibrium methods (***Chapter 4***) or advanced numerical models such as finite element modeling (***Chapter 5***).

Finally, some interesting considerations regarding the design and installation of anchors are given below (Norrish & Wyllie, 1996b):

- If the anchor is installed with a flatter angle of inclination than the normal to the potential failure surface, the shear strength generated by the anchor is increased.
- Resins, mechanical elements or cement grouts can be used to secure the end of the anchor in the drill; when choosing the product, factors to consider include the required capacity of the anchor, the speed of installation, the strength of the intact rock and the ease of access to the anchor installation site.
- Active anchors installation requires following a defined procedure to verify that the design load is applied at the proper depth and there are no significant stress losses over time.
- Corrosion protection must be provided to all anchors planned to be permanent to ensure their durability, even though they are not subject to corrosion at the time of installation.

4.4.2. Rock Bolts

Rock bolts or simply bolts are steel bars that are inserted into the slope and can be considered of low capacity (González de Vallejo & Ferrer, 2011), especially when compared to anchors. Bolts are normally materialized by corrugated bars from 16 to 40 mm, with lengths ranging from 3 to 6 m, although sometimes they can reach 12 m or more. Bolts transfer loads from the unstable exterior mass to the confined interior of the rock mass. In addition, they provide a certain resistance which opposes to the movement of the unstable mass.

Bolts are not recommended to be used in soil slopes, but are usual in rock slopes, where they are especially useful for solving slopes affected by wedge failures. Their efficacy is increase by arranging them in meshes at various heights in a staggered manner, so bolts cover the greatest possible area of influence and "sew" the greatest number of potentially unstable intersection lines.

Bolts are inserted into drillings made in the rock mass and completely filled with resin or cement, ensuring both their direct contact with the ground and their protection against corrosion.

Similar to the case of anchors, in the design of the bolts, both their bearing capacity and their adherence to the ground must be calculated to avoid failure of these elements. The necessary force to be provided by rock bolts can be estimated using limit equilibrium methods or advanced numerical models such as finite element modeling.

The bolt section can be design from their tensile yield stress using the following expression (Portillo, 2003):

$$Q \cdot \gamma_l = \frac{0.9 \cdot f_y}{\gamma_l} \cdot A_\alpha$$ **Equation 4.2**

Where Q is the load of the bolt; γ_l is the safety coefficient for the load, normally ranging from 1.4 to 2.0; f_y is the steel yield stress of the bolt; γ_s is the reduction coefficient of the steel strength (normally 1.15); and A_α is the steel bolt section.

Additionally, pull-out of the bolt must be verified, so that it does not occur when the load Q established is applied. Such calculation needs computing the adhesion between the cement grout of the bolt and the geological materials where the bolt is installed, which can be determined from experimental tests or based on empirical results. Pull-out calculations allow defining the minimum length of the bolt.

Rock bolts can also be used as a corrective measure in rock slopes prone to rockfalls. In that case, bolts are installed fix the unstable blocks; if the dimension of those block is very large, anchors are used instead.

Other uses of rock bolts in geotechnical engineering include civil tunneling support where they are an essential component of the New Austrian Tunneling method.

4.4.3. Walls

Walls are structural elements generally used as retaining elements, i.e. they do not stabilize the slope in a similar way as anchor, bolts, drainage or some geometrical measures do, but they solve the stability problem by preventing (stopping) the sliding of the unstable mass. Walls can also be used as resisting elements (similar to berms) when located at the toe of the slope.

Walls are normally used in soil slopes. The main advantage of using walls is that they enable building a vertical slope, something very useful when lack of space exist. However, when designing walls, drainage measures of its back must be taken into account to allow the dissipation of the pore pressures and to avoid accumulation of water which can result in increasing forces and future corrosion problems.

As Fig. 4.4 shows, walls may be mainly classified as (Jiménez Salas et al., 1976):

- *Retaining walls*, when their objective is containing and supporting the ground; these walls can be separated from the slope with a filling in their back (backfill) or excavated directly in the slope.
- *Revetment walls*, when their objective is basically protecting the ground surface, even though they can also contribute to the slope support (however this function is lower than in the case of the retaining walls).

In addition, there are a great number of types of walls in terms of their geometry, the materials used or the way of developing the mechanical work, for instance:

- Gravity walls.
- Buttress walls.
- Gabion walls.
- Retaining walls.
- Reinforced earth walls.
- Anchored walls.
- Diaphragm walls.
- Piles and micropiles retaining walls.
- Injection walls.

In highly fractured rock masses where a circular failure similar to that of a soil-type material can occur, anchored concrete walls are of common use, pulling the anchors against the wall to stabilize the slope (Norrish & Wyllie, 1996b). This wall thus serves as a protection against rock crumbling and as a large reaction plate that distributes the force of the anchors and compresses the rock mass. In this kind of walls, drainage is provided by drilling some holes in the concrete, letting the water to "cross" the wall.

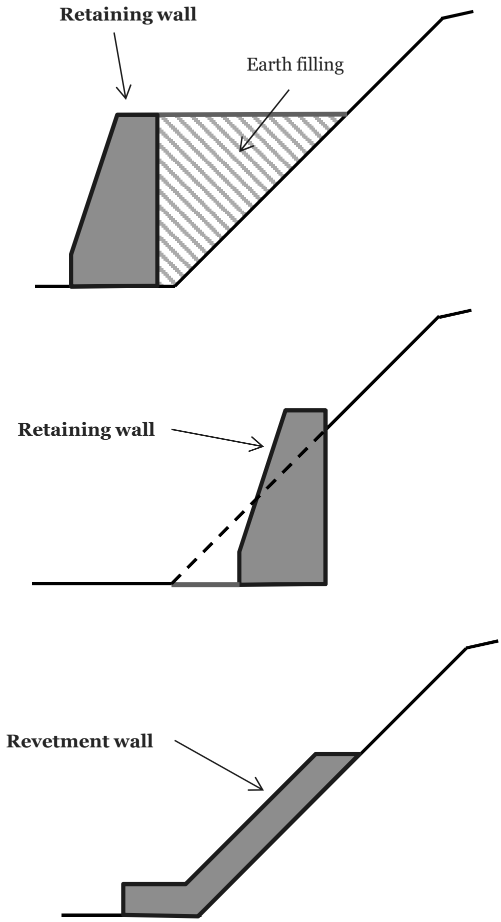

Source: Modified from Jiménez Salas et al. (1976)

Fig. 4.4. Main Wall typologies.

4.5. Surface Protection

4.5.1. Soil Slopes

Surface protection measures are applied to the soil slope surface and therefore only affect and protect the most superficial layers. However, these measures are highly important since they are aimed at preventing the erosions of the surface of the slope and the formation of small local failures.

The most effective surface protection measure in soils is showing them. The seeding of the slopes facilitates the superficial drainage of the soil surface and the roots of the seeded plants increase the shear strength of the soil.

These measures need using native species or ones that can be adapted properly to the weather where they will develop. The chosen species should have deep roots and a high degree of transpiration in order to increase water consumption. Besides, sowing slopes is only possible at a relatively low slope angles, not giving good results on vertical slopes.

As an alternative to sowing, flexible elements like meshes anchored to the slope can be used. These meshes provide a protective function and they also have a certain stabilizing effect on the surface area of the slope (da Costa García, 2004). High resistance meshes can be used and in some cases the anchors are post-tensioned, giving the system an active behavior.

4.5.2. Rock Slopes

Those areas of the rock masses highly fractured or susceptible to weathering can be protected by shotcrete. Although shotcrete should not be considered a resistant element in a slope stability analysis, it does have a positive functionality in protecting the slope surface, controlling both the fall of small rock blocks and the progressive weathering of the slope (Norrish & Wyllie, 1996b). Shotcrete should be combined with drainholes to avoid pore overpressures in the back of the slope which may cause shotcrete spalling.

In rock slopes prone to rockfalls, apart from using bolts to fix the unstable blocks, such instability may be mitigated (Norrish & Wyllie, 1996b; González de Vallejo & Ferrer, 2011) by the application of "rockfall control and direction methods", so rockfalls are allowed to occur, but danger is minimized and infrastructure and services located at the toe of the slope are protected. This can be achieved by using trenches, ditches, barriers and double or triple twist meshes hanging from the crest of the slope and weighted or not at the toe.

Double or triple twist meshes can also be used as a general surface protection measure instead of shotcrete to prevent local instabilities in rock slopes. Sometimes, these meshes are fixed to the ground by bolts or anchor, which also help in stabilizing the slope.

Chapter 5

Use of Finite Element Modeling

5.1. Introduction

Stress-strain methods are alternative calculation procedures to the use of the traditional limit equilibrium methods to analyze the stability of soil and rock slopes. Stress-strain methods consider both forces and the strains and displacements of the ground. Therefore, such methods are more comprehensive ones than limit equilibrium methods (which only consider forces), but they are also much more complex.

Nowadays, the most common stress-strain calculation method is finite element modeling (FEM). The use of FEM is increasingly common for studying the stability of soil and rock slopes as it enables simulating nearly every slope case as well as introducing any corrective measure, and provides much more information about the slope behavior when compared to limit equilibrium method whose main output is the safety factor.

However, the use of FEM requires some experience by part of the practitioner who uses this mathematical tool. Otherwise, the great potential of FEM may not be drawn and even some interpretation errors can arise.

The following sections deal with the most relevant aspects to consider in the stability analysis of soil and rock slopes using FEM. It is important to note that it is not intended here to delve into general aspects of the use of FEM in engineering geology or geotechnical engineering. Thus, discussion about issues like the area to be modeled, the mesh size, the elements to be used and the boundary conditions to be considered are not considered. Such aspects are outside the scope of this work.

5.2. Concept, Advantages and Limitations

5.2.1. Main Concept of Finite Element Modeling

The finite element modeling (FEM) technique consists of discretizing a continuous problem into a series of elements, following a given pattern of triangular or square shapes (or linear ones, in the case of a 1D element). For instance, a soil layer can be divided into several squared element. Each element is defined by its nodes, i.e. a series of significant points normally located on the border of the element, e.g. the vertices of the element.

The relationship between the different nodes of an element is provided by the common kinematic equations of classic mechanics. From that point, the constitutive equation of the material that forms the element can be applied, resulting in the internal forces that can be developed in the element.

Putting together all the elements of a model, a balance of forces can be established by means of the virtual work theory. The problem is then reduced to solve a numerical equation system that involves the exterior forces applied that must equal the internal forces developed in all elements so that displacements are viable. The system considers in the internal forces the stress-strain relationships given by the constitutive equations of all the materials involved in the model.

FEM transforms a continuous problem into a discrete one and provides an approximate solution to the geotechnical and mechanical problem. The solution, although not exact when compared to classical mathematical solutions, is quite approximate to be considered correct. This allows dealing with very complex problems which are otherwise not possible to be addressed using a rigid physical formulation.

5.2.2. Advantages and Limitations

The main advantage of FEM is the flexibility that it provides. In a numerical simulation by FEM, any slope geometry can be analyzed, any load applied and any corrective measure introduced (e.g. anchors or walls). FEM also allows considering water tables and flow nets. Besides, FEM calculation procedure takes into account both stress and strains, unlike limit equilibrium method which only consider forces (stresses). Thus, the results of using FEM not only provide a safety factor, but they also generate a great quantity of output material that facilitates analyzing the slope stability problem.

However, FEM has two main limitations: (i) the great complexity of the model requires in nearly all cases the help of computers, specific software and some experience in interpreting the results; and (ii) knowledge of all boundary conditions and the constitutive behavior of all materials involved in the simulation are need, which may be problematic when dealing with geotechnical materials, as some parameters like the Young modulus are somewhat difficult to obtain in most of cases.

5.3. Constitutive Models

5.3.1. Soils

Soil is normally simulated in FEM as a linear isotropic elastic material following Hooke's law (i.e. defined by the Young modulus E, and the Poisson ratio ν), but considering that the maximum stresses that can be attained in a soil element are controlled by the classical Mohr-Coulomb failure criterion:

$$\tau_{\max} = c + \sigma \cdot \tan \phi \qquad \textbf{Equation 5.1}$$

Where τ_{max} is the maximum tangential stress that can be reached; σ is the normal stress; and c and ϕ and are the cohesion and the friction angle of the soil, respectively.

Once the maximum tangential stress (failure criterion) is attained, usually a plastic behavior of the soil element is considered, following an unassociated plasticity, with the plastic potential controlled by the dilatation angle of the soil (which is generally taken equal to zero for clays and equal to ϕ – 30º for sands, unless proper data is available).

Suitable drainage conditions should be considered when modeling the soil behavior. Thus, all parameters must be defined in terms of drained or undrained conditions, so they are provided in effective terms (e.g. c', ϕ', E', ν') or undrained terms (e.g. c_u, $\phi_u = 0$, E_u, ν_u), respectively. Geotechnical FEM software normally includes the drainage conditions of each material involved in the simulation as an input, so they directly require the user to introduce the corresponding parameter. However, when working with general-purpose FEM software, drainage conditions must always be specifically considered both in terms of parameters and the different hypothesis to assume (e.g. variation or not of pore pressures with time).

Shear strength parameters (c and ϕ) are usually obtained from laboratory tests. Direct shear tests are used for obtaining c' and ϕ ' in granular soils and cohesive soils under drained conditions (performed according to standards such as ASTM D3080) while the uniaxial compression strength test is used for obtaining the undrained shear strength c_u (performed according to standards such as ASTM D2166).

However, the definition of soils elastic parameters is often problematic as the Young modulus and Poisson ratio cannot always be obtained from laboratory tests. In those cases, correlations with other parameters are used. The Young modulus (E')

of a granular soil can be established using different geotechnical correlations with common field test, such as the Standard Penetration Test (SPT). This test (Torrijo et al. 2020) is an in-situ test (normalized in Spain by UNE 103800) carried out during the drilling of a borehole, in the bottom of it and consists of driving on the ground a thick-walled sampler tube of 18 in (45 cm) of length, 2 in (51 mm) of outside diameter and 13/8 in (35 mm) of inside diameter, placed on the bottom of the drilling rods, by a 63.5 kg hammer that is dropped freely 30 in (76 cm). The result of the test is the *N* index, equal to the number of strokes necessary to push the core tube 30 cm (12 in).

If the *N* index is known, some correlations can be used. A common correlation is the one given by D'Apolonia et al. (1970):

$$E' = 215 + 10.6 \cdot N$$ **Equation 5.2**

In this formulation, E' is given in kg/cm^2.

An alternative correlation is the one proposed by Meigh & Nixon (1961):

$$\begin{cases} E' = 8 \cdot N & \text{for silts} \\ E' = 5 \cdot N & \text{for sands} \end{cases}$$ **Equation 5.3**

In this formulation, E' is given in MPa.

Other useful correlations include Wrench & Nowatzki (1986) or Bowles (1988).

For granular soils, the Poisson ratio (ν') is normally found in the range 0.3 – 0.35.

In the case of clays working under undrained conditions, the Poisson ratio (ν_u) is always 0.5 (as water is a non-compressible material). The undrained Young modulus value (E_u) can be obtained from the value of the undrained shear strength (c_u) according to the expression (Wroth, 1971; Castanedo, 2000):

$$E_u = 220 \cdot c_u$$ **Equation 5.4**

Where c_u must be introduced in kPa and E_u is obtained in the same unit.

The undrained Young modulus of a soil will always be greater than the effective one ($E_u > E'$), since under undrained conditions the water absorbs the entire applied load, resulting in a more rigid material. There is a theoretical relationship between both moduli based on the fact that the shear modulus must be equal in both total and effective terms (G_u and G') since water does not transmit tangential stresses:

$$G = \frac{E}{1+\nu} \quad ; \quad G_u = G' \rightarrow \frac{E_u}{1+\nu_u} = \frac{E'}{1+\nu'}$$ **Equation 5.5**

It should be mentioned that the use of this equation may provide *E′* values not in accordance with the real ones, so the use of correlations with field tests is advisable.

Besides mechanical parameters (c, ϕ, E and ν), the density of the soil (γ) is require to conduct any FEM simulation. Depending on the water table location and/or the existence of a flow net, that value will correspond to the bulk density or the saturated one. Both values can be obtained in laboratory.

Dry density is not recommended to be used in FEM simulations as all soils always have at least a small amount of water content.

It is interesting to note that there are other more complex and specific models than the one based on the Mohr-Coulomb failure criterion. For example, the Hardening-Soil Model is based on the observed hyperbolic relationship between the deviatoric stress and the axial deformation in a cohesive soil and does not assume a constant stiffness but considers different Young moduli. Anyway, the Mohr-Coulomb failure criterion is used straightforward in any calculation and especially in the FEM analysis of slopes.

5.3.2. Rock Masses

Simulation of rock masses may be conducted based on two possible approaches:

- Simulating the rock mass as a unique material.
- Considering as independent materials the intact rock and the discontinuities.

As seen in ***Chapter 3***, the main slope instabilities associated with rock masses are planar failures, wedge failures and toppling failures. Discontinuities play an important role in all these types of failures, since instabilities are mainly the consequence of the orientation of the discontinuities to the orientation of the slope under study.

Therefore, the stability analysis of rock slopes by FEM should considerer two independent materials modeled separately: the intact rock and the discontinuities.

Table 5.1. Values of parameter m_i for the Hoek & Brown criterion

Intact rock	**m_i [-]**
Carbonated rocks (limestone, marble, dolomite)	7
Clayed lithified rocks (argillite, slate, shale)	10
Sandy rocks (sandstone, quartzite)	15
Fine grain igneous rocks (diabase, andesite)	17
Coarse grain igneous rocks and metamorphic rocks (granite, gabbro, gneiss, diorite)	25

Source: Adapted from Hoek et al. (2002)

The intact rock may be modeled using the Hoek-Brown failure criterion (Hoek & Brown, 1980), a non-linear quadratic function based on the experimental data and ideas of Griffith (1921) about the formation and propagation of cracks in rocks:

$$\sigma'_1 = \sigma'_3 + \sigma_{ci} \cdot \sqrt{m_i \cdot \frac{\sigma'_3}{\sigma_{ci}} + 1}$$ **Equation 5.6**

Where σ'_1 and σ'_3 are the major and minor principal effective stresses at failure, respectively; σ_{ci} is the uniaxial compression strength (UCS) of the intact rock; and m_i is a parameter that depends on the type of the rock (Table 5.1) and which is related with the fragility of the intact rock and the way that cracks propagate on it.

If σ'_1 is reduced to zero, σ'_3 will represent the tension strength of the intact rock σ_t. For Hoek-Brown criterion expression, after doing some arrangements, σ_t yields:

$$\sigma_t = \frac{1}{2} \cdot \sigma_{ci} \cdot \left(m_i - \sqrt{m_i + 4}\right)$$ **Equation 5.7**

The Hoek-Brown criterion fits well with the compression behavior of real intact rocks and consequently, this is the recommendable failure criterion to be used in a numerical simulation. However, the intact rock is sometimes modeled assuming the Mohr-Coulomb failure criterion, even though this criterion does not perfectly match the behavior of the intact rock, which is not linear. If Mohr-Coulomb failure criterion is defined in principal stresses, this is written as:

$$\sigma_1 = \sigma_c + N_\phi \cdot \sigma_3 \quad ; \quad \sigma_c = \frac{2 \cdot c \cdot \cos\phi}{1 - \sin\phi} \quad ; \quad N_\phi = \frac{1 + \sin\phi}{1 - \sin\phi}$$ **Equation 5.8**

In this expression, σ_c is the uniaxial compression strength (UCS) that depends on the cohesion (c) and friction angle (ϕ) of the rock. As the criterion is linear, tensile strength of the intact rock σ_t is necessarily defined as (intersection of the failure line with the minor principal stress axis σ_3):

$$\sigma_1 = 0 \rightarrow \sigma_t = \sigma_3 = \frac{2 \cdot c \cdot \cos\phi}{1 - \sin\phi} \cdot \frac{1 - \sin\phi}{1 + \sin\phi}$$ **Equation 5.9**

This result shows the main limitation of the Mohr-Coulomb criterion applied to the intact rock: it is not possible to give independent values for the compressive strength and tensile strength of the intact rock. However, the Mohr-Coulomb criterion is of common use in geotechnical practice and is implemented in nearly any finite element software, both general-purpose ones and those designed for Geotechnical

Engineering. Conversely, not all software packages allow using the Hoek-Brown criterion. To apply the Mohr-Coulomb criterion to the intact rock, suitable values of cohesion and friction angle must be established. This can be done by conducting experimental tests or by "linearizing" the Hoek-Brown's strength curve σ'_1 vs. σ'_3 (Eq. 5.6) in the range of interest.

Nevertheless, in rock masses, the Mohr-Coulomb criterion (Eq. 5.1) is still used in FEM simulations, finding its niche for modeling the rock mass discontinuities. Commonly, the discontinuities cohesion is neglected, so there is only one strength parameter, the friction angle. The value of the friction angle can be obtained conducting tilt tests on rock fragments of the real discontinuities.

For typical cases, modeling the discontinuities by the Mohr-Coulomb criterion is enough. If a deep analysis is needed, the discontinuities may be modeled using the Barton-Choubey (1977) and Barton-Bandis (1981) models, which are much more comprehensive, but also require more parameters.

Table 5.2. Usual values of elastic parameters of intact rocks

	Young modulus [MPa]	**Poisson ratio [-]**
Andesite	30000 – 40000	0.23 – 0.32
Sandstone	3000 – 61000	0.10 – 0.40
Basalt	32000 – 100000	0.19 – 0.38
Limestone	15000 – 90000	0.12 – 0.33
Quartzite	22000 – 100000	0.28
Diabase	69000 – 96000	0.08 – 0.24
Shale	6000 – 39000	0.01 – 0.31
Gabbro	10000 – 65000	0.12 – 0.20
Gneiss	17000 – 81000	0.08 – 0.40
Granite	17000 – 77000	0.10 – 0.40
Marble	28000 – 72000	0.10 – 0.40

Source: Adapted from González de Vallejo & Ferrer (2011)

Besides the strength parameters, the elastic ones must also be defined. Even though the intact rock and the discontinuities are modeled separately in terms of its strength behavior, typically the Young modulus to consider corresponds to the whole rock mass, E_m. This is done to avoid an excess of stiffness in the numerical model. The value of E_m can be established from different correlations such as (Hoek & Diederichs, 2006):

$$E_m = 100 \cdot \frac{1 - \frac{D}{2}}{1 + \exp\left(\frac{75 + 25 \cdot D - GSI}{11}\right)}$$ **Equation 5.10**

Where *D* is the *disturbance factor* (Hoek et al., 2002; Hoek & Diederichs, 2006), which depends on the degree of disturbance to which the rock mass has been subjected by blast damage and/or stress relaxation, varying from 0 for undisturbed in situ rock masses to 1 for very disturbed rock masses; and GSI is the *Geological Strength Index*, a geomechanical index defined by Hoek and obtained using the chart given in Fig. 5.1.

For completeness, Table 5.2 shows the usual values of the elastic parameters of different intact rocks (note that these values of Young modulus are higher than E_m).

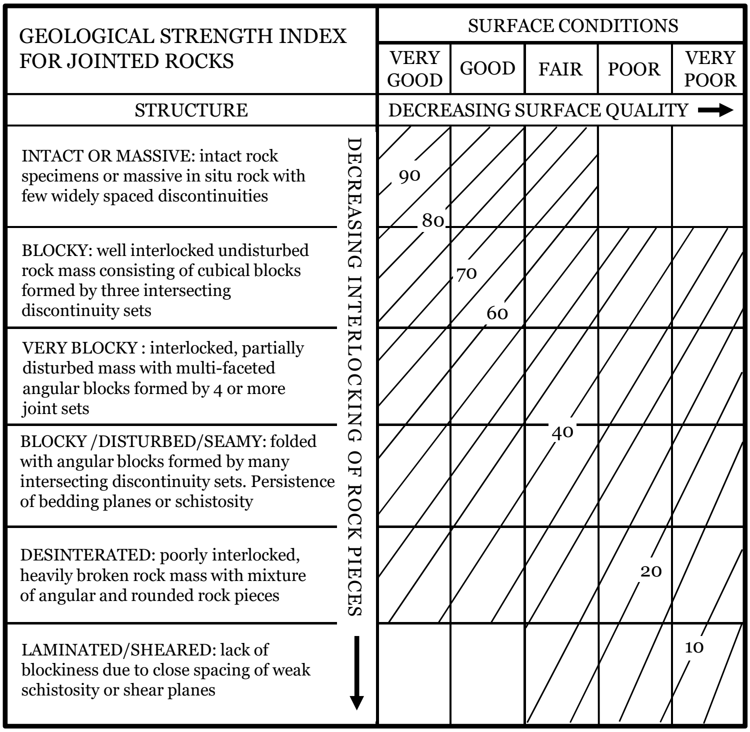

Source: Hoek & Brown (1997)

Fig. 5.1. GSI chart.

Given their nature, discontinuities do not normally are accounted in terms of weight. Thus, all the weight of the rock mass is due to the intact rock, and as in the case of soils, this is considered in the simulation by its density (bulk density or saturated density depending on the water table location and/or the existence of a flow net).

5.3.3. Highly Fractured Rock Masses

The approach showed in the previous section should be applied to any rock mass except in highly fractured rock masses or when the intact rock has very low strength. In such particular cases, the rock mass is assimilated to a soil, and it is modeled accordingly, using the Mohr-Coulomb failure criterion (Eq. 5.1) or, alternatively, the Hoek-Brown failure criterion for rock masses (Hoek et al., 2002):

$$\sigma'_1 = \sigma'_3 + \sigma_{ci} \cdot \left(m_b \cdot \frac{\sigma'_3}{\sigma_{ci}} + s \right)^a$$ **Equation 5.11**

Where σ'_1 and σ'_3 are the major and minor principal effective stresses at failure, respectively; σ_{ci} is the uniaxial compression strength (UCS) of the intact rock; m_b is the reduced value of the constant m_i (see Table 5.1); and s and a are two non-dimensional coefficients that depend on the rock mass properties. The values of m_b, s and a are given based on the GSI value (Fig. 5.1) for the rock mass under study:

$$m_b = m_i \cdot \exp\left(\frac{GSI - 100}{28 - 14 \cdot D} \right)$$ **Equation 5.12**

$$s = \exp\left(\frac{GSI - 100}{9 - 3 \cdot D} \right)$$ **Equation 5.13**

$$a = \frac{1}{2} + \frac{1}{6} \cdot \left[\exp\left(-\frac{GSI}{15} \right) - \exp\left(-\frac{20}{3} \right) \right]$$ **Equation 5.14**

Where D is the *disturbance factor* (Hoek et al., 2002; Hoek & Diederichs, 2006), which depends upon the degree of disturbance to which the rock mass has been subjected by blast damage and/or stress relaxation and varies from 0 for undisturbed in situ rock masses to 1 for very disturbed rock masses.

5.3.4. Reinforcing and Resisting Elements Modeling

The use of FEM for analyzing slope stability problems enables the introduction in the ground model of corrective measures like anchors, bolts and walls, enabling the assessment of the influence and efficacy of those elements on the slope under study.

Similar to ground materials (soil and rocks), the implementation of reinforcing and resisting elements in FEM requires defining their behavior by means of a constitutive model. The most common approach is considering linear elastic models (i.e. only defined by a Young modulus and a Poisson ratio) and controlling that yielding and/or failure of the reinforcing elements does not occur by comparing the stresses obtained in the simulation with those that cause the element yielding/failure. However, if necessary, reinforcing and resisting elements can also be modeled following an elastoplastic behavior.

In the case of a 2D modeling, mechanical parameters values are normally required to be introduced in the model "per meter of depth". For instance, in the case of modeling anchors and their grout bodies, an equivalent area will be needed to be computed based on the true areas of the anchors and grout bodies, respectively.

Thus, if anchors are arranged in a mesh *L* x *L* and their grout bodies have a given diameter d_{grout}, the equivalent area can be computed as:

$$A_{eq} = A_{total\ per\ unit\ length} = n_{grouts\ per\ unit\ length} \cdot A_{grout} = \frac{1}{L} \cdot \frac{\pi}{4} \cdot d_{grout}^2 \qquad \textbf{Equation 5.15}$$

5.4. Water Consideration

5.4.1. Soils

Water should be considered in any soil slope analysis using FEM in a similar way as this is commonly addressed in any geotechnical calculation. In soils, water presence is normally the consequence of one of two causes: water table and flow nets.

Water table (and any phreatic level) can be easily included in FEM by "drawing" a horizontal line at its location. Thus, all the materials above that line are dry (the bulk density is used) while all the materials below that line are saturated (the saturated density is used). Besides, below the water table pore pressures exist, and pore overpressures may be developed if no drainage is allowed. Geotechnical FEM software usually enables the implementation of the water table and any phreatic level, and directly takes into account its consequences (e.g. selecting the appropriate density or accounting for pore pressures). However, if general-purpose FEM software are used, the previous issues must be considered in the numerical simulation.

If a flow net exists in the soil slope, this must be solved prior to addressing the slope stability problem. For simple cases, classical hand methods can be applied, like obtaining the pore pressure at different points by potential and flow lines. Specific software can also be used to solve the flow net, then using the given values as inputs for the slope stability stress-strain problem. Fortunately, geotechnical FEM software usually contains packages to solve basic flow nets once hydrological boundary conditions are established to the slope model (Fig. 5.2).

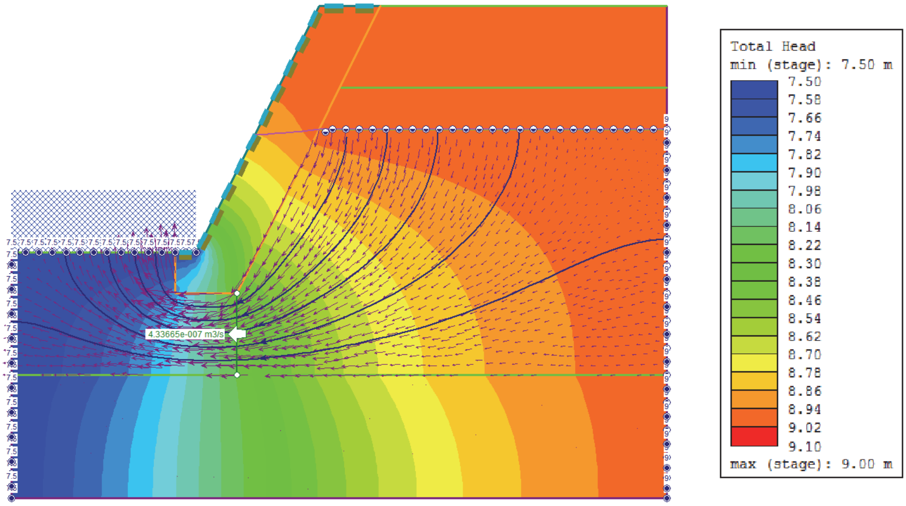

Source: Self-elaboration

Fig. 5.2. Example of flow net in a soil slope.

5.4.2. Rocks

Water should be considered in any rock slope analysis using FEM in a similar way as commonly addressed in any geotechnical calculation of a rock mass.

Water table and any phreatic levels can be considered following the ideas given above for soils. Thus, geotechnical FEM software usually enables the implementation of both the water table and any phreatic level, directly taking into account its consequences. However, if general-purpose FEM software are used, these consequences must be considered “manually” in the numerical simulation.

Flow nets are very common in rock masses, and they need to be solved prior to addressing the slope stability problem. However, the resolution of a flow net in a rock mass can be quite problematic (Nastev et al., 2008) since water mainly flows through discontinuities (Fig. 5.3). This makes necessary the use of specialized hydrogeological software to solve the flow net and then implementing the obtained results as inputs in the slope stability stress-strain FEM simulation, which can also be a complex issue.

Consequently, some simplifications are assumed to reduce such complexity and solve the problem. For example, in the stability of planar failures, it may be feasible considering the simplification assumed when calculating the safety factor (see ***Chapter 3***), consisting of taken a certain depth of water in the tension crack and defining a phreatic surface that decreases linearly towards the slope and that exits at the toe of the slope.

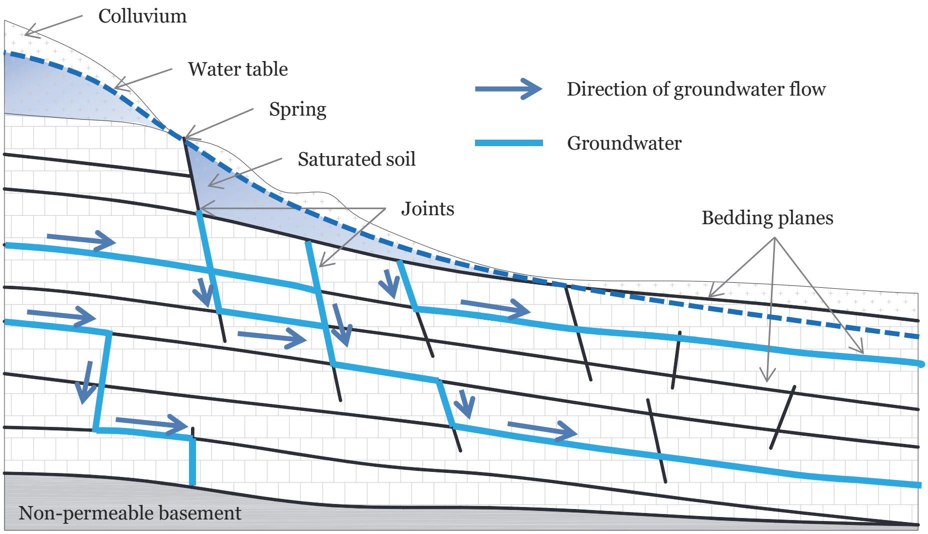

Source: Modified and based on Nastev et al. (2008)

Fig. 5.3. Example of flow net in a rock mass.

5.5. Calculation Issues

5.5.1. Stage Construction

Infrastructures such as slopes rarely are the result of a simple process. On the contrary, a slope is normally the result of a series of construction phases. Each of those phases may include different actions like a partial excavation, the installation of anchors, a wall construction, the application of a certain load and the variation of the water table. Besides, each phase needs time to be executed and during that time the terrain is able to adapt itself to the new stress-strain conditions. Therefore, the end of a phase will set the initial conditions of the next phase, conditions that will be different to those considered for the previous phase.

Analysis of soil and rock slopes by FEM should take into account the different construction phases, so a numerical model of a slope should be decomposed in a series of evolutionary models ranging from the initial condition of the slope (which may correspond to the natural soil state before any excavation is conducted) until the final state of the slope (when all corrective measures are installed). In addition, at each phase, water conditions (due water table/phreatic levels or flow nets) should be updated if necessary.

As all these aspects are specific and typical of geotechnical engineering projects (not only slopes, but other geotechnical problems such as foundations also), specialized geotechnical FEM software normally allow an easy definition of the numerical model by means of stage construction phases, so at any stage the practitioner can remove ground clusters to reproduce an excavation, add structural elements (e.g. anchors), activate load (e.g. a load due to a next foundation), activate/deactivate phreatic levels and so on.

5.5.2. Safety Factor

The classic definition of the safety factor as the ratio between the resisting forces to the driving forces cannot be obtained directly by FEM. However, equivalent definitions of the safety factor are used instead. One of the most common calculation techniques is applying the *shear strength reduction method* which is implemented in much geotechnical FEM software. This technique consists of carrying out several independent FEM simulations, gradually reducing the value of the shear strength parameters of the geotechnical materials, until reaching a failure situation.

Thus, in each of these simulations a shear strength reduction factor F^* is considered. That factor reduces the value of the shear strength parameters of the geotechnical materials and the stresses and deformations are then obtained. For example, the cohesion (c) and the friction angle (ϕ) of a soil can be reduced, respectively, as:

$$c^* = \frac{c}{F^*}$$ **Equation 5.16**

$$\tan\phi^* = \frac{\tan\phi}{F^*}$$ **Equation 5.17**

Where c^* is the reduced cohesion and ϕ^* the reduced friction angle. A similar approach can be developed for the friction angle of a discontinuity and the parameters of the Hoek-Brown model that define the intact rock behavior.

The process of reducing the shear strength parameters continues until reaching an unstable model (i.e. results of the analysis are non-convergent). At that moment the critical value of F^* has been attained. That value of F^* corresponds to the safety factor of the slope.

5.5.3. Output Information

A FEM simulation provides a lot of output information which can be used to analyzed and understand the behavior of the soil or rock slope under study. Besides the safety factor, the most common output information includes:

- *Displacements*: they are given in terms of displacements in the three axes (*x*, *y* and *z*) as well as of total displacements resulting from the vector composition of the previous ones.

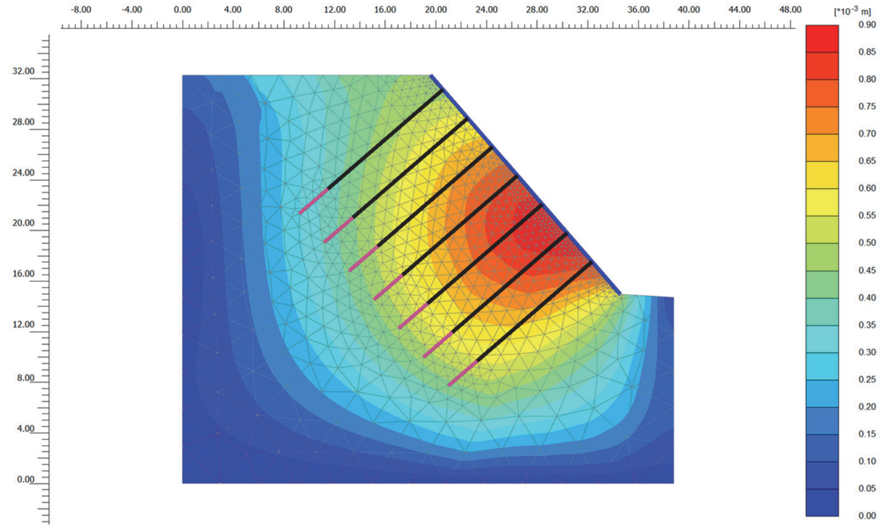

(a)

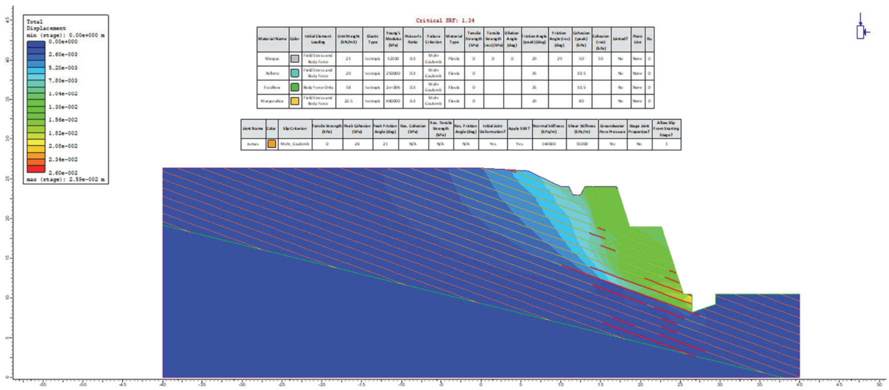

(b)

Source: Self-elaboration

Fig. 5.4. Examples of FEM output information: (a) total displacements obtained in a FEM analysis of a soil slope where a series of anchors are used; (b) total displacements and safety factor obtained in a FEM analysis developed in a rock slope (note that here the shear strength reduction factor is applied to the set of discontinuities, appearing in red the critical lengths where the slope failure is expected to occur).

- *Strains*: they are given according to the main stresses directions as well as to the three axes (*x*, *y* and *z*). Some software also provides inelastic strains, i.e. the strains developed in an element after yielding of the material and/or reaching a failure criterion.
- *Total stresses*: they are given according to the main stresses directions as well as to the three axes (*x*, *y* and *z*). Some software also provides composition of stresses following classical formulations like Von Misses and Tresca, which is useful for analyzing the results on structural elements (e.g. anchor or bolts).
- *Effective stresses*: they are given according to the main stresses directions as well as to the three axes (*x*, *y* and *z*). They are the result of subtracting pore pressures to total stresses.
- *Pore pressures*: they are given according to the main stresses directions as well as to the three axes (*x*, *y* and *z*). They are the result of the water table (and phreatic levels) and/or the flow net.
- *Plastic points*: they are given at the points where an element reaches yielding of the material and/or a failure criterion. Instead of plastic points, some software provides plastic stresses, which represent analogous information.

As an example, Fig. 5.4 shows the results of two FEM simulations. Fig. 5.4a shows the total displacements in a soil slope stabilized with anchors, while Fig. 5.4b shows for a rock slope with a set of discontinuities, total displacements at the failure state.

Bibliography and References

Recommended Bibliography

Ayala, F.J., Andreu, F.J., Fe, M., Ferrer, M., de Simón, A., Fernández, I., Olalla, C., Gómez, J., Sanpedro, J. & Cienfuegos, F.J. (1987). *Manual de Taludes*, IGME Serie Geotecnia, Madrid.

González de Vallejo, L. & Ferrer, M. (2011). *Geological Engineering*. London: CRC Press.

ISRM (2014). *The ISRM Suggested Methods for Rock Characterization, Testing and Monitoring: 2007-2014*. Edited by R. Ulusay. Berlin: Springer.

Ministerio de Fomento (2001). *Guía para el diseño y la ejecución de anclajes al terreno en obras de carretera*. Dirección general de Carreteras, Madrid.

Norrish, N. I. & Wyllie, D.C. (1996a). Chapter 15 – Rock slope stability analysis. In: A.K. Turner & R.L. Schuster (eds.), *Landslides: Investigation and mitigation, Special Report 247*, Transport Research Board, National Research Council, 247, 391-425.

Norrish, N. I. & Wyllie, D.C. (1996b). Chapter 18 – Stabilization of rock slopes. In: A.K. Turner & R.L. Schuster (eds.), *Landslides: Investigation and mitigation, Special Report 247*, Transport Research Board, National Research Council, 247, 474-504.

Torrijo, F.J., Garzón Roca J. & Cobos, G. (2020). Geotechnical Engineering, Techniques and Methods. Valencia: Editorial Universitat Politècnica de València.

References

Alonso Pérez de Ágreda, E. (2005). *Estabilidad de Taludes*. Departament d'Enginyeria del Terreny, Cartogràfica i Geofísica, ETS d'Enginyeria de Camins, Canals i Ports, Universitat Politècnica de Catalunya.

ASTM (2016). Annual Book of ASTM standards. American Society of Testing Materials.

Ayala, F.J., Andreu, F.J., Fe, M., Ferrer, M., de Simón, A., Fernández, I., Olalla, C., Gómez, J., Sanpedro, J. & Cienfuegos, F.J. (1987). *Manual de Taludes*, IGME Serie Geotecnia, Madrid.

Bandis, S.C., Lumsden, A.C. & Barton, N. (1981). Experimental studies of scale effects on the shear behaviour of rock joints. *International Journal of Rock Mechanics and Mining Sciences*, 18, 1-21.

Barton, N. & Choubey, V. (1977). The shear strength of rock joints in theory and practice. *Rock Mechanics*, 10(1-2), 1-54.

Bieniawski, Z.T. (1979). The geomechanics classification in rock engineering applications. *4th International Conference on Rock Mechanics*, Montreaux, Switzerland.

Bieniawski, Z.T. (1989). *Engineering rock mass classifications*. New York: John Wiley and Sons.

Bishop, A.W. (1955). The use of the slip circle in the stability analysis of slopes. *Geotechnique*, 5, 1-17.

Bishop, A.W. (1967). Progressive failure with special reference to the mechanism causing it. *Proccedings of the Geotechnical Conference in Oslo*, 2, 3-10.

Bowles, J.E. (1988). *Foundation Analysis and Design*. New York: McGraw Hill.

Castanedo, F.J. (2000). Cimentaciones superficiales. Aspectos geotécnicos. *Jornadas Geotécnicas sobre Cimentaciones, ICOG, AIGE*, Madrid.

Choquet, P. & Tanon, D.D.B. (1985). Nomograms for the assessment of toppling failure in rock slopes. *Proccedings of the 26th U.S. Symposium on Rock Mechanics*, South Dakota, School of Mines and Technology, Rapid City.

Corominas, J. & García Yagüe, A. (1997). Terminología y cartografía de movimientos de ladera. *Jornadas Técnicas de Taludes y Laderas*, ICOG, Madrid.

Corominas, J. (1989). Clasificación y reconocimiento de los movimientos de ladera. *Monografia S.E.G., nº 3*, Zaragoza.

D'Appolonia, D.J., D'Appolonia, E. & Brissete, R.F. (1970). Discussion on Settlement of Spread Footings on Sand. *ASCE Journal SMFD*, 96, SM2.

da Costa García, A. (2004). *Inestabilidades por Degradación Superficial de Taludes en Suelos. Corrección mediante Sistemas de Refuerzo Anclados*. PhD Thesis, Universidad de Cantabria.

Fellinius, W. (1927). *Erdstatische Berechnungen mit Reibung un Kohäsion und unter Annahme Kreiszilindrescher Gleiftalächen.* Berlin: W. Ernst & Sohn.

Giani, G.P. (1992). *Rock slope stability analysis*. Rotterdam: A. A. Balkema.

González de Vallejo, L. & Ferrer, M. (2011). *Geological Engineering*. London: CRC Press.

Goodman, R.E. & Bray, J.W. (1976). Toppling of rock slopes. *Proccedings of the Specialty Conference on Rock Engineering for Foundations and Slopes*, Boulder, Colorado.

Goodman, R.E. (1976). *Methods of Geological Engineering in Discontinuous Rocks*. St. Paul, Minnesota: West Publishing Co.

Griffith, A.A. (1921). The Phenomena of Rupture and Flow in Solids. *Philosophical Transactions of the Royal Society (Series A)*, 221, 163-198.

Highland L., & Bobrowski, P.T. (2008). The Landslide Handbook – A Guide to Understanding Landslides. Reston, Virginia: US Geological Survey.

Hittinger, M. (1978). *Numerical analysis of Toppling failures in jointed rock masses*. PhD Thesis, University of California, Berkeley.

Hoek E. & Diederichs, M.S. (2006). Empirical estimation of rock mass modulus. I*nternational Journal of Rock Mechanics and Mining Sciences*, 43(2), 203-215.

Hoek, E. & Bray, J.W. (1981). *Rock slope engineering*. London: Institution of Mining and Metallurgy.

Hoek, E. & Brown E.T. (1997). Practical estimates of rock mass strength. *International Journal of Rock Mechanics and Mining Sciences*, 34(8), 1165–1186.

Hoek, E. & Brown, E. T. (1980). *Underground Excavations in Rock.* London: Institution of Mining and Metallurgy.

Hoek, E., Carranza-Torres C. & Corkum, B. (2002). Hoek-Brown failure criterion – 2002 Edition. In: R. Hammah, W. Bawden, J. Curran and M. Telesnicki (Eds.), *Proceedings of NARMSTAC 2002, Mining Innovation and Technology*, Toronto.

ISRM (1981). *Suggested methods for rock characterization, testing and monitoring*. Oxford: Pergamon Press.

ISRM (2007). *The Complete ISRM Suggested Methods for Rock Characterization, Testing and Monitoring: 1974-2006*. Edited by R. Ulusay and J.A. Hudson. Berlin: Springer.

ISRM (2014). *The ISRM Suggested Methods for Rock Characterization, Testing and Monitoring: 2007-2014*. Edited by R. Ulusay. Berlin: Springer.

Janbu, N. (1954). Application of composite slip surfaces for slope stability analysis. *European Conference on Stability of Earth Slopes*, Sweden.

Janbu, N. (1954). Earth pressure and bearing capacity calculations by generalized procedure of slices. *IV Int. Conf. on Soil Mechanics and Foundation Engineering*, London.

Jimenez Salas, J.A., Justo Alpañes, J.L. & Serrano, A.A. (1976). *Geotecnia y Cimientos II. Mecánica del Suelo y de las Rocas*. Madrid: Editorial Rueda.

Meigh, A.C. & Nixon, I.K (1961). A comparison of in situ test for granular soils. *5th ICOSOMEF*, Paris.

Ministerio de Fomento (2001). *Guía para el diseño y la ejecución de anclajes al terreno en obras de carretera*. Dirección general de Carreteras, Madrid.

Morgenstern, N. R. & Price, V. (1965). The analysis of the stability of general slip surfaces. *Geotechnique*, 15 (1), 79–93.

Nastev, M., Morin, R., Gordin R. & Rouleau, A. (2008). Developing conceptual hydrogeological model for Potsdam sandstones in southwestern Quebec, Canada. *Hydrogeology Journal*, 16, 373-388.

Norrish, N. I. & Wyllie, D.C. (1996a). Chapter 15 – Rock slope stability analysis. In: A.K. Turner & R.L. Schuster (eds.), *Landslides: Investigation and mitigation, Special Report 247*, Transport Research Board, National Research Council, 247, 391-425.

Norrish, N. I. & Wyllie, D.C. (1996b). Chapter 18 – Stabilization of rock slopes. In: A.K. Turner & R.L. Schuster (eds.), *Landslides: Investigation and mitigation, Special Report 247*, Transport Research Board, National Research Council, 247, 474-504.

Ortuño, L. (1992). *Taludes en suelos*, I Master de Ingeniería Geológica, UCM Madrid.

Piteau, D.R. & Peckover, F.L. (1978). Engineering of rock slopes. In: R.L.Schuster & R.J. Krizek (eds.), *Special Report 176: Landslides: Analysis and Control*, Transport Research Board, National Research Council, 192-234.

Portillo, E. (2003). Estabilización de taludes mediante anclajes. In: C. López (ed.), *Ingeniería del Terreno*, IngeoTer 2. UD Proyectos ETSI Minas – UPM, Madrid, Cap. 92.

Ritchie, A.M. (1963). *Evaluation of Rockfall and its Control*. Highway Research Board.

Romana, M. (1986). New adjustment ratings for application of Bieniawski classification to slopes. *International Symposium on the role of rock mechanics, ISRM*, Zacatecas.

Romana, M. (1995) The geomechanics classification SMR for slope correction. *Procceddings of the 8th International ISRM Congress*.

Skempton, A. W. & Hutchinson, J.N. (1969). Stability of natural slopes and embankment foundations. *7th Int. Conf. on Soil Mechanics*, México.

Spencer, E. (1967). A Method of analysis of the Stability of Embankments Assuming Parallel Inter-Slice Forces. *Geotechnique*, 17, 11-26.

Taylor, D. W. (1937). Stability of earth slopes. *Journal of Boston Society of Civil Engineering*, 24, *197–246*.

Taylor, D.W. (1948) *Fundamentals of Soil Mechanics*. New York: Wiley.

Torrijo, F.J., Garzón Roca J. & Cobos, G. (2020). Geotechnical Engineering, Techniques and Methods. Valencia: Editorial Universitat Politècnica de València.

Varnes, D.J. (1978). Slope movement types and processes. In R.L. Schuster and R.J. Krizek (eds.), *Landslides: analysis and control*, Transportation Research Board, Special Report 176, 11-33.

Wrench, B.P. & Nowatzki, E.A. (1986). A Relationship between Deformation Modulus and SPT-N for Gravels. *Proccedings of the ASCE Special Conference on In-situ Test*, Blacksburg, Virginia.

Wroth C. P. (1971). Some aspects of the elastic behaviour of aver consolidated clay. *Foulis, Henley on Thames*, 347-361.